

<https://doi.org/10.15388/vu.thesis.136>

<https://orcid.org/0000-0002-5660-9048>

VILNIUS UNIVERSITY

CENTER FOR PHYSICAL SCIENCES AND TECHNOLOGIES

Povilas
ŠIMONIS

Investigation of yeast cell responses to pulsed electric field treatment

DOCTORAL DISSERTATION

Natural sciences,
Chemistry (N 003)

VILNIUS 2021

This dissertation was carried out from 2016 to 2020 at the Center for Physical Sciences and Technology.

The research was supported by the Research Council of Lithuania.

Academic supervisor:

Dr. Arūnas Stirkė (Center for Physical Sciences and Technology, Natural sciences, Chemistry – N 003)

This doctoral dissertation will be defended in a public/closed meeting of the Dissertation Defense Panel:

Chairman – prof. dr. Gintautas Saulis (Vytautas Magnus University, Natural sciences, Biophysics – N 011).

Members:

prof. dr. Aidas Alaburda (Vilnius University, Natural sciences, Biophysics – N 011);

dr. Henri Gerken (Arizona State University, Natural sciences, Biology – N 010);

prof. dr. Gediminas Niaura (Center for Physical Sciences and Technology, Natural sciences, Chemistry – N 003);

prof. dr. Rasa Pauliukaitė (Center for Physical Sciences and Technology, Natural sciences, Chemistry – N 003).

The dissertation shall be defended at a public meeting of the Dissertation Defence Panel at 18.00 on 15th February 2021 in a meeting room D401 of the Center for Physical Sciences and Technology.

Address: Saulėtekio av. 3, D401., Vilnius, Lithuania

Tel. +370 63492894; e-mail: simonis.povilas@gmail.com

The text of this dissertation can be accessed at the libraries of Center for Physical Sciences and Technology, and Vilnius University, as well as on the website of Vilnius University: www.vu.lt/lt/naujienos/ivykiu-kalendarius

<https://doi.org/10.15388/vu.thesis.136>

<https://orcid.org/0000-0002-5660-9048>

VILNIAUS UNIVERSITETAS
FIZINIŲ IR TECHNOLOGIJOS MOKSLŲ CENTRAS

Povilas
ŠIMONIS

Mielių ląstelių atsako į impulsinio elektrinio lauko sukeltą poveikį tyrimas

DAKTARO DISERTACIJA

Gamtos mokslai,
Chemija (N 003)

VILNIUS 2021

Disertacija rengta 2016-2020 metais Fizinių ir technologijos mokslų centre.

Mokslinius tyrimus rėmė Lietuvos mokslo taryba.

Mokslinis vadovas:

Dr. Arūnas Stirkė (Fizinių ir technologijos mokslų centras, gamtos mokslai, chemija – N 003).

Gynimo taryba:

Pirmininkas – **prof. dr. Gintautas Saulis** (Vytauto Didžiojo universitetas, gamtos mokslai, biofizika – N 011).

Nariai:

prof. dr. Aidas Alaburda (Vilniaus universitetas, Vytauto Didžiojo universitetas, gamtos mokslai, biofizika – N 011);

dr. Henri Gerken (Arizonos Valstijos universitetas, gamtos mokslai, biologija – N 010);

prof. dr. Gediminas Niaura (Fizinių ir technologijos mokslų centras, gamtos mokslai, chemija – N 003);

prof. dr. Rasa Pauliukaitė (Fizinių ir technologijos mokslų centras, gamtos mokslai, chemija – N 003).

Disertacija ginama viešame Gynimo tarybos posėdyje 2021 m. vasario mėn. 15 d. 18 val. Fizinių ir technologijos centro D401 auditorijoje. Adresas: Saulėtekio al. 3, D401, Vilnius, Lietuva, tel. +370 63492894; el. paštas simonis.povilas@gmail.com

Disertaciją galima peržiūrėti Fizinių ir technologijos mokslų centro ir Vilniaus universiteto bibliotekose ir VU interneto svetainėje adresu: <https://www.vu.lt/naujienos/ivykiu-kalendorius>

Table of Contents

ABBREVIATIONS.....	7
INTRODUCTION.....	8
STATEMENTS OF THESIS	9
RESEARCH DIRECTIONS	10
1. Fundamentals of electroporation and yeast cell responses to pulsed electric field.....	10
1.1. Literature overview	10
1.2. Importance of further research	18
1.3. Tasks of the research work	19
1.4. Main results	19
1.5. Novelty and relevance	22
2. Signal modulation of yeast-modified electrodes via pulsed electric field treatment.....	24
2.1. Literature overview	24
2.2. Importance of further research	29
2.3. Task of the research work.....	30
2.4. Main results	30
2.5. Novelty and relevance	31
3. The effects and applications of nanosecond pulsed electric fields.....	33
3.1. Literature overview	33
3.2. Importance of further research	35
3.3. Tasks of the research work	36
3.4. Main results	36
3.5. Novelty and relevance	38
CONCLUSIONS.....	39
METHODS EMPLOYED IN THIS RESEARCH WORK.....	40
AUTHOR CONTRIBUTION	45
BIBLIOGRAPHY	46

SANTRAUKA	59
ACKNOWLEDGEMENTS	70
LIST AND COPIES OF PUBLICATIONS	71

ABBREVIATIONS

d – membrane thickness;
DNA – deoxyribonucleic acid;
DTT – dithiothreitol;
EDTA – ethylenediaminetetraacetic acid;
 E – electric field strength;
 E_n – enzymes;
FAD – flavin adenine dinucleotide;
 M – menadione;
 MH_2 – menadiol;
MREs – menadione reducing enzymes;
NADH – nicotinamide adenine dinucleotide;
NADPH – nicotinamide adenine dinucleotide phosphate;
nsPEFs – nanosecond electric field pulses;
PCD – programmed cell death;
PEF(s) – pulsed electric field(s);
PEG – polyethylene glycol;
 R – cell radius;
RNA – ribonucleic acid;
ROS – reactive oxygen species;
 S_{Ox} – oxidized form of substrate;
 S_{Re} – reduced form of substrate;
ssDNA – single stranded deoxyribonucleic acid;
 TPP^+ – tetraphenylphosphonium ion;
 U_m – transmembrane voltage;
YCA1 – yeast metacaspase 1;
 σ_e – electric conductivities of the extracellular medium;
 σ_i – electric conductivity of the cytoplasm;
 σ_m – electric conductivity of the membrane;
 ϵ_m – dielectric permittivity of the membrane;
 θ – the angle between the site on the cell membrane where U_m is measured and the direction of external electric field;
 τ_m – the time constant of the membrane charging.

INTRODUCTION

Yeast *Saccharomyces cerevisiae* is one of the most well-studied and understood eukaryotic organisms. From a long time ago till now they have been widely used in bakery and alcohol production. Interestingly, the same microorganisms in a different environment like juice or dairy products cause spoilage. The demand for nutritious foods is ever-growing and requires safer and more efficient production processes. Meanwhile, the metabolic activity of yeast cells is also successfully employed in biotechnology where cells are used in the whole-cell bioprocesses such as biocatalysis and recombinant protein production. These applications are dependent and are often hindered by the natural barrier functions of the cell wall and cell membrane. They retard the entry of substrates and release of products and thus limit the efficiency of biotechnological procedures. Since yeast cells are an essential part in the food industry, biotechnology as well as research, technology which could enhance or diminish yeast productivity in a desired fashion will have a significant worldwide impact in respective fields.

Pulsed electric field (PEF) is one of techniques which could be used to improve permeability for target molecules. Growing experience suggests a variety of applications, yet the integration of PEF technology into yeast-related biotechnologies is not successfully developed. One of the reasons being the lack of fundamental knowledge of yeast cell responses to such treatment. There is very little detail about PEF effects on cell wall permeability and death related pathways. It is known that PEF can be used as a non-thermal processing technology for extending shelf-life of some products. However, there is still a lack of data related to the effects of PEF on yeast cells used for whole-cell bioprocesses. Use of yeast cells as a model for the investigation of PEF induced effects is untapped and could provide insights for both prospective applications and eukaryotic cell response mechanisms.

Loading cells with DNA, enzymes and antibodies for research purposes, introduction of probes and molecules for drug delivery and transporting molecules into, out of cells and tissue are expected to depend quantitatively on the extent of molecular transport. Fundamental description of cellular responses, mechanical, electrical and molecular transport induced by exposure to pulsed electric fields will be increasingly important. What is more, modern instruments allow generation of high voltage electric field pulses with nanosecond duration which could provide new prospective applications and solutions to previously unsolvable problems. Such insights will open new

applications in therapeutics as well as food industry fields while increasing efficiency and decreasing energy consumption.

In my dissertation I focus on answering questions needed to clarify steps for successful knowledge transfer from fundamental yeast electroporation research to biotechnological applications. The research and overview were divided into three parts covering: 1 — fundamental research on yeast cells, 2 — evaluation of PEF induced effects via mediated amperometry and 3 — yeast cell responses to, and application of electric field pulses with nanosecond duration.

STATEMENTS OF THESIS

1. Permeability of yeast *Saccharomyces cerevisiae* cell wall and plasma membrane after exposure to electric field pulse with strength of up to 6 kV/cm changes similarly and stabilises within 100 seconds, thus confirming involvement and importance of both structures in the recovery process.
2. Mediated amperometry can be employed for the investigation of electric field effects on yeast membrane permeability to hydrophilic mediators as well as activity of menadione reducing enzymes.
3. High voltage electric field pulses (up to 220 kV/cm) with nanosecond duration (up to 90 ns) induce caspase-dependent cell death in yeast cells and can be employed for their selective inactivation.

RESEARCH DIRECTIONS

1. Fundamentals of electroporation and yeast cell responses to pulsed electric field

1.1. Literature overview

Yeast *Saccharomyces cerevisiae* is a single-cell microorganism. It is widely used as a model for eukaryotic cell biology, functional genomics as well as systems biology¹. Due to simple genetic manipulations, yeast became the first eukaryotic organism with complete genomic sequence². Comparison of yeast genomic sequences with those of other model systems showed that both protein amino acid sequences and functions had been conserved well enough that annotations of function could be transferable from one eukaryotic species to another. Furthermore, around 1000 yeast genes are members of orthologous gene families associated with human disease³. Studies of gene expression provided knowledge about transcriptional regulatory networks and the transcription factors that control them^{4,5}. Analysis of marked mutants with double deletions provided quantitative genetic interaction profiles for around 75 % *S. cerevisiae* genes^{6,7}. Relatively easy, safe and fast procedures required for yeast cultivation led to efficient high throughput experiments.

Yeast cells can be considered as ellipsoid objects with an average diameter of 5-10 μm ⁸. Typically, they replicate by forming a bud which grows throughout the cell cycle and later leaves its mother cell when mitosis is completed⁹. Unlike mammalian cells, yeast cells are surrounded by an elastic wall which maintains the shape of the cell, stabilizes internal osmotic conditions, protects against physical stress and acts as a scaffold for proteins¹⁰.

The configuration of the cell wall is tightly controlled. Thickness, structure as well as composition vary considerably depending on environmental conditions and its mass in terms of dry weight may account for up to 30 % of total cell mass¹¹. β 1,3- and β 1,6-linked glucans, mannoproteins (glycoproteins which contain 15 to 90 % mannose by weight) and chitin are covalently joined to form higher-order complexes¹². The outer layer of a cell wall has a brush-like surface consisting mostly of mannoproteins¹³ and can be removed by proteolysis¹⁴. The inner layer has a microfibrillar structure consisting mainly of glucans which are β -glucanase-digestible¹⁴. In yeast, cell wall proteins and proteins often have glycosyl-phosphatidylinositol anchors residing in plasma membrane^{15,16}. Overall, the cell wall is a tightly packed dynamic structure with $\sim 2 \times 10^6$ cell wall proteins¹⁷.

The porosity of yeast cell wall is an extensively investigated topic. In studies which investigate permeability by measuring passive absorption, permeability is distinguished into one limited by the membrane ($M \approx 110$ Da, Einstein-Stokes hydrodynamic radius ≈ 0.42 nm) and cell wall ($M \approx 620$ - 760 Da, Einstein-Stokes hydrodynamic radius ≈ 0.81 - 0.89 nm)¹⁸. In contrast, other researchers show that under specific conditions it is possible to detect influx¹⁹ as well as leakage²⁰ of whole proteins through the cell wall. Permeability measurements performed under hyperosmotic conditions cause a decrease in cellular volume and subsequent increase in its density²¹ also highlighting the dynamic nature of the cell wall structure. A review article by De Nobel and Barnett concluded that yeast cells in the exponential phase of growth are permeable to molecules of up to 400 kDa with hydrodynamic radius of 5,8 nm²². The outermost layer is packed with mannoproteins which give negative a charge to the cell wall and seems to be the main permeability determining barrier since its removal results in higher wall's permeability to horseradish peroxidase ($M = 40$ kDa)²³ and dextrans²⁴. The entry of dextrans ($M \approx 70$ kDa) can be facilitated by modifying cell walls with EDTA and DTT, yet there is a question about whether dextrans are internalized²⁵ or only trapped²⁶ in the cell wall. Pre-treatment with DTT (which reduces disulphide bridges) increased release of invertase (320 kDa) from periplasmic space²⁵. EDTA opens up the wall by removing divalent cations from it and induce only minor changes in permeability²⁷. Permeability measurements are highly variable and depend on numerous parts of methodology, including the strain of microorganisms, growth phase, osmotic, ionic conditions as well as probes for permeability detection. Some researchers hypothesize that cell wall contains some big pores through which globular proteins could enter even if the average pore size is quite small. In order to efficiently manipulate permeability of cell walls (to increase or decrease it), more research on defining their structural changes and dynamics after exposure to abiotic stresses is needed.

The space between the membrane and the cell wall is called as periplasmic and it hosts various enzymes (invertase, acid phosphatase, α -galactosidase) needed for efficient metabolism. This zone of the cell is very dynamic, interacting both with the inner part of a cell wall and plasma membrane²⁸.

The plasma membrane consists of lipids and proteins in approximately equal proportions. Heterogeneous composition allows a wide range of distinct roles and functions²⁸:

1. Acts as a barrier against free diffusion of solutes.
2. Catalyse specific exchange reactions.
3. Stores energy in the form of transmembrane ions and solute gradients.
4. Regulates the rate of energy dissipation.
5. Provides sites for binding specific molecules to invoke catabolic signalling pathways.
6. Provides organized support matrix for the site of enzyme pathways involved in the biosynthesis of the cell components.

The lipid bilayer is composed of phospholipids, glycosphingolipids and ergosterol which forms a hydrophobic barrier and supports the structure of integral proteins. Leaflets of the membrane are asymmetrical, thus maintaining membrane surface potential as well as membrane protein activity²⁹. Relative amounts of major phospholipids (phosphatidylcholine, phosphatidylethanolamine, phosphatidylinositol, phosphatidylserine and phosphatidic acid with minor amounts of cytidine-diphosphate-diacylglycerol) depend on yeast strain, growth phase, temperature as well as nutrient availability³⁰⁻³². Bilayer structure with the lipophilic area surrounded by hydrophilic lipid head groups provides a three-dimensional area for transmembrane proteins and channels. Accurate structure and orientation of enzymes are essential for their activity and are maintained within membranes.

Some proteins actively transport charged ions and molecules across the membrane, therein generating an electric membrane potential difference³³. The electric gradient at both sides of the plasma membrane contributes to the driving force for the uptake of cations and other molecules through their respective transporters^{34,35}. Since membrane acts as an insulator separating charged species, it can be described as a capacitor with specific conductance and resting membrane potential. Physiological ranges of transmembrane voltage, the mechanical pressure exerted by it and the capacitive energy stored in the membrane do not perturb the integrity of a membrane. Selective permeability maintained by hydrophobicity of a membrane and specific channels within it is important for efficient transport of nutrients as well as protection against toxic compounds. Due to the mobile nature of lipid molecules, hydrophobic pores are formed by spontaneous thermal fluctuations of membrane lipids within membranes. Many applications like the introduction of target molecules or extraction of intracellular compounds require fast and efficient improvement of permeability.

One of the techniques which can be used to permeabilize cells and improve molecular transport is exposure to the pulsed electric field. During exposure,

the additional component of the voltage across the membrane superimposes onto resting voltage and exists only as long as the external field is present³⁶. The induced transmembrane voltage is proportional to the strength of the external electric field, and can induce transmembrane voltages far exceeding their physiological range³⁷. The very presence of an induced transmembrane potential provides the free energy necessary for structural rearrangements of membrane phospholipids and thus enables hydrophilic pore formation^{38,39}. Such perturbation, often termed electroporation or electropermeabilization, can lead to structural rearrangements of lipids in the membrane bilayer resulting in the formation of and stabilization of pores^{40,41}. The extent of permeabilization depends on experimental conditions, duration of exposure as well as cell type⁴¹.

Potential distribution in the region surrounding a spherical cell with a non-conducting membrane can be described by the Laplace equation:

$$U_m = 1.5RE \cos \theta \quad (1)$$

where U_m is the transmembrane voltage, R is cell radius, and θ is the angle between the site on the cell membrane where U_m is measured and the direction of external electric field E ³⁶. Transient behaviour during initial microseconds is described with some modifications:

$$U_m = 1.5RE \cos \theta (1 - e^{-t/\tau_m}) \quad (2)$$

where τ_m is the time constant of the membrane charging, and can be expressed as:

$$\tau_m = \frac{R\epsilon_m}{2d \frac{\sigma_i \sigma_e}{\sigma_i + 2\sigma_e} + R\sigma_m} \quad (3)$$

Important components in these processes are σ_i , σ_m and σ_e being the electric conductivity of the cytoplasm, cell membrane and extracellular medium respectively; ϵ_m being the dielectric permittivity of the membrane; and d being membrane thickness³⁶. These equations are applicable to situations where spherical cells in dilute suspensions are exposed to electric field pulses longer than 1 μ s. In concentrated suspensions, where cell volume fraction exceeds 10 %, the local field around each cell starts affecting adjacent cells^{36,42}. It is important to consider that slight differences in cell size and shape could result in distinct values of induced transmembrane potential⁴³. It was shown that

optimal electrical field strength for permeabilization of cells with different size (radius ratios *S. cerevisiae*/*K. lactis* = 1.56) is different⁴⁴. Cells of *H. polymorpha* which are even smaller in average size, need stronger pulses in order to achieve the same results⁴⁵. Critical values of induced transmembrane potential above which the permeabilization usually occurs ranges from 0.25 V up to 1 V³⁶. According to the standard model of electroporation, the formation of hydrophilic pores is followed by rearrangement into aqueous pores which are then stable due to a local minimum of free energy. This state is reversible until chemical and/or mechanical breakdown of membrane structure occurs. The concept of hydrophilic pore formation is supported by measured membrane conductivity changes and increased molecular transport after exposure to an electric field, yet remains theoretical due to lack of visual confirmation of the phenomena³⁸.

Design of controlled treatment procedure for a particular investigation or application involves the choice of various pulse parameters including amplitude, duration, number and repetition frequency. If those parameters exceed the optimal values, irreversible electroporation takes place due to DNA damage⁴⁶ and membrane disintegration⁴⁷. Various pulses can be combined to achieve desired results and should be optimized for specific purposes. Reversible electroporation for various kinds of molecules can be performed by using longer pulses (few milliseconds) or a combination of high-voltage short-duration pulses and low-voltage long-duration pulses^{48,49}. The most frequently used pulse shapes are exponential and square waves. When rise time of pulse amplitude was investigated (2 μ s, 10 μ s, 100 μ s), no significant effects on permeabilization or survivability was detected⁵⁰. Such data suggests that rise time is most important for short pulses where its duration is comparable to the whole pulse width. Study on bipolar pulses revealed that the main permeabilization defining parameter is the time during which the pulse amplitude exceeds certain threshold⁵⁰. It was previously proposed that a train of sufficiently strong pulses will cause permeability which increases within a population of cells with a rise in pulse number while E controls the area of permeabilization⁵¹. Exposure to multiple pulses causes cumulative perturbations in membrane structure and increase the probability of aqueous pore formation. Such an outcome can be beneficial to specific applications like pasteurization, but may conceal fundamental subtleties⁵² due to change of the system after each consecutive pulse⁵³.

The solution surrounding the cells has a significant impact on its own. Solutes in the suspension define conductivity and osmolarity of a system, conditions under which the abiotic stress will be experienced by the cell. Under ideal circumstances for fundamental experiments, the composition of a

solution should not be toxic both before and after permeabilization. During pulsed electrical field treatment, both intracellular and extracellular charged components will be affected by a potential difference between electrodes thus producing measurable currents. Higher conductivity leads to stronger currents within a solution and causes Joule heating which can affect viability as well as permeability on its own, especially when long pulses are used⁵⁴. Experimental evidence on how conductivity affects electroporation is ambiguous. Irreversible electroporation can be enhanced⁵⁵ or diminished⁵⁶ by higher conductivity. Such ambiguity is possibly facilitated by different cell lines and composition of solutions. Results of successful reversible electroporation are achieved in suspensions with lower conductivity⁵².

Osmolarity is another parameter of a suspension which affects electroporation results. It is easier to permeabilize cells in a hypertonic media while the rate of resealing is greater in under hyperosmotic conditions⁵⁷. In mammalian cells, permeabilization in isotonic medium can result in a volume increase of up to 100 % while the increase is significantly lower in hypertonic medium⁵⁸. Regarding transformation and other applications, osmolarity conditions should be optimized to each specific organism.

Research on yeast and other microorganisms provided various insights on electroporation phenomena and can roughly be classified into 3 categories related to applications: genetic transformation of microorganisms, inactivation of microorganisms and extraction of biomolecules.

Introduction of exogenous compounds

One of the most extensively introduced molecules into a wide range of cells is DNA. The first transformation after PEF treatment was successfully performed in mouse cells⁵⁹. It soon became the standard procedure for transforming plant cells⁶⁰ and bacteria⁶¹. It is assumed that exposure to pulsed electric fields results in the pore formation across the membrane which in turn allows entry of macromolecules⁶². Electroporation of yeast spheroplasts was first performed by Karube et al.⁶³ while electrotransformation of whole *Saccharomyces cerevisiae* cells followed soon after⁶⁴. Efforts for simplification of procedure and varying access to instrumentation resulted in plenty of protocols emphasizing different aspects of the treatment. Delorme used log-phase cells within a fresh medium with plasmid DNA and exposed to 2.25 kV/cm with 25 μ F capacitance reaching up to 4.5×10^3 transformants/ μ g plasmid DNA⁶⁵. Multiple other studies have shown that replicating cells in early or mid-log phase can be transformed up to 10 times more efficiently than stationary cells^{66,67}. According to Rech et al.

electroporation can facilitate entry of both circular and linear yeast artificial chromosomes resulting in up to 320 transformants/ μg ⁶⁸. By adding PEG into a buffer, the electroporation procedure was successfully applied for integrative transformation⁶⁹. The electrotransformation was further enhanced (up to 3.0×10^5 transformants/ μg) by treating cells in a buffer containing 1 M sorbitol and plating them onto media supplemented with 1 M sorbitol⁷⁰. Incubation of intact yeast under hyperosmotic conditions improved electrotransformation efficiency⁷¹ without change in survival. It was suggested that rise in transformation efficiency is related to alteration of membrane ultrastructure during shrinkage under hypertonic conditions⁷¹. Electrotransformation in hypotonic medium was more efficient, but higher percentage of cells died after such treatment⁷². In order to limit leakage of intracellular material and to prevent cell death electroporation of yeast is usually performed in a hypertonic solution of 1.0 M sorbitol^{70,72}. Another group showed that it is even possible to transform cells straight from the colony⁷³. Additional pre-treatment of yeast cells by DTT can enhance efficiency by up to 5-fold, suggesting that during transformation cell wall act as a major barrier for molecules like DNA⁷⁴. It was also shown that electrotransformation can be performed with both exponential⁷⁵ and squarewave⁷⁶ formats. When compared to other techniques used for transformation, electroporation provides simple, efficient and short protocols⁷⁷.

Similar permeabilization guidelines and tendencies in yeast are valid for a wide range of molecules. According to the literature, the cell wall is fully permeable to the molecules that are smaller than 760 Da; thus, the main barrier for charged species should be plasma membrane¹⁸. Validation of electroporation in yeast is usually performed with propidium iodide which after entering the cell starts to shine⁴⁵. Multiple studies used small fluorophores to validate that permeability of yeast cells increases with a rise in electric field strength and pulse duration^{26,44}. A weaker electric field can be compensated by longer pulses and vice versa⁴⁴. Pulses with longer duration led to higher permeability both before and after recovery. The fast recovery under hypoosmotic conditions was observed during the first 20-25 minutes after permeabilization²⁶. The study showed that labelling of yeast cells with macromolecules depends on the growth phase as efficiency in stationary phase decreases by up to 40 % when compared to early log²⁶. Studies with permeability to bigger molecules showed that even after exposure to PEF entry of fluorescent dextran (M = 71200 Da) into yeast cells was mainly limited by the cell wall. Majority of dextran molecules were washed off or removed enzymatically together with a cell wall after treatment²⁶, thus

indicating that investigation of permeability is quite complicated. The interaction between the plasma membrane and cell wall as well as dynamics of permeability are still open questions for further analysis.

Extraction of intracellular compounds

Introduction as well as extraction of compounds face same barriers of cell envelope. In order to surpass them, various techniques can be used including enzymatic, mechanical and chemical treatments. It has been reported that compounds like adenosine triphosphate⁶⁶, trehalose⁷⁸ and intracellular proteins of different molar mass can be recovered by PEF treatment^{44,79}. The electroextraction of proteins from yeast suspensions was observed after treatment with electric field strengths as low as 3.2 kV/cm⁴⁴. It was observed that the release of intracellular proteins increased with a rise in E^{44} . Exposure to lethal electroporation conditions results in a long-term leakage of intracellular proteins²⁶. Process of glyceraldehyde-3-phosphate dehydrogenase ($M = 145$ kDa) 3-phosphoglycerate kinase ($M = 45$ kDa), hexokinase ($M = 100$ kDa) leakage reach saturation within 4 hours⁴⁴. Higher yields of active enzymes extracted from yeast cells treated by irreversible electroporation than from enzymatically or mechanically disintegrated ones. Such efficiency was lower in treatments with higher E suggesting thermal denaturation⁴⁴. Electric parameters such as voltage, treatment time, applied energy as well as wave form modulates selectivity and efficiency of product release⁸⁰. Due to the smaller size of internal structures, it was possible to induce irreversible permeabilization of plasma membranes of all treated cells while preserving intactness of organelles and preventing leakage of proteolytic enzymes⁴⁴. Investigation of membranes throughout the cell showed that permeabilization primarily occurs in plasma membrane^{79,81}. These effects result in a selective release of intracellular compounds without losing their activity.

It was shown that by increasing electric field strength release of cytoplasmic proteins from cells in stationary phase can be improved and become comparable to the release from cells in exponential phase²⁶, suggesting that difference in efficiency is related to the cell wall structure. The impact of cell wall on extraction efficiency was confirmed by addition of DTT which reduces the integrity of yeast cell wall²⁶. Release of big proteins like β -galactosidase can also be facilitated by increasing glycerol concentration in media, but the addition of DTT has a major impact⁴⁴. PEF assisted extraction of intracellular proteins was further enhanced by the addition of various cell wall digesting enzymes. After optimizing the procedure was possible to

extract functionally active protein complexes with a size of up to 480 kDa⁴⁵. Such pre-treatment is not universal and is effective only for specific strains⁴⁵. Combination of PEF treatment with lytic enzymes can be used to achieve selectivity and efficiency even for very large intracellular proteins while maintaining their significant activity⁸².

Studies performed with scanning electron microscopy on PEF induced damage to cell wall failed to detect any significant changes even after exposure to multiple pulses with a strength of 14 kV/cm⁷⁹. After exposure to extreme electric fields, damage to both cell wall and membrane can be observed via scanning electron microscopy⁸¹. Since an increase in protein release is observed after pre-treatment under relatively mild conditions it is assumed that the primary selectivity determining parameter is the scope of membrane destruction⁸³.

Wide range of media conditions, variety of microorganisms and potential treatment parameters form a complicated picture for potential application of pulsed electric fields in biotechnology. Fundamental research is needed to bring clarity to the optimal design of instruments and tailoring energy efficient procedures for applications both in biotechnology and the food industry.

1.2. Importance of further research

According to the literature discussed in chapter 1.1, pulsed electric field treatment diminishes barrier functions of cell wall as well as of membrane. Protoplasts show higher permeability than intact yeasts suggesting that cell wall acts as the main barrier (at least for compounds with high molecular weight). There is no definite answer to how the permeability of cell wall and the membrane are related and why permeability of a cell wall increases after PEF treatment. There are several plausible, yet unconfirmed scenarios which can explain the observed results. The electric field could distort cell wall structure directly by electromechanically pulling charged components apart. Another option is that during exposure to an electric field, membrane integrity is distorted via oxidation of its components. Subsequently, anchoring structures and proteins (foundation of a cell wall) will be damaged, thus resulting in its higher permeability. Intracellular compounds released after permeabilization of a membrane could also contribute to cell wall permeability by interact with it (neutralizing surface charge and/or reducing disulphide bridges). While influx of extracellular media leads to subsequent swelling of a cell, mechanical thinning of a cell wall and increase of spacing between membrane and cell wall components. All these options take some part in permeabilization of cell walls.

Identification of key players ruling permeabilization process would facilitate combining PEF technology with other chemical/physical treatments for the optimization of biotechnological procedures like biocatalysis, electroextraction and introduction of big molecules. Understanding of resealing dynamics could provide insights for more efficient pulse delivery. My primary focus is to find how the permeability of a membrane and cell wall are related.

Technological advances in electronics allow great control of pulse shape formation. Yet, only a few instruments (suited for fundamental and/or technological research) provide adequate monitoring of the delivered pulse. Lack of control and objective evaluation during pulse delivery could lead to misinterpretation of data, production of unrepeatable results, waste of energy as well as of other resources. It is known that conductivity affects the shape of current pulse (at least its amplitude). Experimental data on conductivity effects on cells during electric field treatment is ambiguous (different groups of researchers came up with conflicting conclusions). Even though conductivity of cell suspension can change (due to leakage of intracellular ions after exposure to every subsequent pulse), most electroporation protocols used in applications include exposure to multiple pulses. Such conductivity changes, in turn, affect the shapes of delivered pulses. Evidence confirming that thorough monitoring during treatment procedure provides important information would bring more awareness to collecting, interpretation and application of pulse delivery data (voltage and current pulses). Ability to distinguish subtleties in effects induced via pulse shapes or conductivity would bring clarity and accuracy to fundamental research. My goal is to analyse pulse shape (with and without controlled back-front) effects on viability and permeability of yeast cells.

1.3. Tasks of the research work

1. To investigate pulse shape effects on the electric field induced cellular responses.
2. To investigate the link between cell wall porosity and plasma membrane permeability after PEF treatment.

1.4. Main results

Investigation of pulse shape effects was started by evaluating pulse shape itself. The influence of the crowbar circuit (module required for controlling the shape of falling voltage pulse) was experimentally investigated using loads with different resistances. The experiments were done using 1 M sorbitol, a

yeast suspension, and a solution of NaCl. The resistances of these substances were the following: 2000 Ω , 220 Ω , and 65 Ω , respectively.

When the circuit without the crowbar was used, the pulse fall time depended on the load impedance, which is disadvantageous in electroporation cause the voltage did not reach zero within 3-10 s. This is a very significant problem with different biological samples (with different conductivities), especially when short pulses are applied. The long fall time means that even during the decay of the pulse, the sample can be uncontrollably affected by the PEF. After connecting the crowbar circuit, the fall part of the pulse was shortened and was the same for all the investigated loads. Therefore, our proposed circuit with the crowbar is suitable for the treatment of biological cells with electric pulses of an identical duration, independent of the buffer type (and its conductivity).

During the next experiments, it was tested whether exposure to the electric field pulses generated by the pulse generator with and without the crowbar circuit could induce different electroporation results. For this purpose, experiments with a yeast cell suspension were performed. The suspension was exposed to a single 5 μ s pulse with an amplitude up to 2600 V (electric field strength was 26 kV/cm). Permeabilization of the membranes was evaluated by exposing the yeast cells to fluorescent SYTOX Green nucleic acid stain. During the investigation, the yeast suspension was kept on ice. Fluorescent dye was added into the suspension 10 s after exposure to the PEF. The final concentration of the dye in the suspension was 125 nM. After incubation for one minute, the specimen was placed into a quartz cuvette with a 1 cm light path and exposed to 480 nm wavelength light. The permeability of the cell membranes was evaluated by measuring the fluorescence intensity at a peak wavelength equal to 525 nm. It was found that both pulses (the electric field strength was 26 kV/cm) generated with and without the crowbar circuit induced electroporation. It was found that the fluorescence intensity (FI) increased from FI = 2.7 ± 0.2 a.u. (untreated sample) up to FI = 5.4 ± 0.4 a.u. and FI = 5.3 ± 0.3 a.u. in samples exposed to pulses generated without and with the crowbar circuit, respectively. Thus, the differences between the induced membrane permeability in both cases was insignificant. It should be noted that the fluorescence was measured when the dye was added into the suspension just 10 s after exposure to PEF; therefore, no influence of the pulse shape (decay time) on the cell damage or other processes was noticed during such short period.

Investigation of permeability was followed by evaluation of the viability. Long-term electroporation effects were measured by counting the number of

colony-forming units (CFUs). The CFUs were expressed as a percentage, where 100 % corresponded to the viability of the yeast cells in an untreated cell suspension. The viability of the yeast cells exposed to the pulses generated without the crowbar circuit was reduced to $CFU = 84.1 \pm 4.5 \%$, thus confirming that the electroporation was at least partially irreversible. The viability of the yeast cells exposed to the pulses generated with a crowbar circuit was higher ($CFU = 96.1 \pm 3.3 \%$) and was comparable to untreated cells. This result is very important for performing electroporation and retaining high viability of the treated cells.

Our previous study showed that the detectable electroporation in yeast cells starts after exposure to $5 \mu s$ pulses with an electric field strength of approximately 5 kV/cm^{84} . Such an electric field corresponds to a 500 V amplitude and such an electric field strength or higher remained for 8.4 s and 5.5 s when generated by systems without and with the crowbar circuit, respectively. The difference in the pulse duration (at the level of the threshold electric field strength) was 3.1 s, while the energy delivered by such pulses differed by 14%. Such a difference in the viability obtained in our experiments was most probably caused by the longer time of exposure during which the voltage exceeded the electroporation threshold.

This research was followed by the extensive investigation of PEF effects on yeast barrier functions. Cell wall permeability was evaluated by employing TPP^+ to which yeast cell walls are weakly permeable under normal conditions. The ability of the yeast cells to accumulate the TPP^+ ions was investigated by measuring the kinetics of the TPP^+ absorption by the cells not treated with the electric field. First stage which lasted $\approx 10 \text{ s}$ appeared immediately after the injection of the yeast cells into the TPP^+ solution; second stage lasted approximately 3-5 minutes after the fast stage, when the concentration remaining TPP^+ in solution didn't change by more than 10 %. In third stage, slow TPP^+ absorption took off and the saturation was reached after ≈ 2 hours.

After exposure to PEF, second stage (delay of the TPP^+ uptake) was absent. In both PEF-treated and untreated cells, the fast stage was similar, but of a slightly different amplitude. It was thus obvious that the PEF treatment significantly improves the TPP^+ absorption rate since saturation is reached much faster.

For a comparison of the PEF action on intact yeast cells containing wall and wall-free spheroplasts, the TPP^+ absorption measurements were performed at different electric field strengths. Amount of accumulated TPP^+ after incubation for 3 min. The influx of TPP^+ in the case of the intact yeast increased with a rise in the PEF strength. However, there were no changes of

the TPP⁺ influx in the case of wall-free spheroplasts. It is thus evident that PEF can affect the TPP⁺ influx only in the yeast cells having walls and that the cell walls are mainly responsible for the changes of the TPP⁺ uptake rates of the yeast cells.

In order to investigate the recovery of barrier functions, permeability of both membrane and cell wall was evaluated at different points of time after exposure to electric field pulse. After exposure to electric field pulse $E = 5.85 \text{ kV/cm}$ permeability increased. The decrease in permeability after PEF action stabilized within approximately 100 seconds. After such treatment permeability of membranes didn't recover completely indicating some permanent damage.

The recovery of the barrier function of the cells walls was investigated by analysing the TPP⁺ absorption process of the yeast cells after exposure to PEF. TPP⁺ was added at different time intervals after PEF treatment. Independently from the electric field strength (2.93 kV/cm to 5.85 kV/cm), the relative TPP⁺ amount absorbed by yeast cells stabilised (dropped to the same permeability as of untreated cells) in approximately 90-110 seconds. Such data indicated that PEF treatment do not induce permanent damage to the cell wall.

Further discussion and figures can be found in articles: Stankevich, V. et al. *Symmetry* (2020)⁸⁵ and Stirke, A. et. al. *Sci. Rep.* (2019)⁸⁶.

1.5. Novelty and relevance

We showed that permeability of yeast cell wall and membrane after exposure to pulsed electric field are tightly related. Integrity of both structures recovered within 100 seconds. Via modelling, we showed that the life-time of pores in cell wall and membrane is around 24 seconds. Such strong similarities between recovery characteristics of structures imply that both membrane and cell wall are affected in a similar fashion. This could be the case if after exposure to PEF, cell experiences swelling and subsequent thinning of barrier imposing structures. These insights provide a new perspective about permeability of cell wall, cellular responses and efficient PEF treatment procedures.

We also showed that control over pulse shape is extremely important for conducting fundamental research. Without necessary control, the back-front of a pulse depends on conductivity, which in turn can change effective pulse duration. In our study we showed that control of a voltage after electric field pulse generation leads to higher viability of yeast cells while maintaining permeability. Pulse shape can be affected by changes in media composition

during treatment which in turn can lead to lower yields, unrepeatable results or misinterpretation. Conductivity can affect changes in the shape of both current and voltage pulses. False conclusions from such results hinder analysis of fundamental research and scale-up studies required for transfer of technology to industrial scale.

2. Signal modulation of yeast-modified electrodes via pulsed electric field treatment

2.1. Literature overview

One of the main PEF targets in cells is the plasma membrane which can be significantly and controllably permeabilized (electroporated)³⁸ to achieve desired applications. The cellular state after exposure to PEF could be determined by measuring various parameters, including membrane permeability⁸⁷, oxidative state⁸⁸, lipid peroxidation⁸⁹. Measurement of increased molecular transport across the membrane is the most common way to confirm electroporation⁹⁰. The extent of permeabilization can be evaluated by measuring the leakage of intracellular compounds⁹¹ as well as signals generated by exogenous compounds after entering the cell⁹². In order to successfully detect permeabilization, exogenous compounds should not enter intact cells and should be easily detectable. On the other hand, some physical methods like measurement of conductivity⁵³, impedance⁹³ or cell swelling⁹⁴ can assist the investigation and detect electroporation without exogenous probes. There is a high number of substances and methods applicable for the detection of electroporation, yet each comes with a set of disadvantages and often indicates only a single very specific characteristic or aspect of a system reliably (Fig 1).

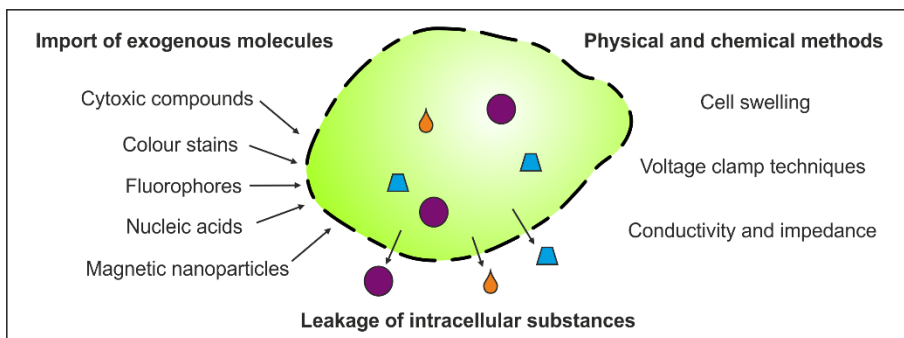


Fig 1. Graphic outline of common methods used for plasma membrane electroporation detection.

Import of non-permeant exogenous substances

The primary function of a plasma membrane is to act as a barrier between the intracellular and extracellular spaces. Under natural circumstances, only small non-polar and uncharged polar molecules can diffuse across a lipid bilayer. In order to absorb large uncharged or charged molecular as well as

ions, cells use various transport proteins⁹⁵. Some molecules can be internalized by endocytosis, whereby portion of extracellular medium including target molecules is enclosed in endocytic vesicles and further processed by various mechanisms⁹⁶. Most exogenous molecules lack transport mechanism and can (at least in theory) be used for the detection of electroporation. Some of these molecules exhibit properties which can be identified through specific detection methods and thus give information about their location. Many molecules can be detected by microscopic and spectroscopic methods, some dyes become visible indicators upon entry of other ions or molecules, while magnetic resonance imaging allow detection of magnetic nanoparticles. Functional molecules can also be used for the detection of electroporation. In such cases, the extent of electroporation will be measured indirectly by evaluating cell death (introduction of e.g. bleomycin) or gene expression (introduction of e.g. DNA).

After permeabilization, transport of charged molecules through the membrane goes along the electrochemical concentration gradient⁹⁷. Ideally detected signal will be proportional to the amount of molecules which pass through and thus correspond to the extent of electroporation^{98,99}. In reality the transport will be affected by changes in the electric field, pores in membranes, solute composition and interaction between transported molecules as well as pore walls¹⁰⁰. Due to the complexity of the task, multiple models were proposed to solve this issue¹⁰¹. By combining different approaches, it is possible to evaluate thresholds of reversible and irreversible electroporation, observe dynamics of permeabilization, estimate pore size, differences between cell types and physiological states.

Leakage of intracellular compounds

Higher permeability of a plasma membrane results not only in increased absorption of exogenous compounds, but also the leakage of cellular components like ions, peptides and ATP leak out of the cell¹⁰². Efflux of compounds like proteins, nucleic acids, pigments, lipids as well as sugars can be used for quantitative evaluation of electroporation and is often used in biotechnology¹⁰³. Protein release patterns were thoroughly analysed in various microorganisms suitable for biotechnology including bacteria¹⁰⁴, yeast¹⁰⁵ and microalgae¹⁰⁶. Some proteins like hexokinase, 3-phosphoglycerate kinase, alcohol dehydrogenase or glutathione reductase could be detected spectrophotometrically^{44,105,107}. Other techniques applicable for such investigation include fluorescence detection^{108,109}, polyacrylamide gel electrophoresis and western blotting^{106,108,110}. The efflux of nucleic acids

(RNA and plasmid DNA) can be detected by gel electrophoresis and anion exchange chromatography. During electroporation, other compounds such as phenolics¹¹¹, carbohydrates, pigments¹¹² and oils¹¹³ are released from microalgae and can be detected via different methods. The drawbacks of these methods are that effluxed compounds will differ between cell types, they are time-consuming, not very sensitive and often additional methods will be required for confirmation of collected data.

Physical and chemical methods

Exposure to the pulsed electric field also cause direct changes to the system which can be detected via physical and chemical methods. Membrane permeabilization results in increased membrane conductivity which can be detected by measuring the impedance of cell suspension¹¹⁴. This technique allows simultaneous evaluation of conductivity and resistivity. After permeabilization, membrane conductivity increases and allows low frequency current to flow through the electroporated cell. At high frequencies, current already flows freely across the membranes of intact cells, thus only frequencies below 10 kHz are used for the detection of electroporation¹¹⁵. The downside of impedance measurements is that the output signal is affected by leakage of intracellular contents, Joule heating in highly conductive mediums and by cell swelling which results in a decrease in conductivity⁵³. These processes mask the membrane conductivity increase due to electroporation and can lead to erroneous results.

Another technique primarily used to investigate PEF effects on a single cell is the voltage clamp. By simultaneously clamping constant voltage across the cell membrane and measuring transmembrane current in membrane patches it enables direct measurements of membrane currents¹¹⁶. Application of voltage steps can be used to investigate breakdown threshold of electroporation¹¹⁷. This technique offers informative μs resolution alongside quick procedure¹¹⁸. Since standard measurement range of covers voltages only from -60 mV to +40 mV, additional electrodes for delivering strong pulses are needed¹¹⁸. With this technique, it is possible to distinguish pulse-induced electroporation from ionic channel currents, evaluate transmembrane potential thresholds of electroporation as well as resealing dynamics^{116,117}. Distribution of pores is highly dependent on the spatial position in an electric field; thus, recording of currents over the entire cell is needed to have a clear picture.

One of the electric field induced physicochemical effects is cell swelling. It occurs due to the osmotic imbalance between intracellular and extracellular space. After permeabilization in hypoosmotic conditions, leakage of ions and

small molecules occurs, followed by water influx which is the leading cause of cell swelling^{119,120}. If the cell survives swelling, it can regulate its size back by the extrusion of osmolytes within 10 minutes¹²¹. The method requires the use of light microscopy. Swelling proved to be a reliable method of determining electroporation in mammalian cells^{119,120,122}. The effects are most prominent in hypotonic buffer¹²³, while the addition of different sugars and PEGs allow estimation of pore size¹²⁰.

Even though PEF is widely investigated, electroporation effects on the output signals of cellular state evaluating methods are poorly understood. Ambiguities appear as the most of methods are primarily used for analysing intact cells. Moreover, the development of new methods for electroporation detection is very important for understanding the mechanism of electroporation and for investigating the cellular state after exposure to PEF.

Electrochemical investigation of cellular redox state

Electrochemical methods provide the ability to monitor redox processes inside the intact cells, thus reflecting their intracellular state^{124,125}. Mediated amperometry can be used for counting cells and evaluation of metabolic activity¹²⁶. The modified physiological state of living cells affects redox activity thus altering electron transport¹²⁷ while non-living cells are electrochemically inactive¹²⁸. Evaluation of cellular redox state can be employed to evaluate oxidative and nutrient stresses, effects of cytotoxic or mutagenic preparations^{126,129,130}. Electron transfer from redox centres of cell enzymes to electrode surface is usually achieved via organic lipophilic electroactive substances like quinone derivatives. Combining organic and inorganic mediators significantly increases electrochemical response¹³¹ and is applicable for a wide range of cells (Fig 2.). After entering a cell, mediators collect electrons from intracellular reducing agents. The most active components of electron exchange reactions are FAD containing dehydrogenases and respiratory chain components^{126,131}. The respiratory chain include multiple NADH/NADPH dehydrogenases which transfer electron to ubiquinone pool^{132,133}. Such experiments are often conducted by transferring whole cells^{134,135} or their parts¹³⁶ onto the surface of an electrode.

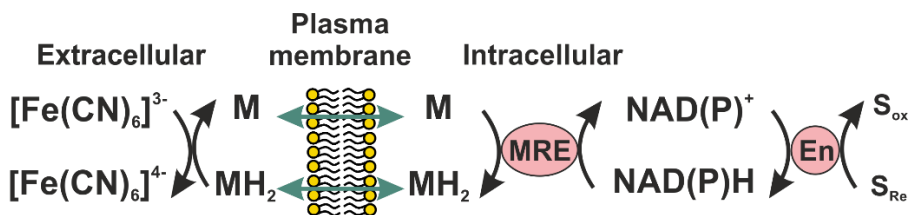
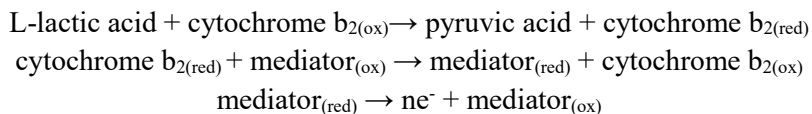


Fig 2. Schematic view of the functional mechanism of the electron transfer mediator-assisted assessment of redox activity in living cells. The lipophilic mediator, menadione (M), can diffuse through the plasma membrane into the intracellular environment, where it can undergo reduction catalysed by menadiol reducing enzymes (MRE) in different subcellular compartments. Intracellular repository of NADH and NADPH are replenished by various enzymes (En) through oxidation of substrates (from reduced (S_{Re}) to oxidized (S_{Ox}) form). Due to its lipophilicity, menadiol (MH_2), the reduced form of menadione, may diffuse back to the extracellular environment, where it is reoxidized by the hydrophilic mediator, ferricyanide ($[Fe(CN)_6]^{3-}$). The formed ferrocyanide ($[Fe(CN)_6]^{4-}$) remains in the extracellular environment as an indicator of the overall menadione reducing capacity of a cell. Description borrowed from Heiskannen et al¹²⁴.

Intracellular and cell membrane redox systems in *Saccharomyces cerevisiae* can be investigated via combinations of mediators and inhibitors¹³⁷. It was shown that via double mediator system it is possible to distinguish mediators which interact with plasma membrane electron transport systems, cross the plasma membrane to interact with cytoplasmic and mitochondrial redox molecules or even inhibit electron transfer from the cell¹³⁷. Structure of mediators has great importance for the strength of redox signal¹³¹. Study of metabolic pathways via amperometric measurements indicated that NADPH is a primary cofactor used for the reduction of quinone-like compounds¹³⁸. Double mediator systems could be employed to screen effects of genetic modifications on intracellular redox environment as well as to assess the impact of chemicals on intracellular cofactor availability¹³⁹.

Single mediator systems usually produce weaker currents but are reduced through more specific reactions. Menadione can be employed as a single mediator in order to monitor intracellular redox activity without cell disruption¹⁴⁰. The addition of glucose results in a rise of measurable current. The pattern of current is specific for yeast strain¹⁴⁰ as well as sugar type¹⁴¹. Hydrophilic mediator systems were used in electrochemical biosensing of

lactic acid¹⁴². The proposed scheme of electrocatalytic detection of lactic acid can be represented as follows:



A study showed that yeast cells could be used as a source of cytochrome b_2 . Meldona blue, Prussian Blue or phenazine methosulphate could be employed as a mediator for the detection of L-lactic acid up to 1 mM^{142,143}. Detected signals with the addition of L-lactic acid were much stronger than with mediator alone. Currents were dependent on mediator as well as on pre-treatment of yeast cells¹⁴⁴. Such data suggests different efficiency of electron transfer to mediators and inconsistent damage to barrier functions caused by pre-treatment.

Mediated amperometry can be applied to investigate permeabilization effects as well. Study of redox activity in intact, chemically permeabilised and lyophilised *Hansenula polymorpha* investigated various hydrophilic ($\text{K}_3[\text{Fe}(\text{CN})_6]$), lipophilic (2,6-dichlorophenolindophenol, 2,4-benzoquinone, 1,2-naphthoquinone) mediators¹⁴⁵. Currents mediated via organic compounds were stronger and significantly decreased after permeabilizing cells. Currents mediated via $[\text{Fe}(\text{CN})_6]^{3-}$ showed an inverse pattern. When cells were grown in the presence of glucose, the addition of formaldehyde (during measurement of current) significantly enhanced the response. Addition of formaldehyde and NAD^+ did not affect the response of permeabilized cells while currents significantly increased in intact cells. The addition of NADH induced a significant surge of the current. It was concluded that permeabilization lead to loss of cofactors and lower activity of dehydrogenases producing NADH. On the other hand, the activity of NADH-ubiquinone oxidoreductase and some components of the electron transport chain was still present¹⁴⁵.

2.2. Importance of further research

Mediated amperometry was never employed to investigate electroporation or even cellular state after exposure to the pulsed electric field. Electrochemical measurements of the cellular state provide a wide range of approaches to investigate redox centres as well as membrane permeability. Single experiment provides complex information involving availability of redox centres, cofactors, changes of cellular state after various pre-treatments. Prospective combination of mediated amperometry with electroporation is important for both fields of research.

Controlled permeabilization of the plasma membrane is supposed to provide a quick gateway to intracellular redox centres. After such pre-treatment hydrophilic mediators could be employed as a standalone probe. After such pre-treatment, the majority of enzymes remain inside the cell and could be investigated in more natural conditions than purified ones. It may even be possible that PEF pre-treatment will open new biosensing capabilities.

Mediated amperometry is a widely applied method to investigate cellular state and abiotic stress. This means that a lot of experience can be quickly transferred between fields of research. Knowledge about different abiotic stresses could be compared for a better understanding and analysis. Beside relatively quick and cheap procedures, mediated amperometry shows perspective to be applicable under flow regime with a wide range of cells. Investigation of cellular redox state could bring clarity into PEF induced effects like stimulation, relation of reversible and irreversible permeabilization (of intracellular structures and/or plasma membrane) to enzymatic activity and homeostasis. Single and double mediator systems combined with various inhibitors could provide a clearer picture about cellular response and death after permeabilization. My main goal was to investigate the applicability of amperometry for the detection of yeast permeabilization and evaluation of cellular redox state.

2.3. Task of the research work

1. To investigate PEF effects on amperometric signals of single mediator systems.

2.4. Main results

The investigation was started by evaluating the viability and permeability of yeast cells with standard methods. Viability was assessed by counting colony-forming units. After exposure to PEF the viability started to decrease considerably when electric field strengths (E) were higher than 4 kV/cm. After exposing yeast cells to a pulse with E stronger than 10 kV/cm, viability decreased to ~2 %.

Permeability was evaluated with membrane-impermeable Sytox green dye intercalating into nucleic acids. Some cells were permeable to the Sytox green fluorescent dye even before exposure to PEF, possibly due to the non-uniform age of cells or nonspecific damage during preparation of cell suspension. The rise in membranes' permeability after the exposure to PEF showed an inverse pattern to the change in the viability. Weak electric field pulses ($E < 4$ kV/cm) did not change either of the measured parameters. Even if the membrane was

permeabilized, it effectively resealed without further damage to cells. Most considerable changes were observed when cells were exposed to a pulse with electric field strength between 4 kV/cm and 10 kV/cm. Stronger electric fields permeabilized yeast cells irreversibly, causing a decrease in the viability, potentially due to the leakage of intracellular compounds.

Next experiment was to evaluate electroporation effects on currents generated by hydrophilic mediator ferricyanide. The results showed marked differences in the responses of electrodes covered with untreated and electroporated yeast cells. Current generated by PEF treated cells in a solution with ferricyanide were stronger ($I = 103 \pm 10$ nA) than ones generated by untreated yeasts ($I = 9 \pm 4$ nA).

To test how permeabilization affects signal mediated by the lipophilic mediator, we employed menadione. When electrodes were covered with untreated cells ($E = 0$ kV/cm), current of 138 ± 15 nA was detected. After exposure to weak electric fields ($E = 4$ kV/cm), current slightly decreased down to 117 ± 14 nA. The further rise in electric field strength ($E = 10$ kV/cm) resulted in even weaker current of 32 ± 15 nA. Exposure to the strongest electric field (16 kV/cm) resulted in a further decrease in current down to 23 ± 12 nA.

I performed the further investigation by adding NAD(P)H into the electrolyte during current measurement and showed that the decrease in menadione current of PEF treated cells could be complemented entirely by adjusting the extracellular concentration of NADH to 1 mM. The addition of NADPH resulted in stronger current as well, but not as high as after the addition of NADH. Supplementing untreated cells with NAD(P)H raised current strength by up to 10 %. Such findings suggest that the decrease of menadione current is indeed observed due to the leakage of intracellular reducing species through permeable membranes. We, therefore, conclude that the formation of hydrophilic pores should not significantly affect the entry of a lipophilic mediator and cause a decrease in current strength by itself.

Further discussion and figures can be found in the following article: Simonis, P. et al. *Sci. Rep.* (2020)¹⁴⁶.

2.5. Novelty and relevance

To our best knowledge we showed for the very first time that yeast-modified electrodes can be used to investigate electroporation of the same cells. Responses to lactic acid were dependent on exposure to PEF and increased with the rise in electric field strength.

Exposure to PEF resulted in lower redox activity which could be compensated entirely by adjusting the extracellular concentration of NADH to 1 mM. Decrease in menadione current after exposure to PEF questions validity of viability kits employing quinone-like mediators. If such mediators are applied to analyse abiotic treatments affecting membrane permeability, they can give ambiguous results.

Our study shows the applicability of PEF technology for modulation of amperometric signals. Yeast-modified electrodes could be used for real-time study of cellular responses to PEF treatment. PEF pre-treatment opens the gateways to intracellular metabolism without cell lysis and allows investigation of both permeability and cellular death mechanisms. We conclude that permeabilization in combination with different growth conditions, inhibitors, mediators, substrates, cofactors will pave the way for the investigation of biochemical pathways through multistep processes.

3. The effects and applications of nanosecond pulsed electric fields

3.1. Literature overview

Theoretical predictions and experiments suggest that pulses with nanosecond duration (1-100 ns) have more profound effect on the cell interior than longer pulses¹⁴⁷. Such insights proposed nanosecond pulses as a promising tool for intracellular manipulation without chemical intervention. Nanosecond electric field pulses (nsPEFs) can affect cell organelles¹⁴⁷⁻¹⁴⁹, increase intracellular calcium¹⁵⁰⁻¹⁵², provoke apoptosis¹⁵³⁻¹⁵⁵, stress responses¹⁵⁶. The plasma membrane is permeabilized as well, but at a lesser extent¹⁵⁷⁻¹⁵⁹. According to the theory of electroporation pulses with duration (1-100 ns) shorter than the charging time of the plasma membrane and thus greater intracellular effects are expected¹⁴⁷. A systematic review of 203 reports concluded that longer pulses are more likely to cause effects related to plasma membrane while shorter pulses induce creation of smaller pores¹⁶⁰. It was also noted that intracellular effects were most likely to be induced by exposing cells to pulses with durations from 10 to 100 ns¹⁶⁰.

To date, there are only a couple of articles which investigated effects induced in yeast cells after exposure to nanosecond high power electrical pulses. One study employed tetraphenylphosphonium (TPP⁺) ions to investigate nsPEF induced effects on walls of *Saccharomyces cerevisiae* cells. It was shown that exposure to pulses with a duration of 60 ns ($E = 190$ kV/cm) increased absorption rate of TPP⁺ ions up to 65 times¹⁶¹. Permeability of yeast cells increased with the rise in electric field strength (up to 190 kV/cm) and pulse duration (10-60 ns). Curiously enough viability of cells was different when evaluated via proliferation kit (~85 %) or colony-forming units (~30 %)¹⁶¹. This phenomenon indicates that membrane permeability alone is not a definite indicator and cause of cell death when pulses with nanosecond durations are used.

Permeability of plasma membrane is often considered as an indicator of necrosis or late apoptosis. This is not the case when cells are exposed to electric fields and membrane permeability can be reversible. Such contradiction in combination with nsPEF-mediated externalization of phosphatidylserine requires new definition and indicators for classification of cellular death. Cell death is an integral part of life in all kinds of organisms. Viral infections, chronological and replicative aging in yeast cells is often followed by physiological death¹⁶². Even though yeast *Saccharomyces cerevisiae* is single-celled microorganism, it expresses apoptotic markers common to multicellular organisms^{163,164}. Yeast cell death is often followed

by DNA fragmentation, externalization of phosphatidylserine, loss of cell integrity and accumulation of reactive oxygen species (ROS)¹⁶⁴. ROS-mediated cell death is primarily executed via activation of yeast caspase YCA1¹⁶⁵ or apoptosis inducing factor¹⁶⁶. Such observations led to the distinction of yeast cell death into caspase-dependent and caspase-independent apoptosis¹⁶².

Cell death occurring during long term development of yeast colonies, stress after exposure to formic acid, copper, sphingolipids, malfunction of N-glycosylation lead to caspase-independent scenarios¹⁶². Upon induction apoptosis inducing factor 1 translocate from mitochondria to the nucleus where it mediates chromatin condensation and DNA degradation leading to cell death. Caspase-dependent means that deletion of YCA1 can protect yeast cells against some forms of lethal insults¹⁶⁵. Multiple conditions like oxidative and salt stress, exposure to valproic acid, short chained fatty acids, excessive iron, manganese, cadmium concentrations lead to so-called programmed cell death (PCD). Furthermore, death-related events like defects in ubiquitination, reduced mRNA stability, mitochondrial fragmentation and aging in yeast cells occurs partly via caspase-dependent fashion¹⁶². Hyperosmotic stress could also induce metacaspase- and mitochondria-dependent apoptosis in *Saccharomyces cerevisiae*¹⁶⁷. Approximately 40% of yeast cell death is caspase dependent. Under normal conditions, yeast metacaspase regulates degradation of oxidized proteins^{168,169}. It was suggested that Ca²⁺ is needed for autocatalytic activation and subsequent proteolytic activity in PCD¹⁷⁰. For now, only one, yet very important substrate of metacaspase (glyceraldehyde 3-phosphate dehydrogenase) is found¹⁷¹. It seems that activation of yeast metacaspases serves as a threshold for a switch from casual cellular oxidative stress maintenance to lethal activity. It was previously shown that pulses with nanosecond duration can induce some sort of oxidative stress in mammalian cells¹⁷². Yet the post pulse metabolism in yeast cells and its fundamental relation to cellular death is poorly described.

Lethal effects induced via exposure of yeast cells to PEF are often studied in the food processing area since the ideal scenario of this application is complete inactivation of all cells¹⁷³⁻¹⁷⁶. In addition to ensuring food safety, PEF treatments have been proposed to prevent the development of spoiling microorganisms, thereby extending food shelf life. Advantages of PEF treatment application for the inactivation of microorganisms in the food industry include non-thermal processing with minimal change in organoleptic and nutritional properties. The disadvantage is that each product has a characteristic chemical, physical and biological composition. This means that most of the time treatment procedures must be tailored to a specific product.

On the other hand, some products already contain substances which enhance PEF induced lethality. To study reversibility and sublethal injuries, researchers often use selective mediums. Such procedures highlight optimal treatment conditions for combining PEF treatment with additional stress which prevents cell repair and subsequent survival. It was shown that PEF treated cells lose viability during subsequent storage under acidic conditions¹⁷⁷ or with citral¹⁷⁸.

With such a variety of media characteristics, it is impossible to have ideal conditions for pasteurization of all products. The focus of research often shifts onto processing of niche products (which could not be thermally pasteurized) and on isolating aspects, which could induce cellular death.

It was previously shown that yeast cells have a significant advantage over mammalian cells for studying cell death in which detection mostly relies on apoptotic markers prone to false positive results. Caspase activation and phosphatidylserine externalization are common indicators, yet caspase activation can occur without cell death and vice versa¹⁷⁹. The precise evaluation of dead versus living yeast cells can be routinely performed using plating assays. Considering the applicability of yeast cells as a model organism, complexity of cellular responses after permeabilization and prospects of direct knowledge transfer to food processing technologies, it is surprising that just a few fundamental studies have investigated PEF induced, death-related aspects of yeast cells.

3.2. Importance of further research

The majority of studies where pulsed electric field is employed to induce death of yeast cells are related to the food industry and pasteurization. This field of research primarily focuses on irreversible electroporation leading to invalidated homeostasis and subsequent cell death. Discovery of pathways related to programmed cell death in yeast cells is relatively new (when compared to electroporation phenomena) and almost no studies on PEF induced cellular death pathways in yeast cells are present. The scope of fundamental studies of yeast cells as a model for investigation of PEF cell responses is very limited as well. There is no information on whether electric field pulses with durations of up to 100 ns could surpass plasma membrane of yeast cells and have any intracellular effects.

Discovery of programmed cell death induced via exposure to nsPEFs would provide a new quick direct death induction method. Cell death for fundamental studies is often induced chemically. Such an approach is highly uncontrollable and often causes extensive damage even upon induction of cell

death. Knowledge on cell death type can also be important for application of PEF technology on food products since non-thermal inactivation can cause release of biochemically active compounds. The goal of a study is to investigate nsPEF induced effects in yeast cells and indicate the type of death (if any).

Shelf life is one of the major concerns in the food industry. Longer shelf life often means safety for a consumer and less waste. Currently, the main technology used for pasteurization of liquid products is thermal treatment. There is a wide range of compounds which lose biochemical activity, nutritional as well as organoleptic characteristics after thermal treatment. Exposure to the pulsed electric field at least to some extent is nonthermal technology. Yet it is not widely accepted and applied.

Another aspect becoming more and more important in the food industry is beneficial bacteria count which is usually lost during processing. Customers want to have access to food which could introduce microorganisms leading to healthy microbiota. The cells of unicellular fungi are often bigger than common bacteria, so according to the theory of electroporation, it should be possible to inactivate fungi while keeping bacteria alive.

For now, there is no reported case where electric field pulses with nanosecond duration have been successfully applied to process food-related products. Efficient non-thermal technology (which PEF treatment under some conditions is) could bring benefits both for food manufacturers (more natural flavour, cheaper processing) and consumers (more nutritious food). The goal of this research direction is to investigate nsPEF effects on yeast cells found in acid whey.

3.3. Tasks of the research work

1. Investigate yeast cell death after exposure to nanosecond pulsed electric field.
2. Evaluate prospects of nanosecond electric field pulse application for acid whey pre-treatment.

3.4. Main results

The viability was evaluated by counting colony-forming units (CFU). After exposure to a single electric field pulse ($\tau = 10\text{-}90$ ns, $E = 25\text{-}220$ kV/cm), the decrease in viability was detected. The smallest number of CFUs (40 ± 3 %) was observed after exposure of the yeast suspensions to a single 60 ns pulse when $E = 190$ kV/cm. To evaluate the effects of repetitive exposure to the electric field, five consecutive pulses were used. After five

50 kV/cm electric field pulses with durations of 90 ns, the viability of the yeast cells decreased by 68 %. Stronger electric fields affected their viability only slightly, reaching its lowest value (CFU = 19 %), when E = 218 kV/cm.

After confirmation that high voltage electric field pulses could reduce the number of colonies forming units in yeast suspensions, expression of markers related to programmed cell death was evaluated. The externalisation of phosphatidylserine was evaluated by enzymatically removing cell walls of PEF treated cells and staining protoplasts with Annexin-V-FITC. Externalisation of phosphatidylserine was confirmed by fluorescent microscopy. DNA fragmentation was evaluated by employing TUNEL assay, which was carried out 1.5-3 h after treatment with nsPEFs ($\tau = 10-90$ ns, E = up to 190 kV/cm). DNA fragmentation, which has previously been defined as an apoptotic marker in yeast, was not observed in our experiments (DNA fragmentation was detected in less than 2 % of the cells and this was independent of nsPEF treatment parameters). Such results could mean that in nsPEF treated cells, metacaspase activation is the primary event and that DNR fragmentation occurs only later during the process of apoptosis.

For the detection of cells with active metacaspases (YCA1+), the caspase inhibitor FITC-VAD-FMK was used. Cells with active caspase showed bright-green fluorescence and were detected by using fluorescence microscopy. To obtain more quantitative results and to establish a possible link between metacaspase activation and the effects of the electric fields on membrane permeability, the yeast cells were treated with propidium iodide, a caspase inhibitor and analysed using a flow cytometer. Size of population in which yeast cells were with active metacaspases and permeable to propidium iodide increased with rise in electric field strength. Strongest induction of 72.7 ± 2.7 % was observed in a suspension which was exposed to 5 consecutive pulses when E = 219 kV/cm. The change in the viability was dependent on the pulse parameters and shows a similar pattern as in the activation of metacaspases in cells treated with pulses with increasing electric field strength.

Applicability of pulses with nanosecond duration was tested on acid whey microorganisms. The suspension was poured into a cuvette and exposed to electric field pulses (pn = 1, 5, 10, 30, 50, 70, 100) of different duration ($\tau = 60$ ns, 90 ns, 1000 ns) and field strength (E = 95 kV/cm, 92 kV/cm). Efficacy of microbial inactivation was evaluated by log reduction (LR), defined by equation (4):

$$LR = -\log\left(\frac{N}{N_0}\right) \quad (4)$$

where N and N₀ are numbers of colony forming units in treated and untreated suspensions respectively. For simplicity purposes, PEF parameters are shown as $LR_{\text{pulselength(ns_fieldstrength_pulsenumber)}}$. When shorter pulses $\tau < 1000$ ns were applied, a minimal increase of bacterial LR values was observed ($LR_{60_95_100} = 0.08 \pm 0.01$ and $LR_{90_95_100} = 0.08 \pm 0.01$). However, the higher sensitivity of yeast cells was observed ($LR_{60_95_100} = 0.99 \pm 0.08$, $LR_{90_95_100} = 1.34 \pm 0.36$), which suggests that PEF can be used for selective pasteurization. At pulse lengths of 60 ns and 90 ns yeast cells were up to 14 times more sensitive to PEF treatment than bacterial cells. After acid whey samples were exposed to longer pulses, LR values were higher, but the difference of PEF effects on yeast ($LR_{1000_92_50} = 1.79 \pm 0.12$) and bacterial ($LR_{1000_92_50} = 1.47 \pm 0.05$) cells was smaller.

Further discussion and figures can be found in articles: Simonis, P. et al. *Bioelectrochemistry* (2017)¹⁸⁰ and Simonis, P. et al. *Int. J. Food Microbiol.* (2019)¹⁸¹.

3.5. Novelty and relevance

To my best knowledge, this study is the first to show that exposure of yeast cells to electric field pulses with nanosecond duration causes expression of features characteristic to caspase-dependent death. Exposure to PEF was followed by activation of yeast metacaspases, permeability to propidium iodide as well as externalized phosphatidylserine. Such data indicate that yeast cells could be used as a model for the analysis of the death-related pathways induced in cells after exposure to nsPEFs.

We showed that electric field pulses with varying duration induce selective inactivation of different microorganisms. Such observation indicates applicability of pulses with nanosecond duration for food processing. Such pre-treatment could keep beneficial bacterial while decreasing the viability of yeast cells. This is the first time the pulses of such magnitude were applied on a commercial food-related product.

CONCLUSIONS

1. Permeability of yeast cells to TPP⁺ is limited by cell walls and not the plasma membranes even though exposure to PEF improves overall permeability of both structures. Exposure to electric field pulse with a strength of ≈ 6 kV/cm induces irreversible damage to the plasma membrane and not the cell wall.
2. Fall time of voltage after electric field pulse formation depends on load conductivity. Active regulation of fall time can lead to a decrease in effective pulse duration by up to 35 %, which in turn can diminish the lethal effects of pulsed electric field. Such unaccounted pulse duration defects can cause up to 10 % of death in yeast cells.
3. Mediated amperometry with hydrophilic mediator ferricyanide can be employed to evaluate irreversible electroporation in yeast cells. Current strengths generated by electroporated cells ($E = 16$ kV/cm, $\tau = 300$ μ s) increased by more than one order of magnitude when compared to currents from untreated yeast cells.
4. A decrease in menadione-mediated current strength by up to 6 times in electroporated yeast cells ($E = 16$ kV/cm, $\tau = 300$ μ s) represents rise in membrane permeability and subsequent leakage of NAD(P)H which are needed for menadione reduction. The decrease in current strength can be compensated entirely by adjusting the extracellular concentration of NADH to 1 mM.
5. Exposure to 5 consecutive electric field pulses with nanosecond duration ($E \geq 220$ kV/cm, $\tau = 90$ ns) results in the expression of markers related to caspase-dependent death in ≈ 73 % of yeast cells.
6. Electric field pulses with nanosecond duration can selectively inactivate yeast cells in acid whey solution. Yeast cells were more susceptible to PEF treatment ($E = 95$ kV/cm, $\tau = 90$ ns, $p_n = 100$) by up to 14 times when compared to bacteria cells.

METHODS EMPLOYED IN THIS RESEARCH WORK

Cultivation and preparation of yeast cells

Yeast strains: BY4742 (MAT α ; his3 Δ 1; leu2 Δ 0; lys2 Δ 0; ura3 Δ 0) yeast cells (Euroscarf, Germany), BY4741 (MAT α ; his3 Δ 1; leu2 Δ 0; met15 Δ 0; ura3 Δ 0) from Euroscarf (Germany), SEY6210 (MAT α , leu2-3, leu2-112, ura3-52, his3- Δ 200, trp1- Δ 901, lys2-801, suc2- Δ 9, GAL), wild type yeast found in acid whey.

Laboratory strains were grown on solid and/or liquid media YPD (1 % yeast extract (Biocorp, Poland), 2 % peptone ex casein (Carl Roth GmbH, Germany), 2 % glucose (Merck KGaA, Germany), 1.3 % agar (Alfa Aesar, Germany) at 30 °C in the incubator for up to 48 hours. Cells were then collected, washed and resuspended in electroporation buffer (EPB) (20 mmol/L Tris (Applichem, Germany), HCl (Merck KGaA, Germany), pH 7.4), which in some cases was supplemented with 1 mol/L sorbitol (Applichem GmbH, Germany). Acid whey samples were treated without any specific preparation.

The conductivity of yeast cell suspension in electroporation buffer was \approx 1.5 mS/cm (Seven2Go conductivity meter with Inlab 738-ISM sensor, Mettler Toledo, USA). Where noted, such cell suspension was lyophilized and kept at 4°C before use in experiments.

Evaluation of cell viability

After exposure to the electric field, the yeast cells were plated onto a solid YPD medium and then incubated in the INCU-Line (VWR, USA) incubator at 30 °C for 48–72 h. After incubation, the number of colony forming units was evaluated.

Evaluation of membrane permeability, metacaspase activation, phosphatidylserine externalization, DNA fragmentation and other fluorescence measurements

Membrane permeability was evaluated by employing propidium iodide (Carl Roth GmbH, Germany) which was added to the yeast cell suspensions immediately or 1.5–2 h after exposure to pulsed electric field with nanosecond duration at a final concentration of 2.5 μ g/mL. Alternatively, recovery of a membrane was measured by employing Sytox Green (Thermo Fisher Scientific, USA). Dye was diluted in anhydrous dimethyl sulfoxide (Thermo Fisher Scientific, USA) to a final concentration of 0.25 mM. The solution was transferred to the cell suspension (final concentration—125 nM) and after

incubation for 60 s, fluorescence intensity was measured using luminescence spectrometer Perkin Elmer LS—50b (PerkinElmer, USA). Leakage of intracellular cofactors was measured by exciting supernatant with 340 nm and measuring fluorescence at 430 nm.

Caspase detection was evaluated using the CaspACE™ FITC-VAD-FMK in situ marker (Promega, USA) and DNR fragmentation was evaluated via FragEL™ DNA Fragmentation Detection Kit (Merck KGaA, Germany). Both procedures were performed according to the producer protocols.

Phosphatidylserine externalisation was analysed by employing Annexin V-FITC (Biovision, USA). Before staining yeast, cells were washed twice with a sorbitol buffer (1.2 M sorbitol, 0.5 mM MgCl₂ (Merck KGaA, Germany), 35 mM KPO₄ (Merck KgaA, Germany), pH = 6.8) and the cells walls were digested with 30 U/mL Lyticase (Sigma-Aldrich, USA) in a sorbitol buffer. After a 2 h incubation at 30 °C, the cells were then collected and washed with a binding buffer (10 mM Hepes, Sigma-Aldrich, USA; NaOH, Sigma-Aldrich, USA; 140 mM NaCl, Sigma-Aldrich, USA; 2.5 mM CaCl₂, Applichem GmbH, Germany; pH = 7.4) with 1.2 M sorbitol and suspended in it. 1 µL Annexin V-FITC was then added to 40 µL of cell suspension and incubated for 20 min. The cells were then washed 3 times and suspended in a binding buffer. For the preparation of the microscopy slides, 0.1% (w/v) poly-L-lizine (Sigma-Aldrich, USA) was used. The fluorescence of at least 200 fixed cells was evaluated on each slide.

In the flow cytometry experiments, at least 20,000 cell events were acquired for each sample with an Amnis Flow Sight Imaging Flow Cytometer (Merck Millipore, Germany) and IDEAS v6.1 software was used for data analysis. The acquired images included a brightfield image, a forward scatter (FSC) (Channel1 457/45 nm), a side scatter (SSC) (Channel6 772/35 nm), FITC (Channel2 532/55 nm) and PI (Channel4 610/30 nm). The FITC, PI and SSC were then excited by 488 nm, 561 nm and 785 nm lasers, respectively. The gating strategy, as detailed in the results and discussion section, was used to assess the event count and the signal intensity of the cells of interest. Non-stained and appropriate single and double stained controls for compensation and gate setting were used. The yeast cells in the EPB supplemented with acetic acid, pH = 2.5 (Merck KgaA, Germany) were used as a positive control for the detection and evaluation of the apoptotic markers.

Cell wall permeability measurements

To investigate the permeability of the yeast cell wall, the concentration changes of TPP⁺ ions as a function of time was measured. A custom-build

mini-potentiostat with a special high sensitivity electronic circuit, protected against static electrical interference, was used for the measurements¹⁸². The electrode with the selective membrane was fabricated according to the protocol found in the literature. During all measurements of the changes of the lipophilic tetraphenylphosphonium (TPP⁺) ion concentrations, the TPP⁺ chloride (Acros Organics, Belgium) was used. For all the measurements, the intact yeast cell and spheroplasts suspension concentrations were the $4\text{-}6 \times 10^9$ colony forming unit (CFU)/mL. For the evaluation of the changes of the TPP⁺ concentration in both yeast suspensions, 200 μL of the yeast suspension was added to 2 mL of a 1 μM concentration TPP⁺ solution and the potentiometric changes were recorded. The concentration of TPP⁺ ions was calculated from the calibration curve. To evaluate the role of the cell wall and cell membrane in the TPP⁺ absorption process, square waveform electrical pulses of 150 μs duration and amplitudes of electric field strength (E) (up to 4.2 kV/cm) were applied to the intact yeast cells and spheroplasts. To investigate the resealing of the yeast cell walls after such PEF treatment, the TPP⁺ was added to the electroporation cuvette with the yeast suspension. The initial TPP⁺ concentration (N_{is}) of 1 μM was added to the cuvette at different time intervals ($\Delta t = 5, 10, 20, 30, 40, 50, 60, 80, 120$ and 180 seconds) after the PEF treatment ($E = 5.85, 4.38$ and 2.93 kV/cm, $\tau = 150$ μs). Each sample was then incubated for 3 minutes at 20 °C and centrifuged in order to get cell-free supernatant. These experiments were repeated three times and presented as means values. The quantity of TPP⁺ (N) absorbed by the yeast cells ($N = N_{is} - [\text{TPP}^+]_{\text{supernatant}}$) was expressed as the accumulation ratio N/N_m , where N_m is the maximal concentration of TPP⁺ that can be accumulated in yeast.

Electrode preparation

Plain carbon paste was prepared by mixing 100 mg of graphite powder (Fluka, Germany) with 50 μl of paraffin oil (Fluka, Germany). The paste was packed into an electrode body consisting of a plastic tube (diameter 2.9 mm) and a copper wire serving as a contact for an electrode. The layers of the yeast cells on the surfaces of plain carbon paste electrodes were formed by covering the conducting area with 10 μl of cell suspension in EPB. The electrodes were allowed to dry at room temperature for 15-20 min and were then covered with a dialysis membrane (Sigma-Aldrich, USA). Due to a relatively long electrode preparation procedure (when compared to membrane resealing time), investigation of permeability is limited to irreversible electroporation.

Electrochemical measurements

Electrochemical experiments were carried out according to previously described procedure¹⁴³ on a BAS-Epsilon Bioanalytical system (USA) and a three-electrode cell arranged with a magnetic stirrer. The platinum wire and Ag/AgCl in 3 M NaCl served as counter and reference electrodes, respectively. Amperometry was carried out in a stirred solution at an operating potential 0.3 V (vs. Ag/AgCl, 3 M NaCl). The yeast-modified carbon paste electrode served as a working electrode. All electrochemical measurements were performed at room temperature.

Hydrophilic mediator

To analyze hydrophilic mediators, yeast cells were employed as biosensors for lactic acid detection¹⁴³. Amperometry for lactic acid-sensing was performed in phosphate buffer: 0.1 M potassium phosphate (Riedel-de Haën, Germany); 0.1 M potassium chloride (Fluka, Germany); potassium hydroxide (Sigma Aldrich, USA) at pH 7.3 and containing 0.5 mM of mediator: N-Methylphezonium methyl sulfate (PMS) (Fluka, Germany), 2,6-Dichlorindophenol sodium salt hydrate (DCPIP) (Fluka, Germany), Potassium ferricyanide (PFC) (Fluka, Germany), 1,2-Naphthoquinone-4-sulfonic acid sodium salt (NQSA) (Fluka, Germany). After reaching a steady state of the background current at the operating potential (0.3 V), L-lactic acid (Riedel-de Haën, Germany) was added into the solution (final concentration 0.2 mM). Data was collected and represented as a change in current strength after the steady-state current was achieved.

Lipophilic mediator

Amperometry for menadione-mediated (Sigma-Aldrich, USA) current detection was performed in phosphate buffer at pH 6.5. The electrode was poised at an operating potential (0.3 V) until the steady-state of the background current was obtained. After that, menadione (dissolved in absolute ethanol (VWR, France)) was added up to a final concentration of 67 μ M. Change in current was evaluated after the steady-state current was reached. Redox activity monitoring was performed by adding NADH disodium salt (VWR, USA) or NADPH tetrasodium salt (MP Biomedicals, France) to a final concentration of 1 mM.

PEF generation systems

Three different pulse generators assembled in the Center for Physical Sciences and Technology were used in the experiments. First one, to generate exponentially decaying pulses of microsecond duration¹⁸³. Second one, to generate square shaped pulses with a duration of up to 300 μs ¹⁸⁴. Third one, to generate squared shaped pulses with nanosecond duration of up to 90 ns¹⁸⁵. Cuvettes and pulsed electric field treatment parameters are described in respective articles.

AUTHOR CONTRIBUTION

The author of this thesis is an experimentalist. He was responsible for the design and execution of experiments with yeast cells, data acquisition and analysis. Complete manuscripts of 3 publications were prepared by the author, while in other 2, he was responsible for systemization of biological parts.

About the author

Povilas Šimonis was born in 1992, in Šiauliai, Lithuania. In 2010, he finished gymnasium of Julius Janonis. In 2014, he received a bachelor degree in bioengineering at Vilnius Gediminas Technical University. In 2016, he received his Biochemistry master's degree at Vilnius University.

BIBLIOGRAPHY

1. Botstein, D. & Fink, G. R. Yeast: An experimental organism for 21st century biology. *Genetics* **189**, 695–704 (2011).
2. Goffeau, A. *et al.* Life with 6000 genes. *Science* **274**, 546–567 (1996).
3. Heinicke, S. *et al.* The Princeton Protein Orthology Database (P-POD): A comparative genomics analysis tool for biologists. *PLoS One* **2**, (2007).
4. Alter, O., Brown, P. O. & Botstein, D. Singular value decomposition for genome-Wide expression data processing and modeling. *Proc. Natl. Acad. Sci. U. S. A.* **97**, 10101–10106 (2000).
5. Eisen, M. B., Spellman, P. T., Brown, P. O. & Botstein, D. Cluster analysis and display of genome-wide expression patterns. *Proc. Natl. Acad. Sci. U. S. A.* **95**, 14863–14868 (1998).
6. Costanzo, M. *et al.* The genetic landscape of a cell. *Science* **327**, 425–431 (2010).
7. Tong, A. H. Y. *et al.* Systematic genetic analysis with ordered arrays of yeast deletion mutants. *Science* **294**, 2364–2368 (2001).
8. Zakhartsev, M. & Reuss, M. Cell size and morphological properties of yeast *Saccharomyces cerevisiae* in relation to growth temperature. *FEMS Yeast Res.* **18**, (2018).
9. Knop, M. Yeast cell morphology and sexual reproduction - A short overview and some considerations. *Comptes Rendus - Biol.* **334**, 599–606 (2011).
10. Klis, F. M., Boorsma, A. & De Groot, P. W. J. Cell wall construction in *Saccharomyces cerevisiae*. *Yeast* **23**, 185–202 (2006).
11. Aguilar-Uscanga, B. & François, J. M. A study of the yeast cell wall composition and structure in response to growth conditions and mode of cultivation. *Lett. Appl. Microbiol.* **37**, 268–274 (2003).
12. Orlean, P. Architecture and biosynthesis of the *Saccharomyces cerevisiae* cell wall. *Genetics* vol. 192 775–818 (2012).
13. Yamaguchi, M. *et al.* Structure of *Saccharomyces cerevisiae* determined by freeze-substitution and serial ultrathin-sectioning electron microscopy. *Microscopy* **60**, 321–335 (2011).
14. Zlotnik, H., Pilar Fernandez, M., Bowers, B. & Cabib, E. *Saccharomyces cerevisiae* mannoproteins form an external cell wall layer that determines wall porosity. *J. Bacteriol.* **159**, 1018–1026 (1984).
15. Kitagaki, H., Wu, H., Shimoi, H. & Ito, K. Two homologous genes, DCW1 (YKL046c) and DFG5, are essential for cell growth and encode glycosylphosphatidylinositol (GPI)-anchored membrane proteins required for cell wall biogenesis in *Saccharomyces cerevisiae*. *Mol. Microbiol.* **46**, 1011–1022 (2002).
16. Caro, L. H. P. *et al.* In silico identification of glycosylphosphatidylinositol-anchored plasma-membrane and cell wall proteins of *Saccharomyces cerevisiae*. *Yeast* **13**, 1477–1489 (1997).

17. Yin, Q. Y., De Groot, P. W. J., De Jong, L., Klis, F. M. & De Koster, C. G. Mass spectrometric quantitation of covalently bound cell wall proteins in *Saccharomyces cerevisiae*. *FEMS Yeast Res.* **7**, 887–896 (2007).
18. Scherrer, R., Louden, L. & Gerhardt, P. Porosity of the yeast cell wall and membrane. *J. Bacteriol.* **118**, 534–540 (1974).
19. Ottolenghi, P. The uptake of bovine serum albumin by a strain of *Saccharomyces* and its physiopathological consequences. *C. R. Trav. Lab. Carlsberg* **36**, 95–111 (1967).
20. Lampen, J. O. Yeast and *Neurospora* Invertases. *Enzymes* **5**, 291–305 (1971).
21. Morris, G. J., Winters, L., Coulson, G. E. & Clarke, K. J. Effect of osmotic stress on the ultrastructure and viability of the yeast *Saccharomyces cerevisiae*. *J. Gen. Microbiol.* **132**, 2023–2034 (1986).
22. De Nobel, J. G. & Barnett, J. A. Passage of molecules through yeast cell walls: A brief essay-review. *Yeast* **7**, 313–323 (1991).
23. Zlotnik, H., Pilar Fernandez, M., Bowers, B. & Cabib, E. *Saccharomyces cerevisiae* mannoproteins form an external cell wall layer that determines wall porosity. *J. Bacteriol.* **159**, 1018–1026 (1984).
24. De Nobel, J. G., Klis, F. M., Priem, J., Munnik, T. & Van Den Ende, H. The glucanase-soluble mannoproteins limit cell wall porosity in *Saccharomyces cerevisiae*. *Yeast* **6**, 491–499 (1990).
25. De Nobel, J. G., Dijkers, C., Hooijberg, E. & Klis, F. M. Increased cell wall porosity in *Saccharomyces cerevisiae* after treatment with Dithiothreitol or EDTA. *J. Gen. Microbiol.* **135**, 2077–2084 (1989).
26. Ganeva, V., Galutzov, B. & Teissié, J. Electric field mediated loading of macromolecules in intact yeast cells is critically controlled at the wall level. *BBA - Biomembr.* **1240**, 229–236 (1995).
27. Ballou, C. Structure and biosynthesis of the mannan component of the yeast cell envelope. *Adv. Microb. Physiol.* **14**, 93–158 (1976).
28. Stewart, G. G. The Structure and Function of the Yeast Cell Wall, Plasma Membrane and Periplasm. in *Brewing and Distilling Yeasts* 55–75 (Springer International Publishing, 2017). doi:10.1007/978-3-319-69126-8_5.
29. Cerbón, J. & Calderón, V. Generation, modulation and maintenance of the plasma membrane asymmetric phospholipid composition in yeast cells during growth: their relation to surface potential and membrane protein activity. *Biochim. Biophys. Acta* **1235**, 100–6 (1995).
30. Carman, G. M. & Han, G.-S. Regulation of phospholipid synthesis in yeast. (2009) doi:10.1194/jlr.R800043-JLR200.
31. Griač, P. & Henry, S. A. The yeast inositol-sensitive upstream activating sequence, UAS(INO), responds to nitrogen availability. *Nucleic Acids Res.* **27**, 2043–2050 (1999).
32. Homann, M. J., Poole, M. A., Gaynor, P. M. & Carman, G. M. Effect

- of growth phase on phospholipid biosynthesis in *Saccharomyces cerevisiae*. *J. Bacteriol.* **169**, 533–539 (1987).
33. Peña, A., Sánchez, N. S. & Calahorra, M. The Plasma Membrane Electric Potential in Yeast: Probes, Results, Problems, and Solutions: A New Application of an Old Dye? in *Old Yeasts - New Questions* (InTech, 2017). doi:10.5772/intechopen.70403.
 34. Peña, A., Cinco, G., Gómez-Puyou, A. & Tuena, M. Effect of the pH of the incubation medium on glycolysis and respiration in *Saccharomyces cerevisiae*. *Arch. Biochem. Biophys.* **153**, 413–425 (1972).
 35. Pena, A. Studies on the mechanism of K⁺ transport in yeast. *Arch. Biochem. Biophys.* **167**, 397–409 (1975).
 36. Kotnik, T., Pucihar, G. & Miklavčič, D. Induced transmembrane voltage and its correlation with electroporation-mediated molecular transport. *J. Membr. Biol.* **236**, 3–13 (2010).
 37. Grosse, C. & Schwan, H. P. Cellular membrane potentials induced by alternating fields. *Biophys. J.* **63**, 1632–1642 (1992).
 38. Weaver, J. C. & Chizmadzhev, Y. A. Theory of electroporation: A review. *Bioelectrochemistry and Bioenergetics* vol. 41 135–160 (1996).
 39. Tsong, T. Y. Electroporation of cell membranes. *Biophysical Journal* vol. 60 297–306 (1991).
 40. Neumann, E. & Rosenheck, K. Permeability changes induced by electric impulses in vesicular membranes. *J. Membr. Biol.* **10**, 279–290 (1972).
 41. Weaver, J. C. Electroporation of Biological Membranes from Multicellular to Nano Scales. *IEEE T. Dielect. El. In.* 754-768 (2003).
 42. Susil, R., Šemrov, D. & Miklavčič, D. Electric field-induced transmembrane potential depends on cell density and organization. *Electro- and Magnetobiology* **17**, 391–399 (1998).
 43. Towhidi, L., Kotnik, T., Pucihar, G., Firoozabadi, S. M. P. & Mozdarani, H. Variability of the Minimal Transmembrane Voltage Resulting in Detectable Membrane Electroporation. *Electromagn. Biol. Med.* **27**, 372–385 (2008).
 44. Ganeva, V., Galutzov, B. & Teissié, J. High yield electroextraction of proteins from yeast by a flow process. *Anal. Biochem.* **315**, 77–84 (2003).
 45. Ganeva, V., Galutzov, B., Angelova, B. & Suckow, M. Electroinduced Extraction of Human Ferritin Heavy Chain Expressed in *Hansenula polymorpha*. *Appl. Biochem. Biotechnol.* **184**, 1286–1307 (2018).
 46. Meaking, W. S., Edgerton, J., Wharton, C. W. & Meldrum, R. A. Electroporation-induced damage in mammalian cell DNA. *BBA - Gene Struct. Expr.* **1264**, 357–362 (1995).
 47. Sale, A. J. H. & Hamilton, W. A. Effects of high electric fields on micro-organisms. III. Lysis of erythrocytes and protoplasts. *BBA -*

- Biomembr.* **163**, 37–43 (1968).
48. Satkauskas, S. *et al.* Mechanisms of in vivo DNA electrotransfer: Respective contribution of cell electropermeabilization and DNA electrophoresis. *Mol. Ther.* **5**, 133–140 (2002).
 49. Wolf, H., Rols, M. P., Boldt, E., Neumann, E. & Teissié, J. Control by pulse parameters of electric field-mediated gene transfer in mammalian cells. *Biophys. J.* **66**, 524–531 (1994).
 50. Kotnik, T., Pucihar, G., Reberšek, M., Miklavčič, D. & Mir, L. M. Role of pulse shape in cell membrane electropermeabilization. *Biochim. Biophys. Acta - Biomembr.* **1614**, 193–200 (2003).
 51. Rols, M. P. Electropermeabilization, a physical method for the delivery of therapeutic molecules into cells. *Biochim. Biophys. Acta - Biomembr.* **1758**, 423–428 (2006).
 52. Silve, A., Leray, I., Poignard, C. & Mir, L. M. Impact of external medium conductivity on cell membrane electropermeabilization by microsecond and nanosecond electric pulses. *Sci. Rep.* **6**, (2016).
 53. Pavlin, M. *et al.* Effect of cell electroporation on the conductivity of a cell suspension. *Biophys. J.* **88**, 4378–4390 (2005).
 54. Pliquett, U., Gift, E. A. & Weaver, J. C. Determination of the electric field and anomalous heating caused by exponential pulses with aluminum electrodes in electroporation experiments. *Bioelectrochemistry Bioenerg.* **39**, 39–53 (1996).
 55. Pucihar, G., Kotnik, T., Kandušer, M. & Miklavčič, D. The influence of medium conductivity on electropermeabilization and survival of cells in vitro. *Bioelectrochemistry* **54**, 107–115 (2001).
 56. Djuzenova, C. S. *et al.* Effect of medium conductivity and composition on the uptake of propidium iodide into electropermeabilized myeloma cells. *Biochim. Biophys. Acta - Biomembr.* **1284**, 143–152 (1996).
 57. Rols, M. P. & Teissié, J. Modulation of Electrically Induced Permeabilization and Fusion of Chinese Hamster Ovary Cells by Osmotic Pressure. *Biochemistry* **29**, 4561–4567 (1990).
 58. Golzio, M. *et al.* Control by osmotic pressure of voltage-induced permeabilization and gene transfer in mammalian cells. *Biophys. J.* **74**, 3015–3022 (1998).
 59. Neumann, E., Schaefer-Ridder, M., Wang, Y. & Hofschneider, P. H. Gene transfer into mouse lyoma cells by electroporation in high electric fields. *EMBO J.* **1**, 841–845 (1982).
 60. Bates, G. W. Electroporation of Plant Protoplasts and Tissues. *Methods Cell Biol.* **50**, 363–373 (1995).
 61. Calvin, N. M. & Hanawalt, P. C. High-efficiency transformation of bacterial cells by electroporation. *J. Bacteriol.* **170**, 2796–2801 (1988).
 62. Potter, H. Application of Electroporation in Recombinant DNA Technology. *Methods Enzymol.* **217**, 461–478 (1993).
 63. Karube, I., Tamiya, E. & Matsuoka, H. Transformation of *Saccharomyces cerevisiae* spheroplasts by high electric pulse. *FEBS*

- Lett.* **182**, 90–94 (1985).
64. Hashimoto, H., Morikawa, H., Yamada, Y. & Kimura, A. A novel method for transformation of intact yeast cells by electroinjection of plasmid DNA. *Appl. Microbiol. Biotechnol.* **21**, 336–339 (1985).
 65. Delorme, E. Transformation of *Saccharomyces cerevisiae* by electroporation. *Appl. Environ. Microbiol.* **55**, 2242–2246 (1989).
 66. Suga, M., Isobe, M. & Hatakeyama, T. Cryopreservation of competent intact yeast cells for efficient electroporation. *Yeast* **16**, 889–896 (2000).
 67. Meilhoc, E., Masson, J. M. & Teissié, J. High efficiency transformation of intact yeast cells by electric field pulses. *Bio/Technology* **8**, 223–227 (1990).
 68. Rech, E. L., Dobson, M. J., Davey, M. R. & Mulligan, B. J. Introduction of a yeast artificial chromosome vector into *Saccharomyces cerevisiae* cells by electroporation. *Nucleic Acids Res.* **18**, 1313 (1990).
 69. Hill, D. E. Integrative transformation of yeast using electroporation. *Nucleic Acids Research* **17**, 8011 (1989).
 70. Becker, D. M. & Guarente, L. High-Efficiency Transformation of Yeast by Electroporation. *Methods Enzymol.* **194**, 182–187 (1991).
 71. Suga, M., Kusanagi, I. & Hatakeyama, T. High osmotic stress improves electro-transformation efficiency of fission yeast. *FEMS Microbiol. Lett.* **225**, 235–239 (2003).
 72. Ganeva, V. & Galutzov, B. Influence of pulsing and postpulsing media tonicity on electrotransformation of intact yeast cells. *FEMS Microbiol. Lett.* **112**, 81–85 (1993).
 73. Grey, M. & Brendel, M. A ten-minute protocol for transforming *Saccharomyces cerevisiae* by electroporation. *Curr. Genet.* **22**, 335–6 (1992).
 74. Ganeva, V., Galutzov, B. & Teissie, J. Fast kinetic studies of plasmid DNA transfer in intact yeast cells mediated by Electropulsation. *Biochem. Biophys. Res. Commun.* **214**, 825–832 (1995).
 75. Yamamoto, T., Moerschell, R. P., Wakem, P., Ferguson, D. & Sherman, F. Parameters affecting the frequencies of transformation and co-transformation with synthetic oligonucleotides in yeast. *Yeast* **8**, 935–948 (1992).
 76. Barre, F. X., Mir, L. M., Lécluse, Y. & Harel-Bellan, A. Highly efficient oligonucleotide transfer into intact yeast cells using square-wave pulse electroporation. *Biotechniques* **25**, 294–296 (1998).
 77. Gietz, R. D. & Woods, R. A. Genetic transformation of yeast. *Biotechniques* **30**, 816–831 (2001).
 78. Jin, Y. *et al.* Optimization of extraction parameters for trehalose from beer waste brewing yeast treated by high-intensity pulsed electric fields (PEF). *African J. Biotechnol.* **10**, 19144–19152 (2011).
 79. Ohshima, T., Sato, M. & Saito, M. Selective release of intracellular

- protein using pulsed electric field. *J. Electrostat.* **35**, 103–112 (1995).
80. Vorobiev, E. & Lebovka, N. Pulsed-Electric-Fields-Induced Effects in Plant Tissues: Fundamental Aspects and Perspectives of Applications. doi:10.1007/978-0-387-79374-0.
 81. Marx, G., Moody, A. & Bermúdez-Aguirre, D. A comparative study on the structure of *Saccharomyces cerevisiae* under nonthermal technologies: High hydrostatic pressure, pulsed electric fields and thermo-sonication. *Int. J. Food Microbiol.* **151**, 327–337 (2011).
 82. Ganeva, V. *et al.* Electroinduced release of recombinant β -galactosidase from *Saccharomyces cerevisiae*. *J. Biotechnol.* **211**, 12–19 (2015).
 83. Zuckerman, H., Krasik, Y. E. & Felsteiner, J. Inactivation of microorganisms using pulsed high-current underwater discharges. *Innov. Food Sci. Emerg. Technol.* **3**, 329–336 (2002).
 84. Stirke, A. *et al.* Electric field-induced effects on yeast cell wall permeabilization. *Bioelectromagnetics* **35**, 136–144 (2014).
 85. Stankevic, V. *et al.* Compact Square-Wave Pulse Electroporator with Controlled Electroporation Efficiency and Cell Viability. *Symmetry (Basel)*. **12**, 412 (2020).
 86. Stirke, A. *et al.* The link between yeast cell wall porosity and plasma membrane permeability after PEF treatment. *Sci. Rep.* **9**, 14731 (2019).
 87. Zhang, Y., Chen, X., Gueydan, C. & Han, J. Plasma membrane changes during programmed cell deaths. *Cell Research* vol. 28 9–21 (2018).
 88. Farrugia, G. & Balzan, R. Oxidative stress and programmed cell death in yeast. *Frontiers in Oncology* vol. 2 JUN (2012).
 89. Eisenberg, T. & Büttner, S. Lipids and cell death in yeast. *FEMS Yeast Res.* **14**, 179–197 (2014).
 90. Batista Napotnik, T. & Miklavčič, D. In vitro electroporation detection methods – An overview. *Bioelectrochemistry* vol. 120 166–182 (2018).
 91. Ganeva, V. & Galutzov, B. Electropulsation as an alternative method for protein extraction from yeast. *FEMS Microbiol. Lett.* **174**, 279–284 (1999).
 92. Peterson, A. D., Jaroszeski, M. J. & Gupta, V. K. Fluorometric assay to compensate for non-viable cells during electroporation. *J. Fluoresc.* **25**, 159–165 (2015).
 93. Granot, Y., Ivorra, A., Maor, E. & Rubinsky, B. In vivo imaging of irreversible electroporation by means of electrical impedance tomography. *Phys. Med. Biol.* **54**, 4927–43 (2009).
 94. Romeo, S., Wu, Y. H., Levine, Z. A., Gundersen, M. A. & Vernier, P. T. Water influx and cell swelling after nanosecond electroporation. *Biochim. Biophys. Acta - Biomembr.* **1828**, 1715–1722 (2013).
 95. Chaffey, N. Alberts, B., Johnson, A., Lewis, J., Raff, M., Roberts, K.

- and Walter, P. Molecular biology of the cell. 4th edn. *Ann. Bot.* **91**, 401–401 (2003).
96. Shete, H. K., Prabhu, R. H. & Patravale, V. B. Endosomal escape: A bottleneck in intracellular delivery. *Journal of Nanoscience and Nanotechnology* vol. 14 460–474 (2014).
 97. Neumann, E., Toensing, K., Kakorin, S., Budde, P. & Frey, J. Mechanism of electroporative dye uptake by mouse B cells. *Biophys. J.* **74**, 98–108 (1998).
 98. Prausnitz, M. R., Milano, C. D., Gimm, J. A., Langer, R. & Weaver, J. C. Quantitative study of molecular transport due to electroporation: uptake of bovine serum albumin by erythrocyte ghosts. *Biophys. J.* **66**, 1522–1530 (1994).
 99. Sözer, E. B., Levine, Z. A. & Vernier, P. T. Quantitative limits on small molecule transport via the electropermeome measuring and modeling single nanosecond perturbations. *Sci. Rep.* **7**, 1–13 (2017).
 100. Breton, M., Delemotte, L., Silve, A., Mir, L. M. & Tarek, M. Transport of siRNA through lipid membranes driven by nanosecond electric pulses: An experimental and computational study. *J. Am. Chem. Soc.* **134**, 13938–13941 (2012).
 101. Kotulska, M., Dyrka, W. & Sadowski, P. Fluorescent Methods in Evaluation of Nanopore Conductivity and Their Computational Validation. in *ADVANCED ELECTROPORATION TECHNIQUES IN BIOLOGY AND MEDICINE* 123–137 (2010).
 102. Teissié, J., Eynard, N., Gabriel, B. & Rols, M. . Electroporabilization of cell membranes. *Adv. Drug Deliv. Rev.* **35**, 3–19 (1999).
 103. Golberg, A. *et al.* Energy-efficient biomass processing with pulsed electric fields for bioeconomy and sustainable development. *Biotechnology for Biofuels* vol. 9 (2016).
 104. Haberl Meglic, S., Marolt, T. & Miklavcic, D. Protein Extraction by Means of Electroporation from *E. coli* with Preserved Viability. *J. Membr. Biol.* **248**, 893–901 (2015).
 105. Ganeva, V. & Galutzov, B. Electropulsation as an alternative method for protein extraction from yeast. *FEMS Microbiol. Lett.* **174**, 279–284 (1999).
 106. Coustets, M., Al-Karablieh, N., Thomsen, C. & Teissié, J. Flow process for electroextraction of total proteins from microalgae. in *Journal of Membrane Biology* vol. 246 751–760 (2013).
 107. Suga, M., Goto, A. & Hatakeyama, T. Electrically induced protein release from *Schizosaccharomyces pombe* cells in a hyperosmotic condition during and following a high electropulsation. *J. Biosci. Bioeng.* **103**, 298–302 (2007).
 108. Matos, T. *et al.* Nucleic acid and protein extraction from electropermeabilized *E. coli* cells on a microfluidic chip. *Analyst* **138**, 7347–7353 (2013).

109. Zhan, Y. *et al.* Release of intracellular proteins by electroporation with preserved cell viability. *Anal. Chem.* **84**, 8102–8105 (2012).
110. Zhan, Y., Martin, V. A., Geahlen, R. L. & Lu, C. One-step extraction of subcellular proteins from eukaryotic cells. *Lab Chip* **10**, 2046–2048 (2010).
111. Pataro, G. *et al.* Effect of PEF treatment on extraction of valuable compounds from microalgae *C. Vulgaris*. *Chem. Eng. Trans.* **57**, 67–72 (2017).
112. Luengo, E., Condón-Abanto, S., Álvarez, I. & Raso, J. Effect of Pulsed Electric Field Treatments on Permeabilization and Extraction of Pigments from *Chlorella vulgaris*. *J. Membr. Biol.* **247**, 1269–1277 (2014).
113. Flisar, K., Meglic, S. H., Morelj, J., Golob, J. & Miklavcic, D. Testing a prototype pulse generator for a continuous flow system and its use for *E. coli* inactivation and microalgae lipid extraction. *Bioelectrochemistry* **100**, 44–51 (2014).
114. Castellví, Q., Mercadal, B. & Ivorra, A. Assessment of Electroporation by Electrical Impedance Methods. in *Handbook of Electroporation* 1–20 (Springer International Publishing, 2016). doi:10.1007/978-3-319-26779-1_164-1.
115. Castellví, Q., Mercadal, B. & Ivorra, A. Assessment of Electroporation by Electrical Impedance Methods. in *Handbook of Electroporation* 1–20 (Springer International Publishing, 2016). doi:10.1007/978-3-319-26779-1_164-1.
116. Chen, W. & Lee, R. C. An improved double vaseline gap voltage clamp to study electroporated skeletal muscle fibers. *Biophys. J.* **66**, 700–9 (1994).
117. Gowrishankar, T. R., Chen, W. & Lee, R. C. Non-linear microscale alterations in membrane transport by electropermeabilization. in *Annals of the New York Academy of Sciences* vol. 858 205–216 (New York Academy of Sciences, 1998).
118. Pakhomova, A. G. P. and O. N. Nanopores: A Distinct Transmembrane Passageway in Electroporated Cells. 197–214 (2010) doi:10.1201/EBK1439819067-14.
119. Romeo, S., Wu, Y. H., Levine, Z. A., Gundersen, M. A. & Vernier, P. T. Water influx and cell swelling after nanosecond electropermeabilization. *Biochim. Biophys. Acta - Biomembr.* **1828**, 1715–1722 (2013).
120. Nesin, O. M., Pakhomova, O. N., Xiao, S. & Pakhomov, A. G. Manipulation of cell volume and membrane pore comparison following single cell permeabilization with 60- and 600-ns electric pulses. *Biochim. Biophys. Acta - Biomembr.* **1808**, 792–801 (2011).
121. Golzio, M. *et al.* Control by osmotic pressure of voltage-induced permeabilization and gene transfer in mammalian cells. *Biophys. J.* **74**, 3015–3022 (1998).

122. Ferret, E., Evrard, C., Foucal, A. & Gervais, P. Volume changes of isolated human K562 leukemia cells induced by electric field pulses. *Biotechnol. Bioeng.* **67**, 520–528 (2000).
123. Ušaj, M., Trontelj, K., Hudej, R., Kandušer, M. & Miklavčič, D. Cell size dynamics and viability of cells exposed to hypotonic treatment and electroporation for electrofusion optimization. *Radiol. Oncol.* **43**, 108–119 (2009).
124. Heiskanen, A. *et al.* Mediator-assisted simultaneous probing of cytosolic and mitochondrial redox activity in living cells. *Anal. Biochem.* **384**, 11–19 (2009).
125. Garjonyte, R., Melvydas, V. & Malinauskas, A. Mediated amperometry reveals different modes of yeast responses to sugars. *Bioelectrochemistry* **107**, 45–49 (2016).
126. Kuznetsov, B. A., Khlupova, M. T., Shleev, S. V, Kaprel'yants, A. S. & Yaropolov, A. I. An Electrochemical Method for Measuring Metabolic Activity and Counting Cells. *Appl. Biochem. Microbiol.* **42**, 599–608 (2006).
127. Kuznetsov, B. A. *et al.* Electrochemical investigation of the dynamics of *Mycobacterium smegmatis* cells' transformation to dormant, nonculturable form. *Bioelectrochemistry* **64**, 125–131 (2004).
128. Pérez, F. G., Mascini, M., Tothill, I. E. & Turner, A. P. F. Immunomagnetic Separation with Mediated Flow Injection Analysis Amperometric Detection of Viable *Escherichia coli* O157. *Anal. Chem.* **70**, 2380–2386 (1998).
129. Li, H. N. & Ci, Y. X. Electrochemical method for analyzing intracellular redox activity changes of the etoposide-induced apoptosis in HL-60 cells. *Anal. Chim. Acta* **416**, 221–226 (2000).
130. Ertl, P., Robello, E., Battaglini, F. & Mikkelsen, S. R. Rapid antibiotic susceptibility testing via electrochemical measurement of ferricyanide reduction by *Escherichia coli* and *Clostridium sporogenes*. *Anal. Chem.* **72**, 4957–4964 (2000).
131. Heiskanen, A. *et al.* Amperometric monitoring of redox activity in living yeast cells: Comparison of menadione and menadione sodium bisulfite as electron transfer mediators. *Electrochem. commun.* **6**, 219–224 (2004).
132. Kerscher, S., Dröse, S., Zwicker, K., Zickermann, V. & Brandt, U. *Yarrowia lipolytica*, a yeast genetic system to study mitochondrial complex I. *Biochim. Biophys. Acta* **1555**, 83–91 (2002).
133. Baronian, K., Downard, A., Lowen, R. & Pasco, N. Detection of two distinct substrate-dependent catabolic responses in yeast cells using a mediated electrochemical method. *Appl. Microbiol. Biotechnol.* **60**, 108–113 (2002).
134. Wu, S. *et al.* Extracellular electron transfer mediated by flavins in Gram-positive *Bacillus* sp. WS-XY1 and yeast *Pichia stipitis*. *Electrochim. Acta* **146**, 564–567 (2014).

135. Chelikani, V. *et al.* Investigating yeast cell responses to oestrogen by electrochemical detection. *Electrochim. Acta* **73**, 136–140 (2012).
136. Giroud, F., Nicolo, T. A., Koepke, S. J. & Minter, S. D. Understanding the mechanism of direct electrochemistry of mitochondria-modified electrodes from yeast, potato and bovine sources at carbon paper electrodes. *Electrochim. Acta* **110**, 112–119 (2013).
137. Rawson, F. J., Downard, A. J. & Baronian, K. H. Electrochemical detection of intracellular and cell membrane redox systems in *Saccharomyces cerevisiae*. *Sci. Rep.* **4**, 1–9 (2014).
138. Spégel, C. F. *et al.* Amperometric response from the glycolytic versus the pentose phosphate pathway in *Saccharomyces cerevisiae* cells. *Anal. Chem.* **79**, 8919–8926 (2007).
139. Kostesha, N. *et al.* Real-time detection of cofactor availability in genetically modified living *Saccharomyces cerevisiae* cells - Simultaneous probing of different geno- and phenotypes. *Bioelectrochemistry* **76**, 180–188 (2009).
140. Garjonyte, R., Melvydas, V., Paškevičius, A., Rašomavičius, V. & Malinauskas, A. Mediated amperometry reveals two distinct modes of yeast responses to glucose. *Cent. Eur. J. Biol.* **9**, 173–181 (2014).
141. Garjonyte, R., Melvydas, V. & Malinauskas, A. Mediated amperometry reveals different modes of yeast responses to sugars. *Bioelectrochemistry* **107**, 45–49 (2016).
142. Garjonyte, R. & Malinauskas, A. Investigation of baker's yeast *Saccharomyces cerevisiae*- and mediator-based carbon paste electrodes as amperometric biosensors for lactic acid. *Sensors Actuators, B Chem.* **96**, 509–515 (2003).
143. Garjonyte, R., Melvydas, V. & Malinauskas, A. Mediated amperometric biosensors for lactic acid based on carbon paste electrodes modified with baker's yeast *Saccharomyces cerevisiae*. *Bioelectrochemistry* **68**, 191–196 (2006).
144. Garjonyte, R., Melvydas, V. & Malinauskas, A. Effect of yeast pretreatment on the characteristics of yeast-modified electrodes as mediated amperometric biosensors for lactic acid. *Bioelectrochemistry* **74**, 188–194 (2008).
145. Khlupova, M., Kuznetsov, B., Gonchar, M., Ruzgas, T. & Shleev, S. Amperometric monitoring of redox activity in intact, permeabilised and lyophilised cells of the yeast *Hansenula polymorpha*. *Electrochem. commun.* **9**, 1480–1485 (2007).
146. Simonis, P., Garjonyte, R. & Stirke, A. Mediated amperometry as a prospective method for the investigation of electroporation. *Sci. Rep.* **10**, (2020).
147. Schoenbach, K. H., Beebe, S. J. & Buescher, E. S. Intracellular effect of ultrashort electrical pulses. *Bioelectromagnetics* **22**, 440–448 (2001).

148. Tekle, E. *et al.* Selective field effects on intracellular vacuoles and vesicle membranes with nanosecond electric pulses. *Biophys. J.* **89**, 274–284 (2005).
149. Napotnik, T. B. *et al.* Electroporabilization of endocytotic vesicles in B16 F1 mouse melanoma cells. *Med. Biol. Eng. Comput.* **48**, 407–413 (2010).
150. Beebe, S. J. *et al.* Diverse Effects of Nanosecond Pulsed Electric Fields on Cells and Tissues. *DNA Cell Biol.* **22**, 785–796 (2003).
151. Vernier, P. T. *et al.* Calcium bursts induced by nanosecond electric pulses. *Biochem. Biophys. Res. Commun.* **310**, 286–295 (2003).
152. Scarlett, S. S., White, J. A., Blackmore, P. F., Schoenbach, K. H. & Kolb, J. F. Regulation of intracellular calcium concentration by nanosecond pulsed electric fields. *Biochim. Biophys. Acta - Biomembr.* **1788**, 1168–1175 (2009).
153. Hall, E. H., Schoenbach, K. H. & Beebe, S. J. Nanosecond pulsed electric fields induce apoptosis in p53-wildtype and p53-null HCT116 colon carcinoma cells. *Apoptosis* **12**, 1721–1731 (2007).
154. Beebe, S. J. *et al.* Nanosecond pulsed electric field (nsPEF) effects on cells and tissues: Apoptosis induction and tumor growth inhibition. in *IEEE Transactions on Plasma Science* vol. 30 286–292 (2002).
155. Beebe, S., Sain, N. & Ren, W. Induction of Cell Death Mechanisms and Apoptosis by Nanosecond Pulsed Electric Fields (nsPEFs). *Cells* **2**, 136–162 (2013).
156. Morotomi-Yano, K., Oyadomari, S., Akiyama, H. & Yano, K. ichi. Nanosecond pulsed electric fields act as a novel cellular stress that induces translational suppression accompanied by eIF2 α phosphorylation and 4E-BP1 dephosphorylation. *Exp. Cell Res.* **318**, 1733–1744 (2012).
157. Thomas Vernier, P. *et al.* Nanoelectropulse-Induced Phosphatidylserine Translocation. doi:10.1529/biophysj.103.037945.
158. Pakhomov, A. G. *et al.* Long-lasting plasma membrane permeabilization in mammalian cells by nanosecond Pulsed Electric Field (nsPEF). *Bioelectromagnetics* **28**, 655–663 (2007).
159. Pakhomov, A. G. *et al.* Lipid nanopores can form a stable, ion channel-like conduction pathway in cell membrane. *Biochem. Biophys. Res. Commun.* **385**, 181–186 (2009).
160. Batista Napotnik, T., Reberšek, M., Vernier, P. T., Mali, B. & Miklavčič, D. Effects of high voltage nanosecond electric pulses on eucaryotic cells (in vitro): A systematic review. *Bioelectrochemistry* vol. 110 1–12 (2016).
161. Stirke, A. *et al.* Permeabilization of yeast *Saccharomyces cerevisiae* cell walls using nanosecond high power electrical pulses. *Appl. Phys. Lett.* **105**, (2014).
162. Madeo, F. *et al.* Caspase-dependent and caspase-independent cell death pathways in yeast. *Biochemical and Biophysical Research*

- Communications* vol. 382 227–231 (2009).
163. Madeo, F., Fröhlich, E. & Fröhlich, K. U. A yeast mutant showing diagnostic markers of early and late apoptosis. *J. Cell Biol.* **139**, 729–734 (1997).
 164. Madeo, F. *et al.* Oxygen stress: A regulator of apoptosis in yeast. *J. Cell Biol.* **145**, 757–767 (1999).
 165. Madeo, F. *et al.* A caspase-related protease regulates apoptosis in yeast. *Mol. Cell* **9**, 911–917 (2002).
 166. Wissing, S. *et al.* An AIF orthologue regulates apoptosis in yeast. *J. Cell Biol.* **166**, 969–974 (2004).
 167. Silva, R. D. *et al.* Hyperosmotic stress induces metacaspase- and mitochondria-dependent apoptosis in *Saccharomyces cerevisiae*. *Mol. Microbiol.* **58**, 824–834 (2005).
 168. Hill, S. M. & Nyström, T. The dual role of a yeast metacaspase: What doesn't kill you makes you stronger. *BioEssays* **37**, 525–531 (2015).
 169. Lee, R. E. C., Brunette, S., Puente, L. G. & Megeney, L. A. Metacaspase Yca1 is required for clearance of insoluble protein aggregates. *Proc. Natl. Acad. Sci. U. S. A.* **107**, 13348–13353 (2010).
 170. Wong, A. H. H., Yan, C. & Shi, Y. Crystal structure of the yeast metacaspase Yca1. *J. Biol. Chem.* **287**, 29251–29259 (2012).
 171. Silva, A. *et al.* Glyceraldehyde-3-phosphate dehydrogenase (GAPDH) is a specific substrate of yeast metacaspase. *Biochim. Biophys. Acta - Mol. Cell Res.* **1813**, 2044–2049 (2011).
 172. Pakhomova, O. N. *et al.* Oxidative effects of nanosecond pulsed electric field exposure in cells and cell-free media. *Arch. Biochem. Biophys.* **527**, 55–64 (2012).
 173. Sale, A. J. H. & Hamilton, W. A. Effects of high electric fields on microorganisms. I. Killing of bacteria and yeasts. *BBA - Gen. Subj.* **148**, 781–788 (1967).
 174. Griffiths, S., MacLean, M., Anderson, J. G., MacGregor, S. J. & Helen Grant, M. Inactivation of microorganisms within collagen gel biomatrices using pulsed electric field treatment. *J. Mater. Sci. Mater. Med.* **23**, 507–515 (2012).
 175. Wang, M. S., Zeng, X. A., Brennan, C. S., Brennan, M. A. & Han, Z. Effects of pulsed electric fields on the survival behaviour of *Saccharomyces cerevisiae* suspended in single solutions of low concentration. *Int. J. Food Sci. Technol.* **51**, 171–179 (2016).
 176. Qin, S. *et al.* Pulsed electric field treatment of *saccharomyces cerevisiae* using different waveforms. *IEEE Trans. Dielectr. Electr. Insul.* **22**, 1841–1848 (2015).
 177. Somolinos, M., García, D., Condón, S., Mañas, P. & Pagán, R. Relationship between sublethal injury and inactivation of yeast cells by the combination of sorbic acid and pulsed electric fields. *Appl. Environ. Microbiol.* **73**, 3814–3821 (2007).
 178. Montanari, C. *et al.* Heat-Assisted Pulsed Electric Field Treatment for

- the Inactivation of *Saccharomyces cerevisiae*: Effects of the Presence of Citral. *Front. Microbiol.* **10**, (2019).
179. Galluzzi, L. *et al.* No death without life: Vital functions of apoptotic effectors. *Cell Death and Differentiation* vol. 15 1113–1123 (2008).
 180. Simonis, P. *et al.* Caspase dependent apoptosis induced in yeast cells by nanosecond pulsed electric fields. *Bioelectrochemistry* **115**, (2017).
 181. Simonis, P. *et al.* Pulsed electric field effects on inactivation of microorganisms in acid whey. *Int. J. Food Microbiol.* **291**, 128–134 (2019).
 182. Balevicius, Z. *et al.* Compact high-sensitivity potentiometer for detection of low ion concentrations in liquids. *Rev. Sci. Instrum.* **89**, 1–6 (2018).
 183. Simonis, P. *et al.* Pulsed electric field effects on inactivation of microorganisms in acid whey. *Int. J. Food Microbiol.* **291**, 128–134 (2019).
 184. Stankevici, V. *et al.* Compact square-wave pulse electroporator with controlled electroporation efficiency and cell viability. *Symmetry (Basel)*. **12**, (2020).
 185. Balevicius, S. *et al.* System for the nanoporation of biological cells based on an optically-triggered high-voltage spark-gap switch. *IEEE Trans. Plasma Sci.* **41**, 2706–2711 (2013).

SANTRAUKA

1. Nagrinėjamos temos apžvalga

Mielės *Saccharomyces cerevisiae* yra vienas iš labiausiai ištyrinėtų eukariotinių mikroorganizmų. Jos yra plačiai naudojamos kepinių bei alkoholinių gėrimų gamybai. Tačiau šis mikroorganizmas patekęs į maisto produktus, pvz.: sultis ar pieno produktus, sukelia gedimą, todėl daugelis maisto produktų, siekiant prailginti jų galiojimo laiką, yra termiškai pasterizuojami. Kadangi maistingos produkcijos poreikis vis labiau auga, reikia naujų technologijų galinčių išsaugoti maistines savybes bei tuo pačiu metu slopinančių gedimą lemiančius mikroorganizmus. Mielių ląstelės taip pat yra sėkmingai naudojamos rekombinantinių baltymų gamybai bei biokatalizei. Šių procesų efektyvumą riboja barjerinės ląstelės membranos bei sienelės savybės. Šios struktūros trukdo substratų, induktorių patekimui bei jau susintetintų viduląstelių produktų išskyrimui, atitinkamai į ir iš mielių ląstelių. Šiuo metu trūksta efektyvių technologijų galinčių veiksmingai kontroliuoti mielių ląstelių pralaidumą bei reguliuoti jų aktyvumą biotechnologiniuose procesuose.

Viena iš technologijų galinčių padidinti ląstelių pralaidumą tikslinėms molekulėms yra impulsinis elektrinis laukas (IEL). Remiantis fundamentinių tyrimų duomenimis galimi įvairūs IEL pritaikymo būdai, tačiau gamybos procesams, kurių metu naudojamos mielės, ši technologija vis dar nėra plačiai naudojama. Yra žinoma, jog IEL gali būti pritaikytas netemperatūriniam skystų maisto produktų galiojimo laiko prailginimui, tačiau vis dar trūksta žinių apie tai kaip poveikis keičia ląstelinius procesus, kas lieka iš mielių ląstelių po IEL poveikio bei kaip tai gali paveikti maisto produktų savybes. Mielių ląstelių, kaip modelinio organizmo, IEL poveikio tyrimuose panaudojimas kol kas taip pat yra retas, nors ir turintis daug perspektyvų dėl gautų žinių pritaikomumo tiek maisto bei biotechnologijos pramonėje. Naujos žinios taip pat galėtų praplėsti suvokimą apie eukariotinių ląstelių atsako į abiotinį poveikį mechanizmus.

Siekiant padidinti ekstraląstelių junginių įvedimo bei viduląstelių komponentų ekstrakcijos efektyvumą vis svarbesnės tampa fundamentinės žinios apie ląstelinį atsaką, mechaninį, elektrinį bei molekulinį transportą po impulsinio elektrinio lauko poveikio. Detalus molekulinio transporto suvokimas būtų naudingas DNR, žymenų, fermentų, antikūnių bei kitų molekulių įvedimui į ląsteles tyrimų bei terapijos tikslais. Šios žinios galėtų būti pritaikomos naujų tvarių IEL technologijų kūrimui bei pritaikymui vėžio terapijoje, maisto pramonės srityse.

Šia disertacija aš analizuoju problemas bei technologinius aspektus svarbius elektroporacijos pritaikymui maisto pramonėje bei biotechnologijose. Tyrimas bei apžvalga apima tris pagrindines kryptis: fundamentinius mielių ląstelių tyrimus, impulsinio elektrinio lauko poveikio vertinimą amperometrijos metodu ir mielių ląstelių atsako į nanosekundžių trukmės elektrinio lauko impulsus tyrimą bei taikymą. Disertacijos problematika bei diskusija yra sugrupuota į penkis poskyrius, kurie siejasi su atitinkamuose straipsniuose publikuotais tyrimais.

2. Ginamieji teiginiai

1. Mielių *Saccharomyces cerevisiae* ląstelių sienelių bei membranų pralaidumas po elektrinio lauko impulso poveikio, kai $E \leq 6$ kV/cm, kinta panašiai ir stabilizuojasi per 100 sekundžių. Tai patvirtina, jog abi struktūros yra svarbios bei dalyvauja ląstelės integralumo atsistatymo procesuose.
2. Amperometrija gali būti pritaikyta elektrinio lauko poveikio mielių ląstelių membranų pralaidumo (hidrofiliniams mediatoriams) bei menadioną redukuojančių viduląstelių fermentų aktyvumo tyrimams.
3. Nanosekundžių trukmės ($\tau \leq 90$ ns) aukštavolčiai elektrinio lauko impulsai ($E \leq 220$ kV/cm) sukelia nuo kaspazių priklausomą mielių ląstelių žūtį bei gali būti panaudoti jų selektyviam gyvybingumo slopinimui.

3. Mokslinio darbo problematika

3.1. Mielių sienelės ir membranos sąveika po impulsinio elektrinio lauko poveikio

Anksčiau atlikti įvairių tyrėjų grupių rezultatai rodo, jog impulsinio elektrinio lauko poveikis susilpnina barjerines sienelės bei membranos funkcijas. Po fermentinio sienelės pašalinimo ląstelės yra pralaidesnės stambiamolekuliniams bei krūvį turintiems junginiams. Tai leidžia daryti prielaidą, jog sienelė yra vienas iš pagrindinių, molekulių patekimą į ląstelės vidų ribojančių barjerų. Šiuo metu nėra galutinai aišku kaip membranos ir sienelės pralaidumas susijęs, bei kodėl po impulsinio elektrinio lauko poveikio sienelės pralaidumas padidėja. Tai būtų galima aiškinti taip:

- Elektrinis laukas suardo sienelės struktūrą veikdamas ją tiesiogiai (elektromechaniškai deformuodamas krūvį turinčius sienelės komponentus);
- Sienelė nėra veikiamą tiesiogiai, bet jos pralaidumas yra susijęs su impulsinio elektrinio lauko poveikiu plazminei membranai. Membranos integralumas gali būti pažeistas dėl komponentų oksidacijos, dėl to gali

būti paveiktos ląstelės sienelė su membrana siejančios struktūros (inkarai) ir taip pažeistas sienelės stabilumas;

- Po elektrinio lauko poveikio dėl padidėjusio membranos pralaidumo į užląstelinę erdvę ištekantys viduląsteliniai komponentai gali sąveikauti su sienele ir taip keisti jos barjerines savybes (neutralizuoti krūvį, redukuoti disulfidinius tiltelius);
- Jei ląstelės elektriniu lauku veikiamos hipoosmosinėmis sąlygomis, tada permeabilizacija lemia vandens patekimą į ląstelę ir jos tūrio padidėjimą. Tokiu atveju sienelės pralaidumo padidėjimas galėtų būti nulemtas sienelės išplonėjimo ir atitinkamai atstumų tarp jos komponentų padidėjimo.

Visos paminėtos priežastys bent dalinai veda į mielių sienelės pralaidumo padidėjimą.

Pagrindinių priežasčių identifikavimas svarbus impulsinio elektrinio lauko technologijos pritaikymui tyrimuose bei pramonėje. Tokios žinios būtų naudingos biokatalizės, elektroekstrakcijos procesų bei stambiamolekulinių junginių įvedimo efektyvumui padidinti. Pralaidumo atsistatymo dinamikos suvokimas reikalingas energetiškai naudingos elektrinio lauko impulsų poveikio procedūrų optimizavimui.

3.2. Elektrinio lauko impulsų formos įtaka mielių elektroporacijos efektyvumui ir ląstelių gyvybingumui

Techninės modernios elektronikos galimybės leidžia labai tiksliai kontroliuoti generuojamo elektrinio lauko impulso formą. Deja tik maža dalis instrumentų (tinkamų fundamentiniams bei technologiniams tyrimams) aktyviai formuoja ir užrašo realią sugeneruoto impulso formą. Kontrolės bei vertinimo stoka impulso poveikio metu gali lemti neteisingą duomenų interpretavimą, neatkartojamų duomenų produkavimą, energijos bei kitų resursų švaistymą. Yra žinoma, jog terpės laidumas veikia generuojamo srovės impulso formą. Vis dėlto duomenys apie terpės laidumo sukeltą poveikį ląstelėms elektrinio lauko generavimo metu yra nevienareikšmiai (skirtingos tyrėjų grupės pateikia prieštarigus duomenis vedančius į skirtingas išvadas). Taip pat, daugelyje elektroporacijos metodų rekomenduojamas daugkartinių impulsų panaudojimas, nors ląstelių elektroporacijos metu laidumas ir kinta po kiekvieno impulso dėl iš ląstelių ištekiančių jonų. Tokie terpės pokyčiai gali paveikti impulsų formą ir skirtingą ląstelių atsaką į vėlesnius impulsus.

Tyrimai patvirtinantys, jog detalus impulsų stebėjimas ir vertinimas jų generacijos metu suteikia reikšmingą informaciją lemtų svarbų pokytį

elektrinio lauko generatorių rinkoje. Žinios leidžiančios atskirti subtilius efektus pasireiškiančius dėl impulso formos skirtumo ar terpės laidumo, suteiktų aiškumo bei tikslumo atliekamiems fundamentiniams tyrimams.

3.3. Amperometrijos metodo taikymas elektroporacijos tyrimams

Šiuo metu amperometrija nėra naudojama elektroporacijos ar ląstelinės būsenos po impulsinio elektrinio lauko poveikio tyrimams. Tuo tarpu, kitose srityse elektrochemija suteikia platų metodų spektrą tinkamą tirti membraniniams ar viduląsteliniais oksidacijos-redukcijos centrams. Individualus amperometrinis eksperimentas gali suteikti didelį informacijos kiekį apie oksidacijos-redukcijos centrus, kofaktorių savybes, ląstelinės būsenos pokyčius po abiotinio poveikio. Perspektyvi amperometrijos bei elektroporacijos sinergija galėtų būti naudinga abiem sritims.

Kontroliuojama plazminės membranos permeabilizacija galėtų suteikti prieigą prie viduląstelinio oksidacijos-redukcijos centrų. Po elektroporacijos hidrofiliiniai mediatoriai galėtų būti naudojami atskirai nuo hidrofobinių. Po tokio ląstelių apdirbimo dauguma fermentų lieka ląstelės viduje, tad jų aktyvumas galėtų būti tyrinėjamas natūresnėje aplinkoje (nei pilnai išgrynintų). Tikėtina, jog plazminės membranos pralaidumo kontrolė elektriniu lauku gali pasiūlyti naujų biojutiklių kūrimo galimybių.

Amperometrija yra plačiai naudojamas metodas viduląstelinės būsenos bei abiotinio streso tyrimams. Ji yra sąlyginai greita ir paprasta, galėtų būti taikoma analitinėse sistemose su įvairiomis ląstelėmis. Šioje srityje sukauptos žinios galėtų būti panaudotos detalesniam elektroporacijos sukeliama ląstelinio streso aiškinimui. Oksidacinės-redukcinės būsenos tyrimai pasitelkiant amperometriją galėtų padėti geriau suprasti tokius impulsinio elektrinio lauko sukeltus efektus kaip stimuliacija, grįžtamos ir negrįžtamos permeabilizacijos (plazminės membranos bei organelių) ryšys su homeostaze bei fermentiniu aktyvumu. Amperometrinės detekcijos sistemos su skirtingomis mediatorių bei inhibitorių kombinacijomis būtų naudingos detaliam ląstelinio atsako analizei bei žūties tyrimui.

3.4. Nanosekundžių trukmės elektrinio lauko impulsais sukeltos mielių ląstelių žūties tyrimas

Didelė dalis tyrimų yra susijusi su impulsinio elektrinio lauko poveikio taikymu maisto pramonėje bei pasterizacijoje. Šie tyrimai koncentruojasi į negrįžtamą elektroporaciją vedančią į sutrikdytą homeostazę bei ląstelės žūtį. Programuotos ląstelės žūties keliai mielių ląstelėse atrasti ganėtinai neseniai (lyginant su elektroporacijos reiškiniu), tad beveik nėra tyrimų apie IEL

poveikio aktyvuojamus žūties kelius. Fundamentinių tyrimų, kuriuose mielių ląstelės būtų naudojamos kaip modelinis organizmas yra labai mažai. Šiuo metu nėra informacijos ar itin trumpi elektrinio lauko impulsai (iki 100 ns) veikia mielių ląstelių vidines membranas ir gali atitinkamai stimuliuoti viduląstelinius efektus.

Duomenys apie programuotos ląstelių žūties indukciją nanosekundžių trukmės elektrinio lauko impulsais būtų naudingi naujų taikomųjų technologijų kūrimui. Žinios apie IEL sukeliama ląstelių žūtį taip pat reikalingos šios technologijos tinkamumo maisto pramonėje įvertinimui, nes žūstančios bei žuvusios ląstelės tampa produkto komponentais.

3.5. Impulsinio elektrinio lauko poveikis rūgščiose išrūgose esantiems mikroorganizmams

Galiojimo laikas yra vienas iš svarbiausių aspektų maisto pramonėje. Ilgesnis galiojimo laikas įprastai reiškia mažesnę tikimybę apsinuodyti maisto produktu bei mažiau atliekų. Šiuo metu pagrindinė skystų produktų pasterizacijai taikoma technologija yra apdorojimas aukšta temperatūra. Tokia procedūra veikia biochemiškai aktyvius junginius, keičia maistines bei organoleptines maisto produktų savybes. Nors poveikis impulsiniu elektriniu lauku yra bent dalinai netemperatūrinis ir galėtų būti taikomas karščiui jautrių produktų pasterizacijai, šiuo metu jis vis dar nėra plačiai taikomas.

Kitas svarbus aspektas į kurį pradeda kreipti dėmesį maisto pramonė yra organizmui naudingos bakterijos, kurios įprastų apdirbimo procedūrų metu žūsta. Mieliagybių ląstelės yra didesnės nei dažniausiai sutinkamos bakterijos, tad remiantis elektroporacijos teorija, elektrinio lauko poveikį turėtų pavykti pritaikyti mielių ląstelių gyvybingumo slopinimui išsaugant bakterijas gyvas. Vis dėlto šiuo metu nėra pavyzdžių apie praktinį tokios teorijos pritaikymą.

Šiuo metu taip pat nėra publikuotų duomenų apie sėkmingai pritaikytus didelės galios nanosekundžių trukmės impulsus su maisto pramone susijusios produkcijos apdirbimui. Nauja energetiškai palanki netemperatūrinė technologija būtų naudinga tiek gamintojams (potencialiai mažesnės energijos sąnaudos) tiek vartotojams (natūralesnis skonis bei maistingesnis produktas).

4. Mokslinio darbo tikslai ir uždaviniai

1. Įvertinti mielių membranos ir sienelės ryšį bei atsistatymo dinamiką po impulsinio elektrinio lauko poveikio.
2. Ištirti impulso formas (su ir be kontroliuojamo galinio fronto) įtaką sukulto poveikio mielių ląstelių gyvybingumui bei pralaidumui.

3. Įvertinti amperometrijos metodo pritaikomumą mielių elektroporacijos tyrimui.
4. Ištirti nanosekundžių trukmės impulsų sukeliama poveikį mielių ląstelėse ir identifikuoti žūties tipą.
5. Ištirti nanosekundžių trukmės elektrinio lauko impulsų poveikį rūgščiose išrūgose randamų mikroorganizmų (mielių bei bakterijų) gyvybingumui.

5. Svarbiausi rezultatai ir naujumas

IEL sukkelto ląstelinio atsako tyrimui, kaip modelinis organizmas, buvo panaudotos mielių *Saccharomyces cerevisiae* ląstelės. Plačiame diapazone įvertinta skirtingų elektrinio lauko parametrų (impulso formos, impulso trukmės, impulsų skaičius bei elektrinio lauko stiprio) įtaka mielių ląsteliniam atsakui.

Ekspimentais parodžiau, jog mielių sienelės ir membranos pralaidumai po IEL poveikio yra labai susiję. Abiejų struktūrų pralaidumas stabilizuojasi per 100 sekundžių. Remiantis matematiniu modeliavimu nustatyta, jog vidutinis tiek sienelės tiek membranos poros užsidarymo laikas yra ≈ 24 sekundės. Barjerinių struktūrų atsistatymo charakteristikų panašumas leidžia manyti, kad tiek membranos tiek sienelės atsistatymo pobūdis yra vienodas. Tai galėtų vykti jei po IEL poveikio ląstelės tūris padidėtų dėl įtekėjusio vandens ir taip lemtų barjerinių struktūrų išplonėjimą bei pralaidumo padidėjimą. Šios išvalgos papildo žinias apie ląstelinį atsaką į IEL poveikį bei leidžia IEL eksperimentus planuoti taip, kad jie vyktų efektyviai.

Ekspimentais patvirtinta, jog impulso formos kontrolė ir vizualizacija atliekant fundamentinius tyrimus yra ypatingai svarbi. Jei impulso galinio fronto forma nėra kontroliuojama, jo forma priklauso nuo terpės laidumo, o tai gali paveikti efektyvią impulso trukmę. Tyrimo rezultatai taip pat parodė, jog terpės laidumo sukeliama krintančio impulso šlaito nuožulnumo pašalinimas lemia didesnę mielių ląstelių gyvybingumą. Įdomu, jog ląstelių plazminės membranos pralaidumas išliko toks pats nepriklausomai nuo impulso formos kontrolės. Rezultatai leidžia manyti, kad tiriamą sistemą veikiant pasikartojančiais impulsais jos laidumas didės ir atitinkamai keis impulsų formą bei išeią. Tai gali lemti neatsikartojančius ar klaidingai interpretuojamus rezultatus. Mano tyrimo rezultatai rodo, jog laidumas daro įtaką tiek srovės, tiek įtampos impulsams. Taigi, norint atlikti tikslią duomenų analizę tiek fundamentiniuose tiek potencialaus elektroporacijos pritaikymo industriniams procesams tyrimuose, būtinas tikslus elektrinių lauko impulsų vaizdinimas bei jų formos kontrolė.

Taip pat man pavyko įrodyti, jog mielėmis modifikuoti elektrodai gali būti naudojami tokių ląstelių elektroporacijos tyrimui – tokie rezultatai niekada anksčiau mokslinėje literatūroje nebuvo publikuoti. Elektrodų atsakas į pieno rūgštį priklausė nuo elektrinio lauko poveikio, o signalas stiprėjo didinant elektrinio lauko stiprį. Po elektrinio lauko poveikio sumažėjo ląstelių redukcinis aktyvumas, tačiau sumažėjimas galėjo būti pilnai kompensuotas tirpalą papildžius 1 mM NADH. Menadiono srovės po elektrinio lauko poveikio tyrimų rezultatai taip pat leidžia kelti klausimus apie gyvybingumo vertinimo rinkinių, kurių sudėtyje yra mediatorių chinono pagrindu, tinkamumą elektroporuotoms ląstelėms. Manau, jog duomenys, gauti naudojant tokius gyvybingumo vertinimo rinkinius turėtų būti vertinami kritiškai, nes membranų pralaidumas gali daryti įtaką jų rezultatams (signalas silpnėnis, nors viduląstelinis fermentų aktyvumas toks pats). Man taip pat pavyko įrodyti, kad IEL technologija yra tinkama amperometrinio signalo moduliacijai. Mielėmis modifikuoti elektrodai gali būti taikomi ląstelinio atsako į elektrinio lauko poveikį tyrimams. IEL poveikis leidžia vertinti viduląstelinį metabolizmą be ląstelių lizės, leidžia tirti pralaidumo dinamiką bei ląstelinės žūties mechanizmus. Apibendrinamas galiu teigti, jog IEL sukelta permeabilizacija kombinuojama su skirtingais ląstelių paruošimo būdais, mediatoriais, inhibitoriais, substratais, kofaktoriais atvers kelią efektyviam daugiapakopiam biocheminių kelių tyrimui.

Mano žiniomis šis tyrimas taip pat buvo pirmasis, kuriame sėkmingai parodyta, jog nanosekundžių trukmės impulsai gali sukelti nuo metakaspazių priklausomai mielių ląstelių žūčiai būdingų žymenų raišką. Po poveikio užfiksuota metakaspazių aktyvacija, pralaidumas propidžio jodidui bei fosfatidilserino išvedimas į išorinę plazminės membranos dvisluoksniu pusę. Šie duomenys patvirtina, jog mielių ląstelės gali būti naudojamos kaip modelis su ląstelės žūtimi susijusių biocheminių kelių tyrinėjimui po nanosekundžių trukmės IEL poveikio.

Nanosekundžių trukmės elektrinio lauko impulsai taip pat pirmą kartą sėkmingai pritaikyti maisto žaliavos apdirbimui. Buvo parodyta, jog priklausomai nuo impulso trukmės, skirtingai veikiamas mikroorganizmų gyvybingumas. Mielių ląstelių gyvybingumas buvo slopinamas iki 14 kartų stipriau nei bakterijų. Toks poveikis gali būti pritaikytas naujų, biologiškai aktyvių produktų kūrimui išsaugant naudingas bakterijas, tačiau slopinant mielių ląsteles.

6. Išvados

1. Mielių ląstelių pralaidumą TPP^+ jonams riboja sienelė, o ne plazminė membrana. Po impulsinio elektrinio lauko poveikio ($E \approx 6 \text{ kV/cm}$) padidėja tiek mielių sienelės tiek membranos pralaidumas, tačiau tik membranoje sukeliama negrįžtamos pažaidos.
2. Stačiakampio formos impulsų įtampos kritimo profilis priklauso nuo bandinio varžos. Aktyvus jo formavimas lemia efektyvios impulso trukmės sumažėjimą per 35 % atitinkamai susilpnindamas potencialiai letalų elektrinio lauko poveikį. Tokie, nuo mėginio varžos priklausantys impulso formos ir trukmės defektai, gali sukelti iki 10 % mielių ląstelių žūties.
3. Amperometrija su hidrofiliu mediatoriumi fericianidu gali būti naudojama negrįžtamos elektroporacijos vertinimui mielių ląstelėse. Srovės stipris gautas tiriant elektrinio lauko impulsu paveiktas ląsteles ($E = 16 \text{ kV/cm}$, $\tau = 300 \mu\text{s}$) gali būti daugiau nei 10 kartų didesnis nei tiriant neveiktas mielių ląsteles.
4. Menadiono laiduojamų srovių stipris tiriant elektriniu lauku paveiktas mielių ląsteles ($E = 16 \text{ kV/cm}$, $\tau = 300 \mu\text{s}$) sumažėja iki 6 kartų ir atspindi padidėjusį membranos pralaidumą bei po to sekantį NAD(P)H kofaktorių reikalingų menadiono redukcijai ištekėjimą iš ląstelės. Matuojamos srovės sumažėjimas gali būti pilnai kompensuotas padidinus užląstelinę NADH kofaktoriaus koncentraciją iki 1 mM.
5. Mielių ląsteles paveikus penkiais nanosekundžių trukmės impulsais ($E \geq 220 \text{ kV/cm}$, $\tau = 90 \text{ ns}$), nuo kaspazių priklausomai programuotai mielių ląstelių žūčiai būdingų žymenų raiška sukeliama $\approx 73 \%$ ląstelių populiacijos.
6. Nanosekundžių trukmės elektrinio lauko impulsai gali atrankiai slopinti mielių ląstelių gyvybingumą rūgščiose išrūgose. Lyginant su bakterijų ląstelėmis, mielės elektrinio lauko poveikiui ($E = 95 \text{ kV/cm}$, $\tau = 90 \text{ ns}$, impulsų skaičius = 100) jautresnės iki 14 kartų.

7. Metodika

Tyrimams naudotos *S. cerevisiae* ląstelės. Elektriniai laukai generuoti Fizinių ir technologijos mokslų centre sukonstruotais unikaliais elektroporatoriais. Gyvybingumas vertintas skaičiuojant kolonijas formuojančius vienetus. Membranos pralaidumas, metakaspazių aktyvacija bei fosfatidilserino išvedimas vertinti fluorescencine mikroskopija, tėkmės citometrija bei fluorimetrija. Sieneles pralaidumas vertintas potenciometrijos metodu. Mielėmis modifikuoti elektrodai buvo panaudoti oksidacijos-redukcijos aktyvumo vertinimui amperometrijos metodu.

8. Autoriaus indėlis

Šio darbo autorius yra eksperimentų vykdytojas ir atliko didžiąją dalį darbe aprašytų eksperimentų. Taip pat yra pagrindinis 3 straipsnių autorius parengęs jas publikavimui.

9. Apie autorių

Povilas Šimonis gimė 1992 metais Šiauliuose. 2010 metais baigė Juliaus Janonio gimnaziją. 2014 metais baigė Bioinžinerijos bakalauro studijų programą Vilniaus Gedimino technikos universitete. 2016 metais baigė Biochemijos magistrantūros studijų programą Vilniaus Universitete. Tais pačiais metais buvo priimtas į doktorantūros studijas Fizinių ir technologijos mokslų centre.

10. Publikacijos darbo tema

1. **Simonis, P.**, Kersulis, S., Stankevich, V., Kaseta, V., Lastauskiene, E., Stirke, A. Caspase dependent apoptosis induced in yeast cells by nanosecond pulsed electric fields. *Bioelectrochemistry*. 2017; 115: 19-25. doi.org/10.1016/j.bioelechem.2017.01.005
2. **Simonis, P.**, Kersulis, S., Stankevich V., Sinkevic, K., Striguniene, K., Ragoza, G., Stirke, A., Pulsed Electric Field Effects on Inactivation of Microorganisms in Acid Whey. *International journal of food microbiology*. 2019; 291: 128-134. doi.org/10.1016/j.ijfoodmicro.2018.11.024
3. Stirke, A., Celiesiute-Germaniene, R., Zimkus, A., Zurauskiene, N., **Simonis, P.**, Dervinis, A., Ramanavicius A., Balevicius., S., The link between yeast cell wall porosity and plasma membrane permeability after PEF treatment. *Scientific Reports*. 2019; 9, 14731 doi:10.1038/s41598-019-51184-y

4. Stankevic, V., **Simonis, P.**, Zurauskiene, N., Stirke, A., Dervinis, A., Bleizgys, V., Kersulis, S., Balevicius S., Compact Square-Wave Pulse Electroporator with Controlled Electroporation Efficiency and Cell Viability. *Symmetry*. 2020, 12, 412. doi.org/10.3390/sym12030412
5. **Simonis, P.**, Garjonyte, R., Stirke, A., Mediated amperometry as a prospective method for the investigation of electroporation. *Scientific Reports*. 2020; 10, 19094. https://doi.org/10.1038/s41598-020-76086-2

11. Konferencijos bei seminarai, kuriuose pristatyti disertacijos rezultatai

1. Žodinis pranešimas “Impulsinio elektrinio lauko poveikio mielių *Saccharomyces cerevisiae* ląstelėms tyrimas amperometrijos metodu”, konferencijoje „Fiztech2019”, Vilnius, Lietuva (2019);
2. Žodinis pranešimas “Pulsed Electric Field Effects on Yeast Cells”, konferencijoje “3rd World Congress on Electroporation”, Tulūza, Prancūzija (2019);
3. Stendinis pranešimas “The Link Between Yeast Cell Wall porosity and Plasma Membrane Permeability After PEF Treatment”, konferencijoje “3rd World Congress on Electroporation”, Tulūza, Prancūzija (2019);
4. Žodinis pranešimas “Electroporation Effects on Mediated Amperometry at Yeast-Modified Electrodes”, konferencijoje “70th Annual Meeting of International Society of Electrochemistry”, Durbanas, Pietų Afrikos Respublika (2019);
5. Kviestinis pranešimas „Pulsed electric field treatment as a nonthermal pasteurization method and its effects on yeast cells“, Biotechnologijos fakultetas, Liubianos universitetas, Slovėnija (2019);
6. Žodinis pranešimas „Pulsed Electric Field (PEF) Effects on Inactivation of Microorganisms in Acid Whey“ dirbtuvėse-konferencijoje „19th Lithuania-Belarus Workshop: Advanced Microwave Devices and Systems”, Vilnius, Lietuva (2018);
7. Žodinis pranešimas „Impulsinio elektrinio lauko poveikio mielių ląstelėms tyrimas amperometrijos metodu“ konferencijoje „Fiztech2018”, Vilnius, Lietuva (2018);
8. Stendinis pranešimas „Electrochemical methods for evaluation of electric effects on yeast cells“, konferencijoje „Baltic Biophysics Conference”, Kaunas, Lithuania (2018);
9. Stendinis pranešimas „The effects of nanosecond pulsed electric fields on *Saccharomyces cerevisiae* cells“ konferencijoje „World Yeast Congress”, Montrealis, Kanada (2018);

10. Stendinis pranešimas „Investigation of a Pulsed Electric Field Effects on *Saccharomyces cerevisiae* Cells Using Mediated Amperometry“, konferencijoje „23rd topical meeting of the international society of electrochemistry“, Vilnius, Lietuva (2018);
11. Stendinis pranešimas „The effects of nanosecond pulsed electric fields on *Saccharomyces cerevisiae* cells“ konferencijoje „Openreadings 2018“, Vilnius, Lietuva (2018);
12. Stendinis pranešimas „Electrochemical methods for evaluation of electric effects on yeast cells“, konferencijoje „The COINS 2018“ Vilnius, Lietuva (2018);
13. Stendinis pranešimas „Caspase dependent apoptosis induced in yeast cells by nanosecond pulsed electric fields“, konferencijoje „2nd World Congress on Electroporation and Pulsed Electric Fields in Biology, Medicine and Food & Environmental Technologies“, Norfolkas, JAV (2017);
14. Stendinis pranešimas „Caspase dependent apoptosis induced in yeast cells by nanosecond pulsed electric fields“, konferencijoje „Openreadings 2017“, Vilnius, Lietuva (2017);
15. Žodinis pranešimas „Nanosekundžių trukmės elektrinio lauko impulsais sukeltos programuotos mielių *Saccharomyces cerevisiae* ląstelių žūties tyrimas“, konferencijoje „Bioaitėtis: gamtos ir gyvybės mokslų perspektyvos“, Vilnius, Lietuva (2016);
16. Žodinis pranešimas „Nanosekundžių trukmės elektrinio lauko impulsais sukeltos programuotos mielių *Saccharomyces cerevisiae* ląstelių žūties tyrimas“, konferencijoje „FizTech16“, Vilnius, Lietuva (2016).

ACKNOWLEDGEMENTS

This dissertation is a big milestone in my academic career, and I would like to sincerely thank my supervisor, Dr. Arūnas Stirkė. His friendly guidance, expert advice and insights have been invaluable throughout all stages of the work.

I have been fortunate to meet many inspiring scientists who gladly shared their knowledge. Prof. Habil. Dr. S. Balevičius and Prof. Dr. N. Žurauskienė taught me about scientific community and shared their knowledge in the field of physics. Dr. Skirmantas Keršulis and Dr. Voitech Stankevič helped me to conduct electroporation experiments and taught me about generation of electric field pulses. Dr. Eglė Lastauskienė facilitated the investigation of yeast programmed cell death. Dr. Vytautas Kašėta taught me to employ flow cytometry. Dr. Rasa Garjonytė taught me to employ mediated-amperometry for the investigation of yeast cell responses. Dr. Eda Demir supervised my work on PEF-assisted freezing of plant tissue. Colleagues from Bioelectrics laboratory helped to plan and perform experiments, proofread articles as well as theses. I take this opportunity to thank them.

I would like to thank government of Lithuania for financial support, Center for Physical Sciences and Technology for opportunity to perform research and alma mater Vilnius university for inspiring mentors.

Special thanks to my fiancée Adelina Skalandytė, for her continuous support and understanding. My thanks are extended to my mother Gaiva Šimonienė, father Laisvūnas Šimonis, sisters Laisvūnė and Saulė Šimonytės, brother Petras Šimonis for their constant encouragement and curiosity.

Finally, I want to thank Airidas Janušauskas, Andrius Pulkauninkas, Aušrinė Remeikienė, Martynas Remeika, Gediminas Drabavičius and Edvardas Golovinas for friendship throughout this journey, inspiration and extensive scientific discussions.

I am grateful to all these people who helped me to extend horizons of understanding, to seek knowledge and to become a better person.

LIST AND COPIES OF PUBLICATIONS

1.The link between yeast cell wall porosity and plasma membrane permeability after PEF treatment.

This article is licensed under Creative Commons Attribution 4.0 International License (<http://creativecommons.org/licenses/by/4.0/>). Full official citation of this open access article and active DOI link are provided:

Stirke, A., Celiesiute-Germaniene, R., Zimkus, A. ., Zurauskiene, N., **Simonis, P.**, Dervinis, A., Ramanavicius, A., Balevicius, S. The link between yeast cell wall porosity and plasma membrane permeability after PEF treatment. *Scientific Reports* **9**, 14731 (2019). <https://doi.org/10.1038/s41598-019-51184-y>

2.Compact Square-Wave Pulse Electroporator with Controlled Electroporation Efficiency and Cell Viability.

This article is open access and is licensed under Creative Commons Attribution 4.0 International License (<http://creativecommons.org/licenses/by/4.0/>). Regarding the request of the journal, official citation and active DOI link are provided:

Stankevici, V.; **Simonis, P.**; Zurauskiene, N.; Stirke, A.; Dervinis, A.; Bleizgys, V.; Kersulis, S.; Balevicius, S. Compact Square-Wave Pulse Electroporator with Controlled Electroporation Efficiency and Cell Viability. *Symmetry* 2020, 12, 412. <https://doi.org/10.3390/sym12030412>

3.Mediated amperometry as a prospective method for the investigation of electroporation

This article is licensed under Creative Commons Attribution 4.0 International License (<http://creativecommons.org/licenses/by/4.0/>). Full official citation of this open access article with active DOI link are provided:

Simonis, P., Garjonyte, R. & Stirke, A. Mediated amperometry as a prospective method for the investigation of electroporation. *Scientific Reports* **10**, 19094 (2020). <https://doi.org/10.1038/s41598-020-76086-2>

4.Caspase dependent apoptosis induced in yeast cells by nanosecond pulsed electric fields.

This is not an open access article, but according to a journal publishing agreement authors retain the right to reuse the article in a dissertation. Full citation and DOI link are provided as requested by the publishers:

Simonis, P., Kersulis, S., Stankevich, V., Kaseta, V., Lastauskiene, E., Stirke, A., Caspase dependent apoptosis induced in yeast cells by nanosecond pulsed electric fields, *Bioelectrochemistry*, 2017, 115, 19-25.
<https://doi.org/10.1016/j.bioelechem.2017.01.005>

5.Pulsed electric field effects on inactivation of microorganisms in acid whey.

This is not an open access article, but according to a journal publishing agreement authors retain the right to reuse the article in a dissertation. Full citation and DOI link are provided as requested by the publishers:

Simonis, P., Kersulis, S., Stankevich, V., Sinkevicius, K., Striguniene, K., Ragoza, G., Stirke, A., Pulsed Electric Field Effects on Inactivation of Microorganisms in Acid Whey, *International journal of food microbiology*. 2019, 291, 128-134. <https://doi.org/10.1016/j.ijfoodmicro.2018.11.024>

Paper 1

The link between yeast cell wall porosity and plasma membrane permeability after PEF treatment

Stirke, A., Celiesiute-Germaniene, R., Zimkus, A., Zurauskiene, N.,
Simonis, P., Dervinis, A., Ramanavicius, A., Balevicius, S.

Scientific Reports **9**, 14731 (2019). <https://doi.org/10.1038/s41598-019-51184-y>

OPEN

The link between yeast cell wall porosity and plasma membrane permeability after PEF treatment

Arunas Stirke¹, Raimonda Celiesiute-Germaniene¹, Aurelijus Zimkus², Nerija Zurauskiene¹, Povilas Simonis¹, Aldas Dervinis¹, Arunas Ramanavicius^{1,3} & Saulius Balevicius¹

An investigation of the yeast cell resealing process was performed by studying the absorption of the tetraphenylphosphonium (TPP⁺) ion by the yeast *Saccharomyces cerevisiae*. It was shown that the main barrier for the uptake of such TPP⁺ ions is the cell wall. An increased rate of TPP⁺ absorption after treatment of such cells with a pulsed electric field (PEF) was observed only in intact cells, but not in spheroplasts. The investigation of the uptake of TPP⁺ in PEF treated cells exposed to TPP⁺ for different time intervals also showed the dependence of the absorption rate on the PEF strength. The modelling of the TPP⁺ uptake recovery has also shown that the characteristic decay time of the non-equilibrium (PEF induced) pores was approximately a few tens of seconds and this did not depend on the PEF strength. A further investigation of such cell membrane recovery process using a fluorescent SYTOX Green nucleic acid stain dye also showed that such membrane resealing takes place over a time that is like that occurring in the cell wall. It was thus concluded that the similar characteristic lifetimes of the non-equilibrium pores in the cell wall and membrane after exposure to PEF indicate a strong coupling between these parts of the cell.

The molecules, which enter cells such as yeast or bacteria, must pass through the cell wall, a periplasmic space and then obtain access to the transporters located in the plasma membrane. The porosity of the yeast cell wall is highly regulated and is dependent on the cell cycle. This is important for water retention in the periplasmic space, where some important proteins, such invertase¹, alpha galactosidase² and acid trehalase³ are located. The cell wall is considered to be a sieve-like structure and does not present an absolute obstacle for solutes since it is being highly charged negatively by the phosphate and carboxyl groups in the cell wall with mannans playing the role of an ion exchanger⁴. Hence, the cell wall acts as the first selective and primary barrier for nutrients, biomolecules and ions⁵. It isn't clear, but there is some evidence that molecules such as bleomycin and tetraphenylphosphonium may also be suspended by this biosorption process^{6–9}. There are many ways to regulate (mainly to increase) the rate at which these various molecules can pass the cell wall barrier. This can be done by using chemical treatment with organic solvents and detergents¹⁰ or by mechanical shearing or treatment with a pulsed electric field (PEF), thus generating pores¹¹.

The other very important barrier for molecules diffusion is the plasma membrane. Besides simple diffusion, when gasses and small lipophilic molecules are being transported, yeast cells have many instruments (transporters and channels) to preserve cell homeostasis¹². This is the reason why the lipid bilayer is always confronted with hyper osmotic pressure at the interior of the cell due to the impermeable intracellular compounds. This osmotic pressure is the main mechanical force that stretches the plasma membrane and this can be at times the reason for cell lysis¹³. It is known that there exists a relationship between the turgor pressure and cell wall pathway integrity¹⁴. Moreover, there is evidence that the plasma membrane fluidity changes the mechanical properties of the cell wall due to the fact that some of the cell wall proteins are linked to the membrane via the GPI (glycosylphosphatidylinositol) anchor¹⁵. However, the actual molecular mechanism of such a connection is not clear.

Our previous work demonstrated that the permeability to the lipophilic ion tetraphenylphosphonium (TPP⁺) across the yeast cell membrane and cell wall may be reversibly changed by their exposure to PEF of microsecond duration⁸. Moreover, the accumulation of these TPP⁺ ions by the yeast is not affected by an electric field when

¹Center for Physical Sciences and Technology, Sauletekio ave. 3, LT-10257, Vilnius, Lithuania. ²Department of Biochemistry and Biophysics, Life Sciences Center, Sauletekio ave. 7, LT-10257, Vilnius, Lithuania. ³Department of Physical Chemistry, Faculty of Chemistry and Geosciences, Vilnius University, Naugarduko st. 24, LT-03225, Vilnius, Lithuania. Correspondence and requests for materials should be addressed to R.C.-G. (email: celiesiute@ftmc.lt)

they reach a steady-state after 90–120 min, while exposure to a high (≈ 100 kV/cm) nanosecond duration PEF speeds this process up to 65 times¹⁶. As far as we know, the influence of post-pulse resealing on the elevated TPP⁺ absorption rate has not been investigated. Moreover, as was noted, the duration and character of the transient pore decay is essential for understanding the mechanism of PEF induced yeast cell permeabilization¹⁷.

In this paper, we investigated yeast cell electrical permeabilization by applying a PEF regime, which does not affect the viability of the cells, i.e. most of the cells can recover to their initial (non-permeabilized) state. These investigations were performed by applying two different methods. One method was based on the study of the TPP⁺ ion absorption kinetics using a potentiometric ion selective electrode, which provides data about the yeast cell wall permeabilization. Another method, based on fluorescent dye measurements, showed the permeabilized state of the cell membrane. These experimental results were analyzed by applying the mathematical model, which took into consideration the decay of the post-pulse transient pores. Experiments and modeling have shown a strong link between the yeast cell membrane and the wall resealing process after PEF action.

Materials and Methods

Yeast strain and cultivation. *Saccharomyces cerevisiae* SEY6210 (*MAT α* , *leu2-3*, *leu2-112*, *ura3-52*, *his3- Δ 200*, *trp1- Δ 901*, *lys2-801*, *suc2- Δ 9*, *GAL*) yeast cells were grown to their early exponential growth phase in a complete medium (YPD) containing 1% (w/v) yeast extract, 2% (w/v) peptone and 2% (w/v) glucose (Merck, Darmstadt, Germany). The yeast cells were then re-suspended in 1 ml of a cold (4 °C) electroporation buffer (EPB) containing 1 M sorbitol and a 20 mM Tris-HCl buffer, pH 7.4 (Applichem, Darmstadt, Germany) while keeping the final concentration of the yeasts at the $(4-6) \times 10^9$ colony forming unit (CFU)/mL. Cell density was determined by measuring the optical density (OD) using an optical absorption spectrophotometer (Halo RB-10, Dynamica Scientific, UK) operating at a wavelength of 600 nm.

Spheroplasts preparation. After the modification cells were pelleted, washed twice and suspended in a lyticase specific buffer, additional control samples of non-modified cells were prepared in parallel. The lyticase buffer containing 1.2 M of sorbitol, 0.5 mM of MgCl₂ and 35 mM of K₂HPO₄ (pH 6.0) was adjusted for this solution according to our previous report¹⁸. The final optical density of the diluted suspension was 1.5 OD (600 nm). A further 50 U/ml of lyticase were added to each cell sample and then incubated at 30 °C for 2 hours. To prove that the lyticase enzyme was active during the experiment, its optical density was measured at 600 nm before and after the incubation cycles of the sample suspensions. After such digestion, both cell samples were inspected with a bright field optical microscope. For spheroplasts preparation, the yeast cells ($\approx 1 \cdot 10^7$ cells/ml) were suspended and washed with sterile water. After that, the cells were harvested by centrifugation and resuspended in a SCEM buffer (1 M sorbitol, 0.1 M sodium citrate (pH = 5.6), 10 mM EDTA and 30 mM 2-mercaptoethanol (Merck KGaA, Germany)). Then 30 U/mL of lyticase (Sigma-Aldrich, USA) was added for digestion by the cell walls. After a 2-hour incubation at 30 °C with occasional inversions, the cells were then collected, washed and re-suspended using a STC buffer (1 M sorbitol, 10 mM Tris-HCl (pH = 7.5), 10 mM CaCl₂ (Merck KGaA, Germany)) by centrifugation at 200-g 5 min.

Pulsed electric field treatment technique. A programmable electroporator for the generation of high-voltage square-wave electric pulses (developed at the Center for Physical Sciences and Technology, Vilnius, Lithuania) was used for the PEF experiments. This electroporator has a variable energy storage capacitor, thus accumulation of high energy is avoided. It generates a single or a sequence of single electrical pulses with widths from 3 μ s to 10 ms and voltages up to 3.5 kV. It has an LCD screen for the monitoring of the input parameters and an additional LCD screen for the display of the pulse waveform (the current passing through the cuvette with the yeast sample) during the experiment. When experiments are performed with a 2 mm gap electroporation cuvette (VWR International, Taiwan) connected to the device, the electric field strength across the cuvette can reach up to about 16 kV/cm.

Cell wall permeability measurements. For the investigation of the permeability of the yeast cell wall, the concentration changes of TPP⁺ ions as a function of time was measured. A custom-build mini-potentiostat with a special high sensitivity electronic circuit, protected against static electrical interference, was used for the measurements¹⁹. The electrode with the selective membrane was fabricated according to the protocol found in the literature²⁰. During all measurements of the changes of the lipophilic tetraphenylphosphonium (TPP⁺) ion concentrations, the TPP⁺ chloride (Acros Organics, Belgium) was used. For all the measurements, the intact yeast cell and spheroplasts suspension concentrations were the $4-6 \times 10^9$ colony forming unit (CFU)/mL. For the evaluation of the changes of the TPP⁺ concentration in both yeast suspensions, 200 μ L of the yeast suspension was added to 2 mL of a 1 μ M concentration TPP⁺ solution and the potentiometric changes were recorded. The concentration of TPP⁺ ions was calculated from the calibration curve¹⁹.

To evaluate the role of the cell wall and cell membrane in the TPP⁺ absorption process, square waveform electrical pulses of 150 μ s duration and amplitudes of electric field strength (E) (up to 4.2 kV/cm) were applied to the intact yeast cells and spheroplasts.

To investigate the resealing of the yeast cell walls after such PEF treatment, the TPP⁺ was added to the electroporation cuvette with the yeast suspension. The initial TPP⁺ concentration (N_{is}) of 1 μ M was added to the cuvette at different time intervals ($\Delta t = 5, 10, 20, 30, 40, 50, 60, 80, 120$ and 180 seconds) after the PEF treatment ($E = 5.85, 4.38$ and 2.93 kV/cm, $t_p = 150$ μ s). It was then incubated for $t = 3$ min. at 20 °C in each case and centrifuged in order to get cell free supernatant. These experiments were repeated three times and presented as means values. The quantity of TPP⁺ (N) absorbed by the yeast cells ($N = N_{is} - [\text{TPP}^+]_{\text{supernatant}}$) was expressed as the accumulation ratio N/N_m , where N_m is the maximal concentration of TPP⁺ that can be accumulated in yeast⁶.

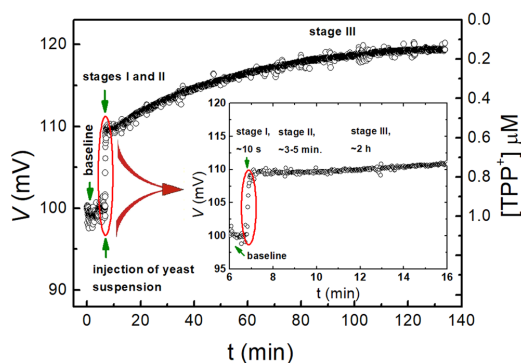


Figure 1. The response signal from the TPP⁺ selective electrode vs. time dependence in the yeast suspension. The stages of the TPP⁺ ions absorption kinetics are outlined in the inset.

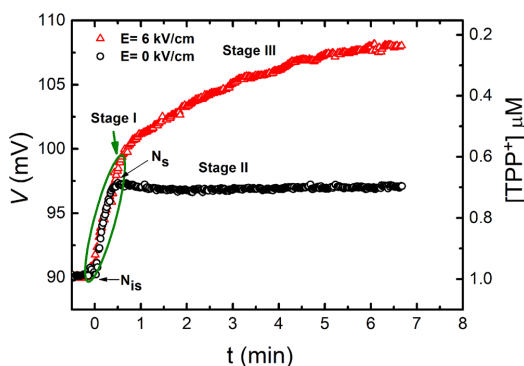


Figure 2. The response of the signal from the TPP⁺ selective electrode vs. time dependence in the yeast suspension, when $E = 0$ kV/cm (circles), and 6 kV/cm (triangles).

Investigation of the resealing of the cell membrane. The resealing of the cell membrane after treatment with PEF (square waveform electric pulses with amplitude of 5.85 kV/cm and duration of 150 μ s) was evaluated using fluorescent dye²¹ (by loading the cell with Fluorescent SYTOX Green nucleic acid stain (ThermoFisher Scientific, USA)). During the investigation, the yeast cell suspension was kept on ice. The fluorescent dye was added to the suspension of up to a 125 nM final concentration at different time intervals in the range from 10 s to 600 s after exposure to the PEF. After incubation for one minute, the specimen was placed into the fluorescence measurements cuvette (light path of 1 cm) of spectrometer LS50B (Perkin Elmer, USA) and exposed to 505 \pm 5 nm wavelength light. The cell membrane permeability was evaluated as the fluorescence spectrum intensity at a peak wavelength equal to 529 nm.

Results

TPP⁺ absorption by yeast cells. The ability of the yeast cells to accumulate the TPP⁺ ions was investigated by measuring the kinetics of the TPP⁺ absorption by the cells not treated with the electric field. For this purpose, 200 μ L of the yeast suspension was injected into a 2 mL solution having different concentrations of TPP⁺ ions. The typical signal of the response from the TPP⁺ selective electrode vs. time dependence reflecting the amount of absorbed TPP⁺ ions is shown in Fig. 1. As it can be seen, the TPP⁺ ions uptake kinetics consisted of three stages. These were (i) stage I, lasting ~10 s. This was the fast stage, which appeared immediately after the injection of the yeast cells into the TPP⁺ solution; (ii) stage II, or the delay stage, which lasted approximately 3–5 minutes after the fast stage, when the concentration of the TPP⁺ changes became no more than 10% (see inset in Fig. 1) and (iii) stage III, when the slow TPP⁺ absorption took place and saturation was reached after ~2 hours.

PEF influence on TPP⁺ absorption. The influence of the PEF on the kinetics of the TPP⁺ uptake is shown in Fig. 2. The circular symbols (black) in Fig. 2 correspond to the TPP⁺ absorption by the yeast cells, which were not affected by the PEF and all show the three TPP⁺ uptake stages as was described in previous section. The

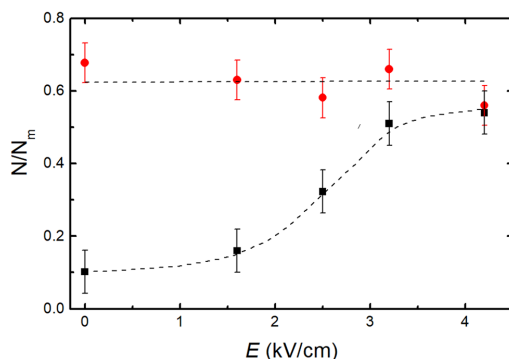


Figure 3. A comparison of the relative change of the TPP⁺ concentration (N) normalized to the maximal value (N_m) accumulated by intact yeast cells (square dots) and wall-free spheroplasts (circular dots) 3 min. after PEF treatment (150 μ s pulse duration, up to 4.2 kV/cm electric field strength).

triangular symbols (red) show the kinetics of the TPP⁺ absorption by the yeast after exposure to PEF of 6 kV/cm strength and 150 μ s duration. As can be seen in the figure, stage II, i.e. the delay of the TPP⁺ uptake is absent and the fast TPP⁺ concentration decrease (response to the voltage increase corresponding to stage I), is changed to a slower one (stage III). In both cases, (the cells affected and not affected by the PEF), the fast stage was of the same rate, but of a slightly different amplitude. It was thus obvious that the PEF significantly changes the TPP⁺ absorption rate, i.e. it eliminates the delay stage.

TPP⁺ absorption by spheroplasts. For a comparison of the PEF action on intact yeast cells containing wall and wall-free spheroplasts, the TPP⁺ absorption measurements were performed at different electric field strengths. Figure 3 presents the ratio N/N_m dependence on E , where N is the TPP⁺ amount accumulated by yeast cells after a 3 min. exposure to 1 μ M of TPP⁺.

As it can be seen from Fig. 3, the influx of TPP⁺ in the case of the intact yeast increased with an increase of the PEF strength. However, there were no changes of the TPP⁺ influx in the case of wall-free spheroplasts. It is thus evident that PEF can affect the TPP⁺ influx only in the yeast cells having walls and that the cell walls are mainly responsible for the changes of the TPP⁺ uptake rates of the yeast cells.

The recovery of cell membrane and wall barrier function after PEF. Our previous investigations demonstrated that high amplitude PEF is able to increase the rate of TPP⁺ ions uptake by several times and that saturation is reached in relatively short period of time. As it was found that PEF amplitude not exceeding 6 kV/cm with pulse duration of 150 μ s does not affect yeast cells viability⁸, thus these PEF parameters were applied in this study.

Cell membrane resealing after PEF. To study the permeability of the cell membrane after treatment with PEF, the fluorescent dye SYTOX Green was used. The fluorescent dye was added to the cell suspension with different time delays ($\Delta t = 10, 30, 90, 180, 360$ and 600 seconds) after treating the cells with PEF (150 μ s pulse duration 5.85 kV/cm electric field strength). Figure 4 shows the intensity of the fluorescent spectrum peak value (529 nm) vs. time (Δt) of the fluorescent dye added to the cells after PEF.

The experimental data presented in Fig. 4 show that the fluorescence intensity drops with the increase of time after cell treatment by PEF down to the level of the residual intensity (I_r). The total decay time showing cell membrane relaxation to their initial state after PEF action is approximately 100 seconds and the fluorescence intensity decay can be well fitted by the exponential expression:

$$I = I_0 \cdot \exp\left(-\frac{\Delta t}{\tau_i}\right) + I_r \quad (1)$$

here I_0 is the fluorescence intensity at $\Delta t = 0$ and τ_i is the characteristic decay time of the lipidic pores. This model describes that part of the resealing process, where the change of fluorescence intensity is fast (see Fig. 4 solid curve a,b). The fitting results show that permeability of a significant part of the cell membrane recovers to its initial state in a characteristic time $\tau_i \approx 20$ s. The difference between fluorescence intensity of untreated cells (Fig. 4, black circle) and the residual intensity (Fig. 4, dashed line c,d) might be related to the extended membrane resealing processes due to the experimental setup where the cells were kept on ice²².

Cell wall recovery after PEF. The recovery of the barrier function of the cells walls was investigated by analyzing the TPP⁺ absorption process of the yeast cells after PEF action with pulse amplitudes of three different electric field strengths. The results of this investigation are presented in Fig. 5.

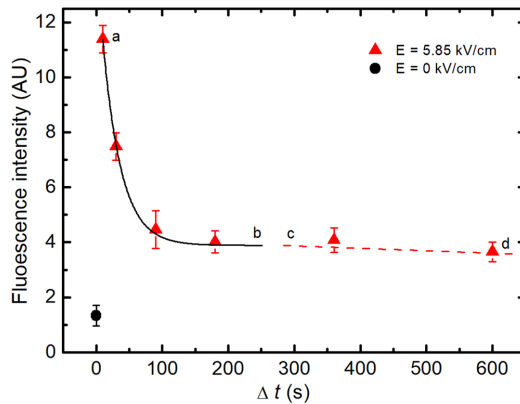


Figure 4. Fluorescence spectrum peak (at 529 nm) intensity vs. time (Δt) of the dye added to the cells after PEF treatment (triangles). The black circle shows the intensity of the fluorescence in the case of the control (untreated) cells. The solid curve (a,b) obtained using Eq. (1), adj. R^2 is 0.99394. The dashed line (c,d) represents the extended membrane resealing processes.

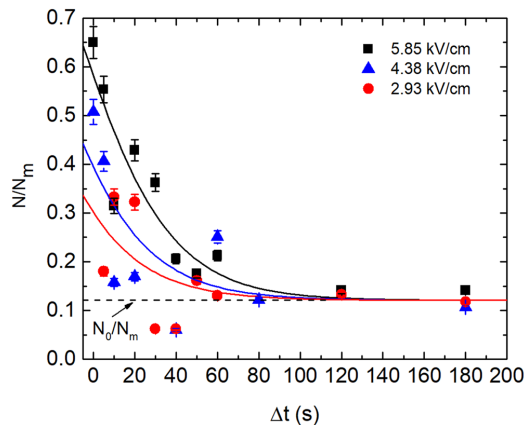


Figure 5. The dependence of TPP^+ absorption by yeast cells over time after PEF treatment. The y axis represents the relative TPP^+ amount accumulated in the yeast cells; the x axis represents the TPP^+ injection time after PEF treatment. The dashed line represents the full recovery of the TPP^+ absorption level by the yeast cells (PEF = 0) after 3 minutes of incubation. The solid curves were obtained by using Eq. (10), adj. R^2 values are 0.854 (rectangles), 0.582 (triangles) and 0.341 (circles).

Here N/N_m is the ratio between the TPP^+ amount (N) accumulated inside the yeast cells after 3 min. exposure in a TPP^+ solution and the maximal amount (N_m) of TPP^+ which can be accumulated in the tested volume of yeast (without PEF action). The dashed line (N_0/N_m) represents the full recovery of the TPP^+ absorption process which corresponds to the relative amount of TPP^+ ($N_0/N_m \approx 0.12$) absorbed during 3 min. of incubation. With the rise of the electric field strength from 2.93 kV/cm to 5.85 kV/cm, the relative TPP^+ amount absorbed by cells drops to the full recovery level in approximately 90–110 seconds. The solid curves in Fig. 5 represent fitting results using model described in the next Section. It has to be noted that the characteristic time evaluated from modelling results was obtained similar for all three electric field strengths.

The modelling of cell wall recovery process after PEF. The experimental results presented in Fig. 5 show that the recovery of the yeast cell wall after PEF action takes place in a relatively short time when compared to the duration of the whole 1.5 h-long TPP^+ ions absorption process (without PEF) until the steady state is reached (see Fig. 1). This means that the post-pulse transient pores in cell wall responsible for the increase of TPP^+ absorption rate exist only for a few minutes after the electric pulse action. At high electric field strength

(more than 6 kV/cm), the TPP⁺ ions uptake by the yeast significantly increases and saturation is reached in a relatively short time⁸. In such case, the TPP⁺ ions absorption process was described while ignoring the cell wall recovery after the PEF action. Thus for the description of TPP⁺ absorption kinetics, the following pseudo-second order differential equation was used⁸:

$$\frac{dN(E, t)}{dt} = k_{\alpha}(E, t) \cdot (N_m - N)(N_s - N); \tag{2}$$

here $N(t)$ is the time dependent concentration of the TPP⁺ ions in the supernatant, N_m is maximal change of the TPP⁺ concentration during the slow period of TPP⁺ accumulation by the yeast and N_s is the concentration of TPP⁺ ions at the beginning of stage II (corresponding to TPP⁺ concentration at the time instant when the absorption process starts (see Fig. 2)), k_{α} is absorption rate coefficient. It was assumed, that k_{α} depends on the electric field strength as follows⁸:

$$k_{\alpha} = k_{\alpha 0} + b(E_p - E_{th,p})^2 f^2 \left[1 - \exp\left(-\frac{t_p}{t_{ch}}\right) \right]^2; \tag{3}$$

here b is the empirical constant, which shows the effectiveness of the electric field on permeabilization, f is the cell shape factor (1.5 for spheres), E_p is the amplitude of electric field strength, $E_{th,p}$ is the threshold electric field strength at which the TPP⁺ absorption rate begins to be dependent on the electric field, t_p is the pulse duration and t_{ch} is the characteristic time required to charge the membrane as a capacitor.

However, at lower amplitudes of electric field strength (less than 6 kV/cm in our case), the decay of the post-transient pores in the cell walls can significantly change the kinetics of the TPP⁺ ions adsorption by the yeast cells. For this reason, the coefficient k_{α} in Eq. (2) was modified by considering that it was not only a function of the pulsed electric field strength and duration, but also depended on the resealing of the transient pores after PEF action.

In order to obtain a mathematical expression of coefficient's k_{α} dependence on time, we made the following assumptions: (a) that the PEF permeabilization which facilitated the TPP⁺ ions diffusion is proportional to the number of pores in the cell wall; (b) that the generation of the additional post-pulse non-equilibrium pores is the result of PEF action and that the number of these pores depends on the PEF energy (amplitude and duration of the square waveform pulses); (c) that the characteristic lifetime of the post-pulse transient non-equilibrium pores and the naturally existing equilibrium pores is different. Based on these assumptions the following expression of k_{α} was suggested:

$$k_{\alpha}(E, t) = k_{\alpha 0} + C \cdot \Delta M_p(E, t); \tag{4}$$

here $k_{\alpha 0}$ is the absorption coefficient at $E = 0$ kV/cm, $\Delta M_p(E, t) = M_p - M_{p,eq}$ is the difference between the whole amount of post-pulse transient non-equilibrium pores (M_p) and the amount of naturally existing equilibrium pores ($M_{p,eq}$), and C is a constant. The dependence of ΔM_p on time can be obtained from the following first order differential equation:

$$\frac{d(\Delta M_p)}{dt} = -k \cdot (\Delta M_p); \tag{5}$$

here $k = 1/\tau_d$ (τ_d is the characteristic lifetime of the PEF induced pore). The solution of the Eq. (5) is the following:

$$\Delta M_p(t) = \Delta M_{p0} \cdot e^{-\frac{t}{\tau_d}}; \tag{6}$$

here ΔM_{p0} is the initial amount of post-pulse transient non-equilibrium pores generated after the PEF action. Taking into account Eqs (3, 4), one can express ΔM_{p0} as a function of electric field strength:

$$\Delta M_{p0} = \frac{b}{C}(E_p - E_{th,p})^2 f^2 \left[1 - \exp\left(-\frac{t_p}{t_{ch}}\right) \right]^2. \tag{7}$$

The solution of Eq. (2) using Eqs (4) and (6) is the following:

$$N(t) = \frac{N_m(1 - S)}{1 - R \cdot S}; \tag{8}$$

$$\text{here } R = \frac{N_m}{N_s} \text{ and } S = e^{(N_m - N_s) \left[k_{\alpha 0} t + C \cdot \Delta M_{p0} \tau_d (1 - e^{-\frac{t}{\tau_d}}) \right]}. \tag{9}$$

We considered the TPP⁺ ions absorption delay at the time intervals Δt after the PEF action (Fig. 5). This could be described by Eq. (8) using modified expression (9). It has to be noted that Eqs (8 and 9) represent the solution of Eq. (2) in which the time t starts from the moment when TPP⁺ was added to the cuvette with the yeast suspension. In order to investigate the absorption delay, an experiment was performed by adding TPP⁺ with a Δt delay after PEF action. Therefore, ΔM_{p0} in Eq. (9) had to be replaced by $\Delta M_{p0} \exp(-\Delta t/\tau_d)$, because the concentration

of the non-equilibrium pores had exponentially decreased during the time Δt . In such case, the S in Eq. (9) is modified as follows:

$$S_{\Delta t} = e^{(N_m - N_0)k_{ad}t + C \Delta M_{p0} \tau_d \left(e^{-\frac{t}{\tau_d}} \right) \left(1 - e^{-\frac{\Delta t}{\tau_d}} \right)}. \quad (10)$$

The solid curves in Fig. 5 show the fitting of the experimental data using modified Eq. (8), when $S_{\Delta t}$ instead of S (see Eq. (9)) was used:

$$\frac{N(t, \Delta t)}{N_m} = \frac{1 - S_{\Delta t}}{1 - R \cdot S_{\Delta t}}. \quad (11)$$

During fitting the incubation time t , after which the absorption of the TPP⁺ was measured, was kept constant $t = 3$ min. The level N_0/N_m marked by the dashed line in Fig. 5 corresponds to the full recovery of the cell wall, where N_0 is the amount of the TPP⁺ absorbed by untreated yeast cells:

$$\frac{N_0}{N_m} = \frac{1 - S_0}{1 - R \cdot S_0}; \quad (12)$$

here S_0 is:

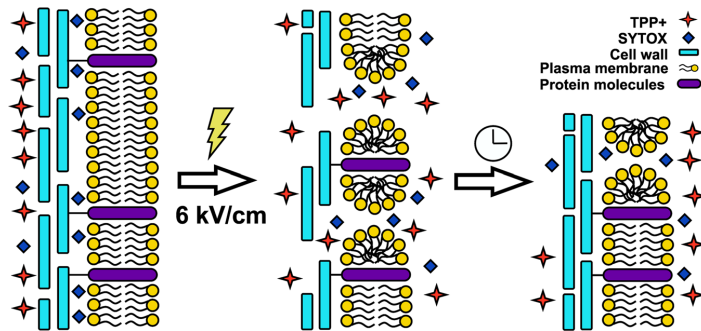
$$S_0 = e^{(N_m - N_0)k_{ad}t}. \quad (13)$$

Thus, the $N/N_m - N_0/N_m$ in Fig. 5 shows the difference between the TPP⁺ amount absorbed by the PEF affected cells (N) at Δt and the amount of TPP⁺ absorbed by the untreated yeast cells (N_0) relative to maximal amount N_m . The data when $\Delta t = 0$ in Fig. 5 represent the N/N_m ratio immediately after the PEF action. One can see that at $\Delta t = 0$ for $E = 5.85$ kV/cm, the ratio $N/N_m \approx 0.65$, which is in good agreement with the results presented in⁸, where the absorption coefficient's k_a dependence on E was expressed as Eq. (3) without considering its dependence on delay time Δt . The fitting results using this model (solid curves in Fig. 5) show that the characteristic time (τ_d) of the wall recovery almost does not depend on the PEF electric field strength. Due to scatter of experimental data the fitting procedure resulted in τ_d values in the range of (21–27) s, thus the solid curves in Fig. 5 were shown for average $\tau_d = 24$ s.

Discussion

Tetraphenylphosphonium (TPP⁺), a lipophilic cation is widely used as a probe for various cells as well as an artificial membrane potential measurements^{20,23–26}. The ability of the aromatic groups to delocalize and shield the electric charge and to increase the lipid solubility facilitates their translocation across the hydrophobic barrier^{27,28}. The accumulation of TPP⁺ ions in yeast cells strongly depends on various factors, such as the yeast strain, the properties of the cell wall, the yeast growth phase, the growing conditions and mutations determining the structure of the cell wall and others^{25,29–31}. Unlike structurally similar compound dibenzyltrimethylammonium, TPP⁺ is not transported via the thiamine transport system, nor via another inducible translocation mechanism. As described in the literature, the uptake of TPP⁺ ions into the yeast cells has distinct stages. Two groups of authors, Eraso *et al.* and Slayman *et al.* observed the biphasic uptake of TPP⁺ when the yeast was collected in the logarithmic phase of growth^{25,32}. In both cases, the exponential and quasi-linear stages were outlined. Ketteter *et al.* experimented with artificial lipid bilayer membranes, which showed a three-stage uptake: (1) adsorption to the membrane-solution interface; (2) passage of the ion to the opposite interface; and (3) desorption into the aqueous solution. The rate-determining step is the jump from the adsorption site into the aqueous phase²⁴. For lipophilic molecules such as TPP⁺, it usually takes from 0.5 up to 2 or more hours to reach the steady state^{25,32}. In our experiments, three stages of TPP⁺ uptake was observed (Fig. 1). Stage I was due to the injection of yeast suspension into the sample; stage II, when the TPP⁺ concentration changes were delayed for several minutes. As far as we know, these were absent in the works of other authors due to the different experimental setups. The last stage, i.e. stage III, consisting of slow TPP⁺ absorption and a plateau, is similar to biphasic TPP⁺ absorption, which is outlined in the works of Eraso *et al.* and Slayman *et al.*^{25,32}.

Stage I in our experiments could be explained by TPP⁺ ions adsorption on the surfaces of negatively charged yeast cells⁴ and the interaction between it and the positive TPP⁺ ions (i.e. sorbate). A similar behavior of the sorbate was observed during the investigation of the yeast cells, when the fast, reversible and metabolically-independent adsorption step was attributed to the cell wall surface complexation with metal cation uptake³³. The stage II, i.e. delay stage, could be explained by the additional time needed for the TPP⁺ ions to reach the surface of the plasma membrane through the cell wall and periplasmic space. The slow stage reflects the process of TPP⁺ absorption deeper inside the yeast cell and through the membrane. It should be noted that due to the large TPP⁺ concentration at the surface of the cell, the expulsion of TPP⁺ ions from the cell to the solution has to be negligible. Thus, the yeast cells accumulate TPP⁺ ions mainly during the last slow stage. As is known, the main ion transport systems into the yeast cell include ion pumps, several transporters, a potassium channel and a non-selective cation current. The presence of a complex structure cell wall adds more complexity for ion transport. Thus, the TPP⁺ absorption experiments were performed in cell wall-free spheroplasts, which were obtained by degrading the wall with the enzyme lyticase. Such spheroplasts provide an easy means to manipulate the experimental system for studies of whole genome transferring³⁴, cell fusion³⁵ or toxin transport³⁶. In our experiments, the system of spheroplasts served for the clarification of the role of the cell wall in TPP⁺ absorption. As seen from Fig. 3 (circular dots), the PEF strength had no effect on TPP⁺ absorption for spheroplasts, which was almost the



Scheme 1. Schematic overview of the cell wall and the resealing of the cell membrane after the PEF treatment.

same at all applied electric field strengths including $E = 0$. This result showed that the main barrier for TPP^+ ion absorption is the cell wall, not the membrane.

The experimental results presented in Figs 4 and 5 demonstrated that both the membrane and the wall relaxation process after PEF lasted for approximately 100 s. Moreover, the characteristic time of these relaxations evaluated by means of mathematical simulations was also of the same order. Good fitting was also obtained at all the different electric field strengths, which had been applied, of the same characteristic lifetime of the post-pulse transient pores in the cell walls. This was $\tau_d = 24$ s, which was close enough to the characteristic lifetime of lipidic pores, which was $\tau_l \approx 20$ s (see Fig. 4). However, as is known from molecular dynamics related with thermal processes, the post-pulse lipidic pore lifetime is in the range from 100 ns⁴⁷ to 3-ms^{37,38}, which is drastically shorter than the characteristic relaxation time observed in our experiments. Moreover, experimental investigation showed that this relaxation time could range from milliseconds³⁹ to several hours if the cells are cooled down after electroporation by putting them on ice²². It is evident, that the lifetimes of the lipid pores may vary along a broad range and depend on the experimental setup or the object⁴⁰. In our case, however, this cannot be attributed to the pores, which disappear via spontaneous thermal fluctuations. Yeast treatment with PEF simultaneously induces permeabilization of the whole cell barrier, i.e. both the cell wall and the membrane. The recovery of these parts to a non-permeabilized state takes a similar time (Scheme 1).

The strong connection between the resealing of the yeast cell membrane and the wall recovery allows one to assume that this recovery process is “mechanical” in nature, which could be related to changes of osmotic pressure during electroporation and the processes taking place after the PEF. The verification of this hypothesis could be an object of future investigations.

In conclusion, our investigations confirmed that the rate of absorption of the TPP^+ ions into the yeast cells is stimulated by the action of the pulsed electric field (PEF). Moreover, as the main barrier to the influx of TPP^+ ions is the cell wall and the PEF stimulates the generation of transient (non-equilibrium) pores in this wall, this is responsible for the increase of the TPP^+ ions absorption rate. It was demonstrated that the treatment of the yeast by the PEF simultaneously induces permeabilization of both parts of this cell barrier, i.e. the cell wall and the membrane. The characteristic time of recovery of these parts to a non-permeabilized state takes several tens of seconds, what demonstrates a strong coupling between these processes.

References

- Carlson, M. & Botstein, D. Two differentially regulated mRNAs with different 5' ends encode secreted and intracellular forms of yeast invertase. *Cell* **28**, 145–154, [https://doi.org/10.1016/0092-8674\(82\)90384-1](https://doi.org/10.1016/0092-8674(82)90384-1) (1982).
- Sumner-Smith, M., Bozzato, R. P., Skipper, N., Davies, R. W. & Hopper, J. E. Analysis of the inducible MEL1 gene of *Saccharomyces carlsbergensis* and its secreted product, alpha-galactosidase (melibiase). *Gene* **36**, 333–340, [https://doi.org/10.1016/0378-1119\(85\)90188-X](https://doi.org/10.1016/0378-1119(85)90188-X) (1985).
- Parrou, J. L., Jules, M., Beltran, G. & François, J. Acid trehalase in yeasts and filamentous fungi: Localization, regulation and physiological function. *FEMS Yeast Res.* **5**, 503–511, <https://doi.org/10.1016/j.femsyr.2005.01.002> (2005).
- Orlean, P. Architecture and biosynthesis of the *Saccharomyces cerevisiae* cell wall. *Genetics* **192**, 775–818, <https://doi.org/10.1534/genetics.112.144485> (2012).
- François, J. M. In *Yeast Membrane Transport* (eds José Ramos, Hana Sychrová, & Maik Kschischo) 11–31 (Springer International Publishing, 2016).
- Aouida, M., Tounekti, O., Belhadj, O. & Mir, L. M. Comparative roles of the cell wall and cell membrane in limiting uptake of xenobiotic molecules by *Saccharomyces cerevisiae*. *Antimicrob. Agents Chemother.* **47**, 2012–2014, <https://doi.org/10.1128/aac.47.6.2012-2014.2003> (2003).
- Yasuda, K., Ohmizo, C. & Katsu, T. Potassium and tetraphenylphosphonium ion-selective electrodes for monitoring changes in the permeability of bacterial outer and cytoplasmic membranes. *Journal of Microbiological Methods* **54**, 111–115, [https://doi.org/10.1016/S0167-7012\(02\)00255-5](https://doi.org/10.1016/S0167-7012(02)00255-5) (2003).
- Stirke, A. *et al.* Electric field-induced effects on yeast cell wall permeabilization. *Bioelectromagnetics* **35**, 136–144, <https://doi.org/10.1002/bem.21824> (2014).
- Ballarín-Denti, A., Slayman, C. & Kuroda, H. Small lipid-soluble cations are not membrane voltage probes for *Neurospora* or *Saccharomyces*. *Biochimica et Biophysica Acta (BBA) - Biomembranes* **1190**, 43–56, [https://doi.org/10.1016/0005-2736\(94\)90033-7](https://doi.org/10.1016/0005-2736(94)90033-7) (1994).

10. Jamur, M. C. & Oliver, C. Permeabilization of cell membranes. *Methods in molecular biology (Clifton, N.J.)* **588**, 63–66, https://doi.org/10.1007/978-1-59745-324-0_9 (2010).
11. Ganeva, V., Galutov, B. & Teissie, J. Evidence that Pulsed Electric Field Treatment Enhances the Cell Wall Porosity of Yeast Cells. *Appl. Biochem. Biotechnol.* **172**, 1540–1552, <https://doi.org/10.1007/s12010-013-0628-x> (2014).
12. José Ramos, H. S. a. M. K. *Yeast Membrane Transport*. Vol. 892 (Springer Nature Switzerland AG, 2016).
13. Cohen, B. E. Membrane Thickness as a Key Factor Contributing to the Activation of Osmosensors and Essential Ras Signaling Pathways. *Frontiers in Cell and Developmental Biology* **6**, <https://doi.org/10.3389/fcell.2018.00076> (2018).
14. Levin, D. E. Cell Wall Integrity Signaling in *Saccharomyces cerevisiae*. *Microbiol. Mol. Biol. Rev.* **69**, 262, <https://doi.org/10.1128/MMBR.69.2.262-291.2005> (2005).
15. Dupont, S., Rapoport, A., Gervais, P. & Beney, L. Survival kit of *Saccharomyces cerevisiae* for anhydrobiosis. *Appl. Microbiol. Biotechnol.* **98**, 8821–8834, <https://doi.org/10.1007/s00253-014-6028-5> (2014).
16. Stirke, A. *et al.* Permeabilization of yeast *Saccharomyces cerevisiae* cell walls using nanosecond high power electrical pulses. *Applied Physics Letters* **105**, 253701, <https://doi.org/10.1063/1.4905034> (2014).
17. Weaver, J. C. a. V. & Thomas, P. Pore lifetimes in cell electroporation: Complex dark pores? *ARXIV eprint arXiv:1708.07478* (2017).
18. Kawai, S., Hashimoto, W. & Murata, K. Transformation of *Saccharomyces cerevisiae* and other fungi: Methods and possible underlying mechanism. *Bioengineered Bugs* **1**, 395–403 (2010).
19. Balevicus, Z. *et al.* Compact high-sensitivity potentiometer for detection of low ion concentrations in liquids. *Review of Scientific Instruments* **89**, 044704, <https://doi.org/10.1063/1.5023443> (2018).
20. Moreno, A. J., Santos, D. L., Magalhães-Novais, S. & Oliveira, P. J. Measuring Mitochondrial Membrane Potential with a Tetraphenylphosphonium-Selective Electrode. *Current Protocols in Toxicology* **65**, 25.25.21–25.25.16, <https://doi.org/10.1002/0471140856.tx2505s65> (2015).
21. Garcia, P. A., Ge, Z., Moran, J. L. & Buie, C. R. Microfluidic Screening of Electric Fields for Electroporation. *Sci. Rep.* **6**, 21238, <https://doi.org/10.1038/srep21238> (2016).
22. Yano, K. I. *et al.* Bioelectrics: Biological Responses. In *Bioelectrics*, 155–274 (2017).
23. Boxman, A. W., Barts, P. W. J. A. & Borst-Pauwels, G. W. F. H. Some characteristics of tetraphenylphosphonium uptake into *Saccharomyces cerevisiae*. *Biochimica et Biophysica Acta (BBA) - Biomembranes* **686**, 13–18, [https://doi.org/10.1016/0005-2736\(82\)90146-8](https://doi.org/10.1016/0005-2736(82)90146-8) (1982).
24. Ketterer, B., Neumcke, B. & Läger, P. Transport mechanism of hydrophobic ions through lipid bilayer membranes. *The Journal of Membrane Biology* **5**, 225–245, <https://doi.org/10.1007/bf01870551> (1971).
25. Eraso, P., Mazón, M. J. & Gancedo, J. M. Pitfalls in the measurement of membrane potential in yeast cells using tetraphenylphosphonium. *Biochimica et Biophysica Acta (BBA) - Biomembranes* **778**, 516–520, [https://doi.org/10.1016/0005-2736\(84\)90402-4](https://doi.org/10.1016/0005-2736(84)90402-4) (1984).
26. Labajova, A. *et al.* Evaluation of mitochondrial membrane potential using a computerized device with a tetraphenylphosphonium-selective electrode. *Analytical Biochemistry* **353**, 37–42, <https://doi.org/10.1016/j.ab.2006.03.032> (2006).
27. Altenbach, C. & Seelig, J. Binding of the lipophilic cation tetraphenylphosphonium to phosphatidylcholine membranes. *Biochimica et Biophysica Acta (BBA) - Biomembranes* **818**, 410–415, [https://doi.org/10.1016/0005-2736\(85\)90016-1](https://doi.org/10.1016/0005-2736(85)90016-1) (1985).
28. Ross, M. F. *et al.* Lipophilic triphenylphosphonium cations as tools in mitochondrial bioenergetics and free radical biology. *Biochemistry. Biokhimiia* **70**, 222–230 (2005).
29. De Nobel, J. G. & Barnett, J. A. Passage of molecules through yeast cell walls: A brief essay-review. *Yeast* **7**, 313–323, <https://doi.org/10.1002/yea.320070402> (1991).
30. De Nobel, J. G., Klis, F. M., Priem, J., Munnik, T. & Van Den Ende, H. The glucanase-soluble mannoproteins limit cell wall porosity in *Saccharomyces cerevisiae*. *Yeast* **6**, 491–499, <https://doi.org/10.1002/yea.320060606> (1990).
31. Daugelavicius, R., Buivydas, A., Sencilo, A. & Bamford, D. H. Assessment of the activity of RND-type multidrug efflux pumps in *Pseudomonas aeruginosa* using tetraphenylphosphonium ions. *International journal of antimicrobial agents* **36**, 234–238, <https://doi.org/10.1016/j.ijantimicag.2010.03.028> (2010).
32. Slayman, C. L., Kuroda, H. & Ballarin-Denti, A. Cation effluxes associated with the uptake of TPP+, TPA+, and TPMP+ by *Neurospora*: evidence for a predominantly electroneutral influx process. *Biochimica et Biophysica Acta (BBA) - Biomembranes* **1190**, 57–71, [https://doi.org/10.1016/0005-2736\(94\)90034-5](https://doi.org/10.1016/0005-2736(94)90034-5) (1994).
33. Fomina, M. & Gadd, G. M. Biosorption: current perspectives on concept, definition and application. *Bioresour. Technol.* **160**, 3–14, <https://doi.org/10.1016/j.biortech.2013.12.102> (2014).
34. Karas, B. J. *et al.* Transferring whole genomes from bacteria to yeast spheroplasts using entire bacterial cells to reduce DNA shearing. *Nature Protocols* **9**, 743, <https://doi.org/10.1038/nprot.2014.045> (2014).
35. Russell, I. & Stewart, G. G. Spheroplast Fusion of Brewers Yeast Strains. *Journal of the Institute of Brewing* **85**, 95–98, <https://doi.org/10.1002/j.2050-0416.1979.tb06834.x> (1979).
36. Becker, B. & Schmitt, M. J. Adapting Yeast as Model to Study Ricin Toxin A Uptake and Trafficking. *Toxins* **3**, 834–847, <https://doi.org/10.3390/toxins3070834> (2011).
37. Vasilkoski, Z., Esser, A. T., Gowrishankar, T. R. & Weaver, J. C. Membrane electroporation: The absolute rate equation and nanosecond time scale pore creation. *Physical review. E, Statistical, nonlinear, and soft matter physics* **74**, 021904, <https://doi.org/10.1103/PhysRevE.74.021904> (2006).
38. Son, R. S., Smith, K. C., Gowrishankar, T. R., Vernier, P. T. & Weaver, J. C. Basic features of a cell electroporation model: illustrative behavior for two very different pulses. *The Journal of membrane biology* **247**, 1209–1228, <https://doi.org/10.1007/s00232-014-9699-z> (2014).
39. Melikov, K. C. *et al.* Voltage-induced nonconductive pre-pores and metastable single pores in unmodified planar lipid bilayer. *Biophysical Journal* **80**, 1829–1836, [https://doi.org/10.1016/s0006-3495\(01\)76153-x](https://doi.org/10.1016/s0006-3495(01)76153-x) (2001).
40. Pakhomov, A. G. *et al.* Long-lasting plasma membrane permeabilization in mammalian cells by nanosecond pulsed electric field (nsPEF). *Bioelectromagnetics* **28**, 655–663, <https://doi.org/10.1002/bem.20354> (2007).

Acknowledgements

This research was funded by the European Regional Development Fund according to the supported activity 'Research Projects Implemented by World-class Researcher Groups' under Measure No. 01.2.2-LMT-K-718-01-0063.

Author Contributions

A.S. performed research; analyzed data; drafted the manuscript, R.C.-G. analyzed and interpreted the data, drafted the manuscript, A.Z., P.S. and A.D. performed the research. A.R. and N.Z. designed the research and contributed the analytic tools, S.B. designed the research and approved the final version of the manuscript to be submitted.

Additional Information

Competing Interests: The authors declare no competing interests.

Publisher's note Springer Nature remains neutral with regard to jurisdictional claims in published maps and institutional affiliations.



Open Access This article is licensed under a Creative Commons Attribution 4.0 International License, which permits use, sharing, adaptation, distribution and reproduction in any medium or format, as long as you give appropriate credit to the original author(s) and the source, provide a link to the Creative Commons license, and indicate if changes were made. The images or other third party material in this article are included in the article's Creative Commons license, unless indicated otherwise in a credit line to the material. If material is not included in the article's Creative Commons license and your intended use is not permitted by statutory regulation or exceeds the permitted use, you will need to obtain permission directly from the copyright holder. To view a copy of this license, visit <http://creativecommons.org/licenses/by/4.0/>.

© The Author(s) 2019

Paper 2





Compact Square-Wave Pulse Electroporator with Controlled Electroporation Efficiency and Cell Viability

Stankevic, V., **Simonis, P.**, Zurauskiene, N., Stirke, A., Dervinis, A.,
Bleizgys, V., Kersulis, S., Balevicius, S.

Symmetry **12** (3), 412 (2020). <https://doi.org/10.3390/sym12030412>

Article

Compact Square-Wave Pulse Electroporator with Controlled Electroporation Efficiency and Cell Viability

Voitech Stankevic ^{1,2}, Povilas Simonis ¹, Nerija Zurauskiene ^{1,2,*} , Arunas Stirke ¹ , Aldas Dervinis ¹ , Vytautas Bleizgys ^{1,2}, Skirmantas Kersulis ¹  and Saulius Balevicius ¹

¹ Center for Physical Sciences and Technology, Department of Functional Materials and Electronics, Sauletekio 3, 10257 Vilnius, Lithuania; voitech.stankevic@ftmc.lt (V.S.); povilas.simonis@ftmc.lt (P.S.); arunas.stirke@ftmc.lt (A.S.); aldas.dervinis@ftmc.lt (A.D.); vytautas.bleizgys@ftmc.lt (V.B.); skirmantas.kersulis@ftmc.lt (S.K.); saulius.balevicius@ftmc.lt (S.B.)

² Vilnius Gediminas Technical University, Faculty of Electronics, Naugarduko 41, 03227 Vilnius, Lithuania

* Correspondence: nerija.zurauskiene@ftmc.lt

Received: 16 February 2020; Accepted: 2 March 2020; Published: 5 March 2020



Abstract: The design and development of a compact square-wave pulse generator for the electroporation of biological cells is presented. This electroporator can generate square-wave pulses with durations from 3 μ s up to 10 ms, voltage amplitudes up to 3500 V, and currents up to 250 A. The quantity of the accumulated energy is optimized by means of a variable capacitor bank. The pulse forming unit design uses a crowbar circuit, which gives better control of the pulse form and its duration, independent of the load impedance. In such cases, the square-wave pulse form ensures better control of electroporation efficiency by choosing parameters determined in advance. The device has an integrated graphic LCD screen and measurement modules for the visualization of the current pulse, allowing for express control of the electroporation quality and does not require an external oscilloscope for current pulse recording. This electroporator was tested on suspensions of *Saccharomyces cerevisiae* yeast cells, during which, it was demonstrated that the application of such square-wave pulses ensured better control of the electroporation efficiency and cell viability after treatment using the pulsed electric field (PEF).

Keywords: pulsed electric field generator; power electronics; square-wave electrical pulses; electroporation; yeast cells

1. Introduction

The use of electroporation in biotechnology and medicine has led to new methods of food pretreatment, gene therapy, drug delivery, and cancer treatment [1–5]. The efficiency of electroporation and its applications strongly depends on the parameters of the pulsed electric field (PEF), namely its amplitude, duration, repetition frequency, number of pulses, and pulse waveforms. Electrical pulses with durations ranging from 10 ns up to 1000 ns are usually used to affect intracellular structures or to create a large number of small pores in the cell plasma membranes [6,7]. Pulses with a microsecond duration (1–1000 μ s) are able to induce a non-thermal, irreversible permeabilization of various cells [1,8], while long pulses, having durations of several milliseconds, can enhance the transfer of large charged molecules (proteins, DNA, RNA) into the cells [9].

Two types of devices are usually used for biological cell electroporation. Those used in industrial facilities for the treatment of large amounts of biomass [10–15] have fixed parameters of the electrical pulses and multi-purpose setups with variable pulse parameters for the investigation

of the electroporation process [16–21]. In the latter case, it is preferable that the electroporator would be able to generate pulses with the widest possible range of amplitudes and durations.

Electropermeabilization appears when the electric field exceeds the threshold value of the transmembrane voltage, above which the formation of pores in cells becomes energetically favorable [22]. Moreover, the time during which the pulse amplitude remains higher than this threshold value has a major role in the efficiency of the electropermeabilization [23]. It is therefore very important during such experiments to know the exact pulse amplitudes, waveforms, and durations. The best solution is to use square-wave pulses [24], since in such cases, it is easier to estimate the energetic and time evolution characteristics of the electroporation process. Electroporation setups using square-waveform electrical pulses are usually based on electrical circuits, which exploit a capacitor discharge by means of a high-power switch. For the generation of nanosecond duration pulses, the capacitor can be a coaxial cable [18] or a micro-strip line configuration [16]. The discharge of this capacitor is realized using a mercury-wetted reed relay [25], a spark-gap switch [26], or fast metal-oxide-semiconductor field-effect transistors (MOSFETs) [27]. Electroporators generating longer pulses, whose durations range from μs to ms , do this by means of electronic circuits containing high-power switch units based on reed relays [28], insulated-gate bipolar transistors (IGBTs) [29], or MOSFET transistors [30]. Most of these setups, however, are state-of-the-art laboratory arrangements, which require specific knowledge and adequate experience on the part of the operator. For this reason, several modifications of compact electroporators that generate square waveform pulses have been designed and can be purchased on the market [31,32].

Most of the commercial devices used for electroporation have maximal operating voltages of up to 3 kV [33]. In order to avoid large energy storage, they can operate within two discrete ranges: low-voltage long pulses (up to 500 V) or high-voltage short pulses (up to 3000 V). Unfortunately, the separation of the voltage range cannot prevent the storage of enormous amounts of energy in their capacitor banks and thus devices with more controlled energy output are required.

The application of fast and powerful MOSFETs or IGBT transistors for connecting and disconnecting the charged capacitor to the load in these devices makes it possible to generate pulses with short rise times (less than $0.1 \mu\text{s}$). However, after the switch-off of these transistors, a current tail occurs in low-current applications, thus the fall time, and consequently the total pulse duration, cannot be strictly determined and are dependent on the load resistance. This phenomenon is very important when the cells are exposed to pulses of microsecond duration because the pulse waveforms can have a significant impact on the cell viability [23]. The value of the load, which depends on the geometry of the cuvette used for electroporation and electrical conductivity of the cell material mixture with the buffer solution, can range from several tens of ohms to a few $\text{k}\Omega$. This means that for a wide range of material applications, the pulse generation circuit needs to be designed such that the generated pulse waveform would be as insensitive as possible to the load value. Moreover, as it was noted in Cukjati et al. [34], it is necessary to control the electric-pulse-induced load resistance changes in real time due to electrical breakdown or Joule heating, making it possible to perform an accurate and safe electroporation process. One of the options for providing continuous quality monitoring of the electroporation process is the visualization of the current pulse shape. This allows for the evaluation of the amplitude, duration, and rise and fall times, as well as the peculiarities of each pulse. To our best knowledge, only one company produces electroporators with a waveform display [35]. Most of them only have an output to an oscilloscope, which is a drawback of most commercially available electroporators.

The main task of this study was to design an easy to use, compact electroporator generating square waveform pulses with a wide range of duration and amplitudes, which could be applicable for different loads (different conductivity of the investigated cell medium), and would be equipped with a simple real-time indicator showing the waveform of the current pulse in the load of the electroporator circuit during the electroporation process.

2. Design of the Generator for Cell Electroporation

In order to develop a universal pulsed power device for the electroporation of biological cells, the required parameters for the output of the device were first determined. The selection of these parameters was influenced by the biological processes that are induced in the biological objects. Therefore, the range of amplitude and duration, repetition frequency, and other output pulse parameters were selected in terms of their applicability in such experiments.

As has already been mentioned above, the microsecond pulse duration range (from 1 μ s to 1 ms) is the one that is most widely used for electroporation. Therefore, our aim was to develop a device that could generate pulses with durations from microseconds to milliseconds and would cover a wide range of electric field amplitudes. High-energy pulses cause Joule heating, which takes place due to the high current flow through the investigated substance. Therefore, the pulse duration, voltage drop during the pulse, and the flowing current needed to be optimal as well. Based on these assumptions, the following parameters were selected: maximal pulsed current: 250 A, voltage amplitude: up to 3.5 kV, pulse duration: from 3 μ s to 10 ms, and shape of the pulse: square-wave.

2.1. Structure of the Electric Pulse Generator

The concept of the generation of square-wave electrical pulses is based on the connection of the load to the charged capacitor for the limited time representing the pulse width. The basic parameters of such square-wave pulses are the following: the pulse amplitude, the voltage drop during the pulse, the pulse duration, and the rise and fall times of the pulse. A simplified block diagram of the proposed square-wave pulse generator is presented in Figure 1. It consists of the high-power, control, load, and pulse-measuring units. The high-power unit includes the high-voltage (HV) supply, energy storage, and pulse-forming units.

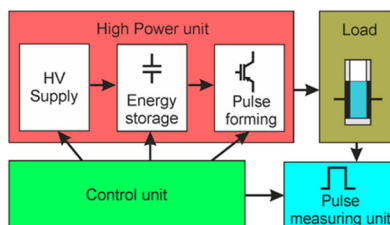


Figure 1. Simplified block diagram of the square-wave pulse generator. HV: High-voltage.

A more detailed block diagram of the generator is shown in Figure 2. Each part of the proposed device described in more detail below.

2.1.1. The High-Power Unit

The HV supply of the high-power unit consists of AC/DC 220/24 V (model SP-240-24) (A1) and the variable DC/DC 24/4000 V (model ISEG EPX40406) (A2) supply sources (see Figure 2). The output voltage and the current of the variable power supply A2 is controlled using the 0–5 V analog signal of the microcontroller, corresponding to a 0–3.5 kV output.

One of the most important parts of the high-power unit is the energy storage unit. It consists (see Figure 2) of the variable capacitance unit, including capacitor banks with commutation relays (A3), which are controlled by the microcontroller (A6 from the control unit) through the linear optocoupler (LOC) (A4). The capacitors in this generator are used for energy storage because the power of the pulse to be generated is much higher than the power of the HV supply source. However, the use of a single capacitor in order to meet all requirements for the high-voltage and long-duration pulses is not suitable for safety reasons. A possible solution is to divide the whole operation range of the electroporator into separate operation ranges and to define the limits of the maximal energy for each range [29]. Therefore,

the capacitor banks in the proposed generator are designed as units of variable capacitance. Moreover, this configuration helps to avoid the undesired Joule heating of the cell suspensions being investigated. The amount of heat dissipating in the cuvette is proportional to the voltage across the cuvette, the current through the medium with the cells, and the pulse duration. During the development of the device, it was specified that the temperature of the cell medium during the pulse could not increase more than 3 °C, and the maximal drop of voltage across the cuvette during the pulse needed to be limited to 10% of the pulse amplitude. The calculations of the maximal pulse duration t_{max} satisfying the mentioned conditions were performed for a 50 μ L cuvette filled with biological medium with a characteristic impedance of 90 Ω .

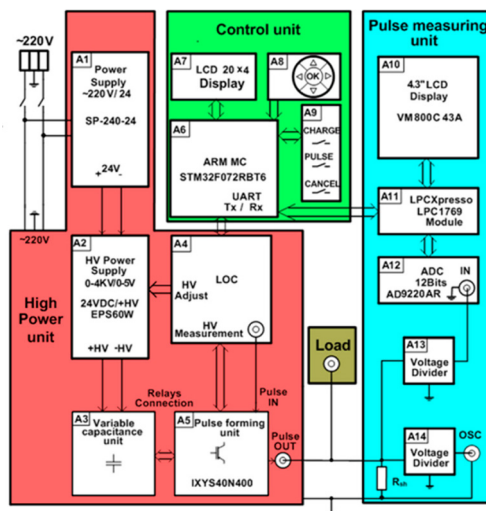


Figure 2. Block diagram of the pulse generator for cell electroporation. LOC: Linear optocoupler.

Based on the calculation results, it was decided that two types of capacitors with different operating voltages and different capacitances were to be used: four high-voltage capacitors $C_{HV} = 52 \mu\text{F} \times 1400 \text{ V}$ and four low-voltage capacitors $C_{LV} = 1000 \mu\text{F} \times 450 \text{ V}$. The switching of the capacitors in parallel and/or in series allows for coverage of all the ranges of the pulse widths and operating voltages that were determined in advance according to the required conditions.

A detailed circuit of the variable capacitance unit is shown in Figure 3. The switching of the capacitors is implemented by using three high voltage relays. A low-power transistor (BT1–BT3) driven by a respective microcontroller port pin results in a three-transistor/relay structure and controls each relay. The opening of these transistors allows for the coverage of all the capacitor commutation variations required for the setup. Four possible connections are realized: range 1—two by two capacitors C_{LV} connected in series (C5 and C6, and C7 and C8), and then interconnected in parallel; range 2—four capacitors C_{LV} (C5–C8) are connected in series; range 3—two by two capacitors C_{HV} (C1 and C2, and C3 and C4) are connected in series and then interconnected in parallel; and range 4—four capacitors C_{HV} (C1–C4) are connected in series. The total capacitance and the maximal operating voltage of the energy storage unit for the different connection configurations (ranges) is presented in Table 1.

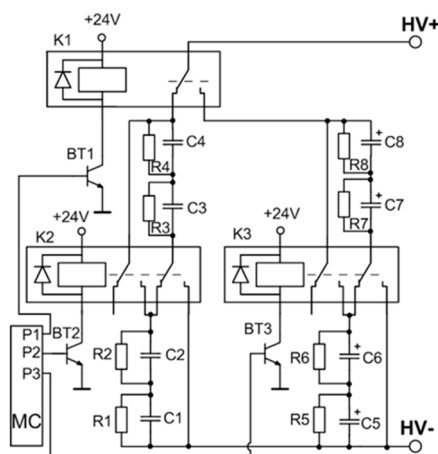


Figure 3. Variable capacitance unit. MC: Microcontroller.

Table 1. Main parameters of the operating ranges of the variable capacitance unit.

Capacitor Connection Configuration	C (μF)	V_{max} (V)	t_{max} (ms)
Range 1	1000	900	15.8
Range 2	250	1800	3.95
Range 3	52	2800	0.84
Range 4	13	5600	0.21

Furthermore, the maximum possible pulse duration t_{max} during which the voltage drop across the load will be lower than 10% is given. These calculations for the different capacitor configurations were performed for a total resistance of 150 Ω after taking into account the load resistance of 90 Ω and the internal (ballast) resistance of the device ($R = 2 \times 30 \Omega$). For other loads, the dependences of the maximum voltage on the pulse duration need to be recalculated. Thus, by dividing the operation range into four ranges, this meets the requirements and allows for the coverage of many areas of presently known biological applications.

Another very important part of the high-power unit of the proposed electroporator is the pulse-forming unit (see A5 in Figure 2). As was mentioned above, the main problem with the electronic switches, such as the MOSFETs or IGBTs, is the inability to turn them off in a sufficiently short time in order to get a square-shaped pulse.

This problem appears due to the minority carriers of these transistors, which contribute to an internal recombination current called the tail current. One of the possibilities is to cut off this current using a crowbar circuit to produce a sharp fall time for the generated pulse. The simplified circuit of this pulse-forming unit with corresponding control and output waveforms is presented in Figure 4. It consists of the main switch VT1 and crowbar switch VT2 transistors, which are controlled by the same microcontroller (see A6 in Figure 2) through a high-speed optically decoupled driver LOC110 (IXYS). The VT1 switch is employed to connect and then disconnect the load to the charged capacitor and thus to form the square-wave pulse. The controlled crowbar circuit, which is synchronized with the VT1, was implemented to achieve a short pulse fall time independent of the load. The insulated-gate bipolar transistors (model IXYS40N400) and snubber diodes are used for both switches. This transistor model has a high collector–emitter operating voltage up to 4000 V and the maximal allowed collector current in a pulsed regime up to 400 A. The $R_D C_D$ snubbers are placed across each of these transistors to protect them against damage. They reduce the peak voltage of the turned-off transistors and

the power dissipation in the turned-on state. Additionally, the non-inductive capacitor C_B is included in the pulse-forming circuit to compensate for the parasitic inductance in the high-power circuit. The main principle of the forming pulse with a short fall time is based on the use of a crowbar circuit: The transistor VT2 is turned on just before the time (see Figure 4) at which the main transistor VT1 is turned off. Such a solution allows for the shortening of the circuit of the load and thus to discharge the remaining electrical charge through the crowbar circuit. This switcher gives the possibility of always having the same fall time of the pulse, independent of the impedance of the load. Such a system allows for the precise generation and evaluation of the pulse in biological loads with highly variable conductivity, thus providing greater control over the treatment procedures and their reproducibility.

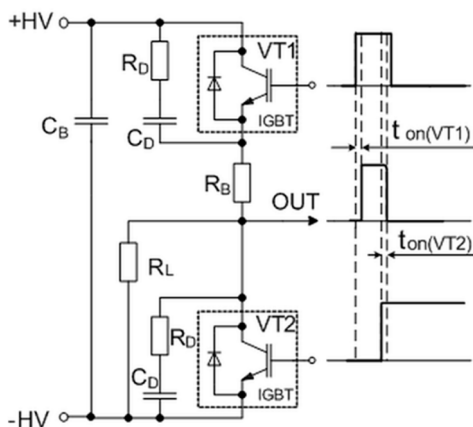


Figure 4. The simplified circuit of the pulse-forming unit with corresponding control and output waveforms. Here, $t_{on}(VT1)$ and $t_{on}(VT2)$ are the delay times between the control pulses of transistors VT1 and VT2 and the rising and falling edges of the output pulses, respectively. IGBT: Insulated-gate bipolar transistor.

2.1.2. Control Unit

The main part of the control unit is the ARM STM32F072RBT6 microcontroller (A6 in Figure 2). It controls the charging voltage and the connection of the capacitors, forms the control pulse (pulse duration and number of pulses) for the switchers VT1 and VT2, and controls the measuring of the output current of the load. The input parameters of the pulse (voltage, pulse duration, and number of pulses) are set by means of the group of five buttons in block A8. All the set parameters are displayed on the liquid crystal display (LCD) display A7.

2.1.3. Pulse-Measuring Unit

For the visualization of the electric pulse, it was decided to image the current pulse through the load. Compared with the voltage value across the load, this current pulse visualization gives more information about the load resistance, the current through the load, the voltage drop across the load, and the different events that can appear during electroporation (spark, electrical short circuit, liquid evaporation, and others). For this purpose, the voltage drops across the shunt connected in series with the load are measured. The unit that measures and displays the current pulse on the screen includes the precision shunt $R_{sh} = 0.1 \Omega$, the voltage divider (A13), the 12-bit 10 MSps analog-to-digital converter (ADC) (model AD9220AR) (A12), the LPCXpresso 1769 module (A11) for the storage of the measured signal, and the 4.3" VM800C43A LC graphic display (A10) (see Figure 2). The LPCXpresso module has an ARM microcontroller, which controls the analog–digital converter and the graphic display. For

a more precise measurement of the signals, a BNC connector is provided, allowing for a connection to an external oscilloscope. The divider A14 is used for this purpose.

2.2. Operation of the Pulse Generator

The operation of the system can be divided into three stages: (1) the input of the pulse parameters, (2) the pulse generation, and (3) the pulse visualization. During the first stage, the microcontroller A6 (see Figure 2) monitors the input and updates the parameters on the LCD screen A7 (see also left screen in Figure 5). The entry and exit of this stage are carried out by pushing the button “OK” in block A8. There are five main parameters that can be altered: the voltage range, the charging voltage, the pulse width, the number of pulses, and the repetition frequency of the pulses. By default, the capacitors’ relay commutation is based on the continuous check of the two input parameters, namely the voltage and the pulse width, with the voltage being given a higher priority. Therefore, based on the voltage setting entered by the user, the microcontroller identifies the connection of the applicable capacitors, followed by a check of the pulse width that is being used to select the optimal operation range calculated for the load of $90\ \Omega$. This ensures that the decrease of the pulse amplitude during the pulse will be no more than 10% for the selected pulses. The system can be easily reprogrammed for applications with different loads. In addition, the microcontroller checks the capacitor charge level before switching the ranges and the change of ranges occurs only after the capacitors have been discharged to a safe level. This prevents distortion of the relays and capacitors due to high current flow during switching.

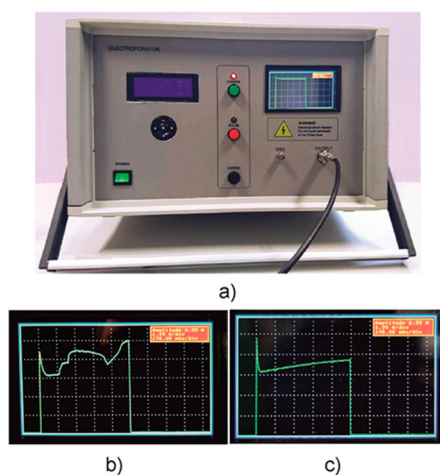


Figure 5. (a) A photograph of the developed compact square-wave generator for electroporation of biological cells. (b,c) Pictures of the display showing when the sparking in the cuvette takes place (b) and when the current during the pulse increases due to heating of the substance in the cuvette (c).

When the main parameters are set, the capacitors can be charged by pushing the “Charge” button from group A9. Starting at this moment, the system is set to the pulse generation stage. Microcontroller A6, through the optical driver A4, gives the command to the HV power supply A2, which starts to charge the capacitors’ connection inside block A3. During this process, the voltage of the capacitors is monitored in real time in the LCD display A7. This stage is also highlighted by the blinking of the red photodiode until the capacitors are charged up to the set voltage. After the capacitors are charged, the pushing of the button “Pulse” starts the discharge of the capacitors through the load. During this time, the microcontroller sends a command to the driver of transistor VT1 and opens it. Before the end of the pulse (the “turn off” of transistor VT1), the microcontroller sends a command to transistor VT2 and turns it on to create a second path for the high current flow through the crowbar circuit. As a result,

the fall time of the pulse is shortened and is dependent only on the type of switches that are used and the parasitic parameters of the circuit. Without the synchronized crowbar circuit, the characteristic tail that depends on the load would appear.

Moreover, when the system is in the pulse generation stage, the ADC A12 in the pulse measuring and imaging unit enters the waiting state, in which the data (voltage drop across the shunt) are being constantly recorded to the buffer until the trigger signal initiates the start of the measurement. After pushing the button "Pulse," the microcontroller A6, through the universal asynchronous receiver-transmitter (UART) protocol, starts to communicate with this ADC and triggers it. After the signal is sampled, it is stored in the memory of the LPCXpresso module A11 and then is imaged onto the LCD A10. At this time, the system is switched to the visualization stage, and after the end of the pulse generation, the measured current pulse is imaged on the LCD A10. For a better visualization of the pulse, the scale of the current (Y scale) on the LCD is adjusted automatically to show the full amplitude of the pulse. The time scale (X scale) is set during the data input mode. The values of the current and time scales are also shown on the display. After visualization, the system goes back into the pulse generation stage and waits for the next command from the user.

2.3. Safety Considerations

The nodes and individual parts of this device are protected against over-current and over-voltage. The variable high voltage power supply ISEG EPX40406 has this inner current limitation. Therefore, it is connected directly to the capacitor array without limiting resistors. In order to establish the precise control of the electroporation unit, accurate and safe pulse parameter choice selections are required for each operation mode. Therefore, multiple limitations are implemented in the software design and in the hardware. Parameters, such as the maximum charging voltage, the maximum pulse length, and the number of pulses, are limited for each capacitor connection for efficient and safe power accumulation. To avoid voltage breakdowns that may occur during relay switching, the switching of the relays is synchronized with the high-voltage power supply. A separate interrupt event has been implemented in the software for the expectation of a change of an operation mode, which shuts the high-voltage source down. When the user changes the operation mode, the power supply is turned off, and after confirming the status, the relay is switched. Such implementation ensures the safe commutation of the capacitors, thus preventing any voltage breakdowns during the operation mode selection. Furthermore, the priority order of the microcontroller tasks during pulsing are clearly specified in order to avoid errors and delays in the task management. The charged high-voltage capacitors are potentially dangerous. If for some reason they become disconnected after charging, they can hold a lethal charge for a long time. In order to eliminate this possibility, bleeder resistors are connected across the terminals of the capacitors (10 M Ω resistors are connected to C_{HV} and 100 k Ω to C_{LV}). Such a configuration ensures the constant discharge of the capacitors, even when disconnected from the pulsing circuit. Moreover, these resistors ensure a uniform voltage distribution across these capacitors and protect these capacitors against over-voltage. In addition, the device has a forced capacitor discharge regime, where discharge takes place through the discharge circuit. The "Cancel" button is used for this purpose. The switchers are also protected against turn-off over-voltage and over-current. The snubber diode connected in parallel to the transistor protects it against a turn-off opposite voltage, which can appear due to an inductive load. Moreover, two ballast resistors of 30 Ω are connected in series with the cuvette for the limitation of the current flow through the transistors in case an electrical short circuit occurs in the cuvette.

2.4. Design of the Device

A photo of the developed electroporation system is presented in Figure 5a. The designed generator was placed into a 43 × 35 × 25 cm³ plastic case. For ease of use, the front panel of the device was visually divided into three parts corresponding to the three stages of the device operation: the parameter input (left), the pulse generation (middle), and the pulse visualization (right). The input of the pulse

parameters of the system is performed via a group of five buttons and the LCD on the left side of the device.

The pulse generation is performed via three buttons in the middle of the device. In addition, this stage of operation is also highlighted by the red photodiode. The LCD is placed on the right side and provides pulse visualization and information. Furthermore, a high-voltage output connector for the load (cuvette with treated substance) and a BNC connector for an external oscilloscope are shown. The current pulse visualization on the display of the device allows for better control of the electroporation process. As an example, two images of the device screen are shown in Figure 5b,c. The first (b) shows the case when some sparking takes place in the cuvette during the experiment. Therefore, one can see the current jumping on the screen. The second picture (c) shows the gradual increase of the current caused by the heating of the contents of the cuvette or the chemical processes in the liquid.

3. Results and Discussion

First, the influence of the operating ranges on the shape of the electric pulse was tested. A cuvette (Lonza, Basel, Switzerland) with electrodes of 2 cm^2 placed 1 mm apart and filled with a NaCl solution was used as the load of the generator. The resistance of the solution was about $90\ \Omega$.

The capacitors of the different connection configurations were charged up to 700 V and a pulse with a duration of 3 ms was generated. The current through the cuvette during the pulses is shown in Figure 6.

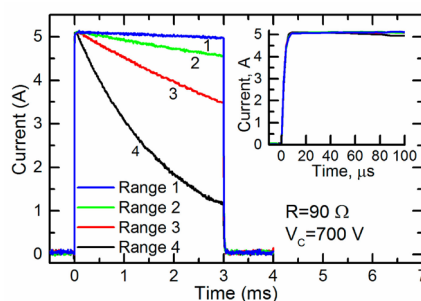


Figure 6. The current through the cuvette having a resistance of $90\ \Omega$ during the 3-ms pulses generated at different ranges of operation. The inset shown the same pulses during the first 100 ms.

One can see that the current through the cuvette was almost constant throughout the whole pulse only in range 1 (see Table 1). For the other ranges 2–4, the current noticeably decreased. Thus, for the generation of a pulse of a given duration for loads with this and lower resistances, range 1 was the most acceptable. At the same time, the inset in Figure 6 shows that the initial part of the same current pulse during the first 100 ms was almost constant at all operating ranges. Thus, all of them could be used for the generation of short pulses. It should be noted that electroporation using short pulses is usually accompanied by a high voltage. Therefore, the fourth range of operation of the generator, in which the maximum charge voltage of the capacitors reached 4 kV, was the most acceptable.

The influence of the crowbar circuit was experimentally investigated using loads with different resistances. For this purpose, a cuvette with various fillings was used. The experiments were done using 1 M sorbitol, a yeast suspension (for more details see below), and a solution of NaCl filling the same cuvette described above. The resistances of these substances were the following: $2000\ \Omega$, $220\ \Omega$, and $65\ \Omega$, respectively. The capacitors were connected according to range 4 and were charged up to a certain voltage, which allowed to produce the same voltage ($\approx 2.6\text{ kV}$) across the cuvette. The obtained results are presented in Figure 7 for the circuit without a crowbar (curve 1: cuvette filled with sorbitol, curve 2: with yeast suspension, and curve 3: with solution of NaCl) and with the crowbar

circuit (curve 1*: with sorbitol and curve 2*: with yeast suspension). As seen from the figure, when the circuit without the crowbar was used, the pulse fall time depended on the load impedance, which is disadvantageous in electroporation. Using this circuit after the switch-off of the transistor, the voltage did not reach zero within 3–10 μs . This is a very significant problem with different biological samples, especially when short pulses are applied. The long fall time means that even during the decay of the pulse, the sample can be uncontrollably affected by the PEF. After connecting the crowbar circuit, the fall part of the pulse was shortened and was the same for all the investigated loads. This is shown in Figure 7 as curves 1* and 2*. Therefore, our proposed circuit with the crowbar allowed for the treatment of biological cells with electric pulses of identical duration, independent of the buffer type (and its conductivity).

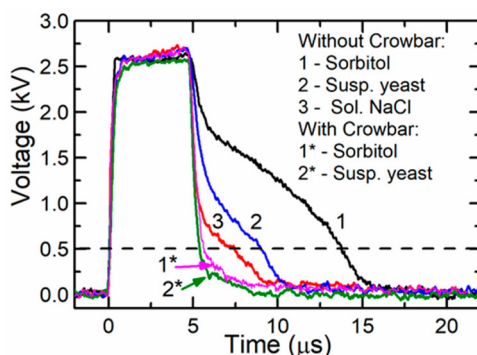


Figure 7. A voltage across different loads when a single pulse was generated with and without the crowbar circuit. The dashed line represents the voltage level corresponding to the threshold electric field strength for the electroporation of yeast cells.

During the next experiments, we tested whether exposure to the electric field pulses generated by the pulse generator with and without the crowbar circuit could induce different electroporation results. For this purpose, experiments with a yeast cell suspension were performed. The yeast suspension for the experiment was prepared as follows: The *Saccharomyces cerevisiae* BY4742 (MAT α ; his3 Δ 1; leu2 Δ 0; lys2 Δ 0; ura3 Δ 0) yeast cells (Euroscarf, Oberursel, Germany) were grown for 24 h in a complete medium (YPD) containing 1% (*w/v*) yeast extract, 2% (*w/v*) peptone, and 2% (*w/v*) glucose (Merck, Darmstadt, Germany). Then, the yeast cells 33.3% (*w/v*) were re-suspended in a cold (4 °C) electroporation buffer (EPB) containing 1 M sorbitol and a 20 mM Tris-HCl buffer at pH 7.4 (Applichem, Nümbrecht, Germany).

In the experiments, the yeast cell suspension was transferred into the same cuvette and exposed to a single 5- μs pulse with an amplitude up to 2600 V (electric field strength was 26 kV/cm). The resistance of the cuvette filled with the yeast suspension was $R \approx 220 \Omega$. Experiments were performed with and without the crowbar circuit. The pulse shapes for both cases were discussed above and presented in Figure 7 (2 and 2* curves, respectively).

Permeabilization of the membranes was evaluated by exposing the yeast cells to fluorescent SYTOX Green nucleic acid stain (ThermoFisher Scientific, Waltham, Mass., USA). During the investigation, the yeast suspension was kept on ice. Fluorescent dye was added into the suspension 10 s after exposure to the PEF. The final concentration of the dye in the suspension was 125 nM. After incubation for one minute, the specimen was placed into a quartz cuvette with a 1-cm light path (Sarstedt, Nümbrecht, Germany) and exposed to 480-nm wavelength light generated using a fluorescence spectrometer LS50B (Perkin Elmer, Waltham, Mass., USA). The permeability of the cell membranes was evaluated by measuring the fluorescence intensity at a peak wavelength equal to 525 nm.

The permeability of the yeast cells after exposure to PEF treatment is presented in Figure 8 as the fluorescence intensity. It was evaluated by employing membrane-impermeable fluorescent dyes intercalated into nucleic acids. Greater amounts of intracellular dye resulted in greater fluorescence intensity (FI), corresponding to the increased permeability [36].

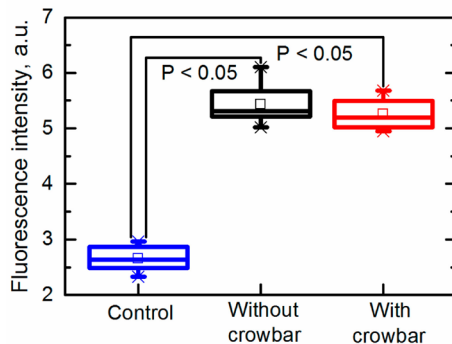


Figure 8. Permeability of yeast cells after exposure to an electric field pulse.

It was found that both pulses (the electric field strength was 26 kV/cm) generated with and without the crowbar circuit induced electroporation. It was found that the fluorescence intensity (FI) increased from FI = 2.7 ± 0.2 a.u. (untreated sample) up to FI = 5.4 ± 0.4 a.u. and FI = 5.3 ± 0.3 a.u. in samples exposed to pulses generated without and with the crowbar circuit, respectively. Thus, the differences between the induced membrane permeability in both cases was insignificant. It should be noted that the fluorescence was measured when the dye was added into the suspension just 10 s after its exposure to PEF; therefore, no influence of the pulse shape (decay time) on the cell damage or other processes was noticed during such short period.

We further investigated the long-term electroporation effects by evaluating the viability by means of the number of colony forming units (CFUs). The viability of the cells was evaluated by the plate count method using solid YPD media with 1.2% (*w/v*) agar (Alfa Aesar, Kandel, Germany). Afterward, the plating yeast cells were grown in an incubator for 48 h at 30 °C. The results are presented in Figure 9. The CFUs are expressed as a percentage, where $100 \pm 8.2\%$ corresponded to the viability of the yeast cells in an untreated cell suspension. The viability of the yeast cells exposed to the pulses generated without the crowbar circuit was reduced to CFU = $84.1 \pm 4.5\%$, thus confirming that the electroporation was at least partially irreversible. The viability of the yeast cells exposed to the pulses generated with a crowbar circuit was higher (CFU = $96.1 \pm 3.3\%$) and was comparable to untreated cells. This result is very important for performing electroporation and retaining a high viability of the treated cells.

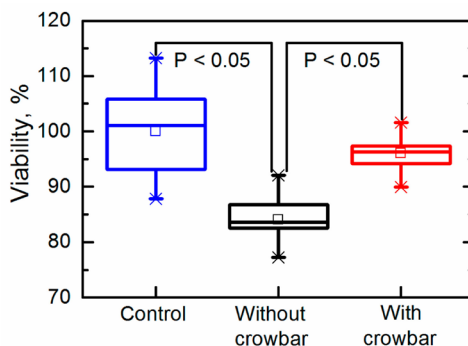


Figure 9. Viability of yeast cells after exposure to an electric field pulse.

Our previous study showed that the detectable electroporation in yeast cells starts after exposure to 5- μ s pulses with an electric field strength of approximately 5 kV/cm [37]. Such an electric field corresponds to a 500-V amplitude (dashed line in Figure 7) and such an electric field strength or higher remained for 8.4 μ s and 5.5 μ s when generated by systems without and with the crowbar circuit, respectively. The difference in the pulse duration (at the level of the threshold electric field strength) was 3.1 μ s, while the energy delivered by such pulses differed by 14%. It was previously shown that the pulse parameters (pulse shape, duration, frequency) could have an effect on the cellular response [23]. In our experiments, the duration of the maximal amplitudes was similar and resulted in similar electroporation. From the viability experiment, however, we can conclude that the total energy input, as well as the pulse shape, could contribute to the reduction of the cell viability and should be accurately reported according to the guidelines [38]. Such a difference in the viability obtained in our experiments was most probably caused by the longer time of exposure during which the voltage exceeded the electroporation threshold.

4. Conclusions

A commercially available, compact, programmable device for high-voltage, square-wave electric pulse generation that is usable for biological cell electroporation has been proposed, designed, and tested. The device has a variable energy storage capacitor bank; thus, the accumulation of high amounts of energy is avoided. The main advantages of such a device are the increased range of possible pulse durations and amplitudes when compared with commercially available electroporators. It can generate a single or a sequence of single electrical pulses with widths from 3 μ s to 10 ms and amplitudes up to 3.5 kV. The rise and fall time of the pulses does not depend on the load impedance and is less than 0.1 μ s. It is equipped with an LCD screen for the monitoring of the input parameters and an additional LCD screen for the display of the pulse waveform during the experiments. The incorporation of this additional screen into the design of the device significantly improved the quality of the investigation of the processes occurring in the test object by providing the possibility of more precise control of the current pulse shape, indicating the preferable conditions of the experiment (e.g., no sparking or heating of the cell suspension). The proposed device was successfully tested in experiments with biological cells. The design of the generator using a crowbar circuit enabled better control of the pulse parameters (especially the pulse duration), which resulted in the increased effectiveness of electroporation and cell viability.

Author Contributions: Conceptualization, V.S. and N.Z.; methodology, V.S. and S.B.; software, V.B.; validation, V.B. and A.D.; investigation, A.D., P.S., S.K., and A.S.; writing—original draft preparation, V.S., A.S., and P.S.; writing—review and editing, N.Z. and A.S.; project administration, N.Z. All authors have read and agreed to the published version of the manuscript.

Funding: This work was partly funded by “Geozondas” Ltd. Implementing an EU structural investment project 01.2.1-MITA-T-851-02-0004 under measure “Inocekiai.”

Conflicts of Interest: The authors declare no conflict of interest.

References

1. Kotnik, T.; Frey, W.; Sack, M.; Haberl Meglič, S.; Peterka, M.; Miklavčič, D. Electroporation-Based Applications in Biotechnology. *Trends Biotechnol.* **2015**, *33*, 480–488. [[CrossRef](#)]
2. Yarmush, M.L.; Golberg, A.; Serša, G.; Kotnik, T.; Miklavčič, D. Electroporation-Based Technologies for Medicine: Principles, Applications, and Challenges. *Annu. Rev. Biomed. Eng.* **2014**, *16*, 295–320. [[CrossRef](#)]
3. Zhu, Z.; Zhang, R.; Grimi, N.; Vorobiev, E. Effects of Pulsed Electric Field Treatment on Compression Properties and Solutes Diffusion Behaviors of Jerusalem Artichoke. *Molecules* **2019**, *24*. [[CrossRef](#)]
4. Brezar, S.K.; Kranjc, M.; Čemažar, M.; Buček, S.; Serša, G. Electrotransfer of siRNA to Silence Enhanced Green Fluorescent Protein in Tumor Mediated by a High Intensity Pulsed Electromagnetic Field. *Vaccines* **2020**, *8*, 49. [[CrossRef](#)]

5. Frandsen, F.; Vissing, V.; Gehl, G. A Comprehensive Review of Calcium Electroporation—A Novel Cancer Treatment Modality. *Cancers* **2020**, *12*. [[CrossRef](#)]
6. Beebe, S.J.; Chen, Y.J.; Sain, N.M.; Schoenbach, K.H.; Xiao, S. Transient Features in Nanosecond Pulsed Electric Fields Differentially Modulate Mitochondria and Viability. *PLoS ONE* **2012**, *7*, e51349. [[CrossRef](#)]
7. Pakhomov, A.G.; Gianulis, E.; Vernier, P.T.; Semenov, I.; Xiao, S.; Pakhomova, O.N. Multiple Nanosecond Electric Pulses Increase the Number but Not the Size of Long-Lived Nanopores in the Cell Membrane. *Biochim. Biophys. Acta Biomembr.* **2015**, *1848*, 958–966. [[CrossRef](#)]
8. Blank, L.M.; Rockenbach, A.; Sudarsan, S.; Berens, J.; Kosubek, M.; Lazar, J.; Demling, P.; Hanke, R.; Mennicken, P.; Ebert, B.E.; et al. Microfluidic Irreversible Electroporation—A Versatile Tool to Extract Intracellular Contents of Bacteria and Yeast. *Metabolites* **2019**, *9*. [[CrossRef](#)]
9. Cervia, L.D.; Chang, C.C.; Wang, L.; Mao, M.; Yuan, F. Enhancing Electrotransfection Efficiency through Improvement in Nuclear Entry of Plasmid DNA. *Mol. Ther. Nucleic Acids* **2018**, *11*, 263–271. [[CrossRef](#)]
10. Golberg, A.; Sack, M.; Teissie, J.; Pataro, G.; Pliquett, U.; Saulis, G.; Stefan, T.; Miklavcic, D.; Vorobiev, E.; Frey, W. Energy-Efficient Biomass Processing with Pulsed Electric Fields for Bioeconomy and Sustainable Development. *Biotechnol. Biofuels* **2016**, *9*, 94. [[CrossRef](#)]
11. Pudasaini, S.; Perera, A.T.K.; Ahmed, S.S.U.; Chong, Y.B.; Ng, S.H.; Yang, C. An Electroporation Device with Microbead-Enhanced Electric Field for Bacterial Inactivation. *Inventions* **2020**, *5*. [[CrossRef](#)]
12. Bluhm, H.; Rusch, D. *Pulsed Power Systems: Principles and Applications*; Springer: Berlin/Heidelberg, Germany, 2006.
13. Bluhm, H.; Sack, M. Industrial-Scale Treatment of Biological Tissues with Pulsed Electric Fields. In *Food Engineering Series*; Springer: Berlin/Heidelberg, Germany, 2008; pp. 237–269. [[CrossRef](#)]
14. Sack, M.; Keipert, S.; Hochberg, M.; Greule, M.; Mueller, G. Design Considerations for a Fast Stacked-MOSFET Switch. *IEEE Trans. Plasma Sci.* **2013**, *41*, 2630–2636. [[CrossRef](#)]
15. Reberšek, M.; Miklavčič, D.; Bertacchini, C.; Sack, M. Cell Membrane Electroporation-Part 3: The Equipment. *IEEE Electr. Insul. Mag.* **2014**, *30*, 8–18. [[CrossRef](#)]
16. Romeo, S.; Sarti, M.; Scarfi, M.R.; Zeni, L. Modified Blumlein Pulse-Forming Networks for Bioelectrical Applications. *J. Membr. Biol.* **2010**, *236*, 55–60. [[CrossRef](#)]
17. Eing, C.J.; Bonnet, S.; Pacher, M.; Puchta, H.; Frey, W. Effects of Nanosecond Pulsed Electric Field Exposure on Arabidopsis Thaliana. *IEEE Trans. Dielectr. Electr. Insul.* **2009**, *16*, 1322–1328. [[CrossRef](#)]
18. Kolb, J.F.; Kono, S.; Schoenbach, K.H. Nanosecond Pulsed Electric Field Generators for the Study of Subcellular Effects. *Bioelectromagnetics* **2006**, *27*, 172–187. [[CrossRef](#)]
19. Kuthi, A.; Gabriëlsson, P.; Behrend, M.R.; Vernier, P.T.; Gundersen, M.A. Nanosecond Pulse Generator Using Fast Recovery Diodes for Cell Electromanipulation. *IEEE Trans. Plasma Sci.* **2005**, *33*, 1192–1197. [[CrossRef](#)]
20. Puc, M.; Čorović, S.; Flisar, K.; Petkovšek, M.; Nastran, J.; Miklavčič, D. Techniques of Signal Generation Required for Electroporation. Survey of Electroporation Devices. *Bioelectrochemistry* **2004**, *64*, 113–124. [[CrossRef](#)]
21. Katsuki, S.; Nomura, N.; Koga, H.; Akiyama, H.; Uchida, I.; Abe, S.I. Biological Effects of Narrow Band Pulsed Electric Fields. *IEEE Trans. Dielectr. Electr. Insul.* **2007**, *14*, 663–668. [[CrossRef](#)]
22. Weaver, J.C.; Chizmadzhev, Y.A. Theory of Electroporation: A Review. *Bioelectrochem. Bioenerg.* **1996**, *41*, 135–160. [[CrossRef](#)]
23. Kotnik, T.; Pucihar, G.; Reberšek, M.; Miklavcic, D.; Mir, L.M. Role of Pulse Shape in Cell Membrane Electroporation. *Biochim. Biophys. Acta* **2003**, *1614*, 193–200. [[CrossRef](#)]
24. Reberšek, M.; Miklavčič, D. Advantages and Disadvantages of Different Concepts of Electroporation Pulse Generation. *Automatika* **2011**, *52*, 12–19. [[CrossRef](#)]
25. Saulis, G.; Saule, R.; Bitinaite, A.; Zurauskiene, N.; Stankevicius, V.; Balevicius, S. Theoretical Analysis and Experimental Determination of the Relationships between the Parameters of the Electric Field Pulse Required to Electroporate the Cells. *IEEE Trans. Plasma Sci.* **2013**, *41*, 2913–2919. [[CrossRef](#)]
26. Balevicius, S.; Stankevicius, V.; Zurauskiene, N.; Shatkovskis, E.; Stirke, A.; Bitinaite, A.; Saule, R.; Maciuleviciene, R.; Saulis, G. System for the Nanoporation of Biological Cells Based on an Optically-Triggered High-Voltage Spark-Gap Switch. *IEEE Trans. Plasma Sci.* **2013**, *41*, 2706–2711. [[CrossRef](#)]
27. White, J.A.; Pliquett, U.; Blackmore, P.F.; Joshi, R.P.; Schoenbach, K.H.; Kolb, J.F. Plasma Membrane Charging of Jurkat Cells by Nanosecond Pulsed Electric Fields. *Eur. Biophys. J.* **2011**, *40*, 947–957. [[CrossRef](#)]

28. Bullmann, T.; Arendt, T.; Frey, U.; Hanashima, C. A Transportable, Inexpensive Electroporator for in Utero Electroporation. *Dev. Growth Differ.* **2015**, *57*, 369–377. [CrossRef]
29. Stankevič, V.; Novickij, V.; Balevičius, S.; Žurauskienė, N.; Baškys, A.; Dervinis, A.; Bleizgys, V. Electroporation System Generating Wide Range Square-Wave Pulses for Biological Applications. In Proceedings of the 2013 IEEE Biomedical Circuits and Systems Conference, BioCAS, Rotterdam, The Netherlands, 31 October–2 November 2013; pp. 33–36. [CrossRef]
30. Flisar, K.; Meglic, S.H.; Morelj, J.; Golob, J.; Miklavcic, D. Testing a Prototype Pulse Generator for a Continuous Flow System and Its Use for E. Coli Inactivation and Microalgae Lipid Extraction. *Bioelectrochemistry* **2014**, *100*, 44–51. [CrossRef]
31. Gene Pulser Xcell™ Electroporation Systems from Bio-Rad|Biocompare.com. Available online: <https://www.biocompare.com/11987-Electroporation-Cell-Fusion-Instruments/4231642-Gen-Pulser-Xcell-Electroporation-Systems/> (accessed on 4 November 2019).
32. ECM 830 Square Wave Electroporation System. Available online: https://www.btxonline.com/media/wysiwyg/tab_content/BTX-ECM-830-User-Manual-0818.pdf (accessed on 4 November 2019).
33. Pakhomov, A.G.; Miklavčič, D.; Markov, M. *Advanced Electroporation Techniques in Biology and Medicine*; Marko, S., Ed.; CRC Press: Boca Raton, FL, USA, 2010.
34. Cukjati, D.; Batiuskaite, D.; André, F.; Miklavčič, D.; Mir, L.M. Real Time Electroporation Control for Accurate and Safe in Vivo Non-Viral Gene Therapy. *Bioelectrochemistry* **2007**, *70*, 501–507. [CrossRef]
35. Celetrix Biotechnology. Available online: http://www.celetrix.com/upfile/doc/Celetrix_Brochure.pdf (accessed on 4 November 2019).
36. Stirke, A.; Celiesiute-Germaniene, R.; Zimkus, A.; Zurauskienė, N.; Simonis, P.; Dervinis, A.; Ramanavicius, A.; Balevicius, S. The Link between Yeast Cell Wall Porosity and Plasma Membrane Permeability after PEF Treatment. *Sci. Rep.* **2019**, *9*, 1–10. [CrossRef]
37. Stirke, A.; Zimkus, A.; Ramanaviciene, A.; Balevicius, S.; Zurauskienė, N.; Saulis, G.; Chaustova, L.; Stankevic, V.; Ramanavicius, A. Electric Field-Induced Effects on Yeast Cell Wall Permeabilization. *Bioelectromagnetics* **2014**, *35*, 136–144. [CrossRef]
38. Cemazar, M.; Sersa, G.; Frey, W.; Miklavcic, D.; Teissié, J. Recommendations and Requirements for Reporting on Applications of Electric Pulse Delivery for Electroporation of Biological Samples. *Bioelectrochemistry* **2018**, *122*, 69–76. [CrossRef]



© 2020 by the authors. Licensee MDPI, Basel, Switzerland. This article is an open access article distributed under the terms and conditions of the Creative Commons Attribution (CC BY) license (<http://creativecommons.org/licenses/by/4.0/>).

Paper 3

Mediated amperometry as a prospective method for the investigation of electroporation

Simonis, P., Garjonyte, R. & Stirke, A.

Scientific Reports **10**, 19094 (2020). <https://doi.org/10.1038/s41598-020-76086-2>



OPEN

Mediated amperometry as a prospective method for the investigation of electroporation

Povilas Simonis , Rasa Garjonyte & Arunas Stirke

Pulsed electric field effects induced in a membrane, as well as intracellular structures, depend on cell type, field and media parameters. To achieve desired outcomes, membranes should be permeabilized in a controlled manner, and thus efficiency of electroporation should be investigated in advance. Here, we present a framework for using mediated amperometry as a prospective method for the investigation of electroporation and its effects on cellular machinery. Whole-cell sensors with single mediator systems comprised of hydrophilic or lipophilic mediators were successfully employed to investigate membrane permeability as well as cellular responses. Exposure of yeast cells to single electric field pulse ($\tau = 300 \mu\text{s}$, $E = 16 \text{ kV/cm}$) resulted in up to tenfold increase of current strength mediated with hydrophilic mediators. Exposure to PEF resulted in decrease of menadione mediated current strength (from 138 ± 15 to $32 \pm 15 \text{ nA}$), which could be completely compensated by supplementing electrolyte with NADH.

In recent years, more and more processes in both medicine and biotechnology depend on the abiotic manipulation of cells. One of the relatively new and prospective techniques used for increasing permeability of cells and tissues is the exposure to pulsed electric fields (PEFs). It is already used for increasing the efficiency of chemotherapy¹, enhancing gene transfection², extending the shelf-life of food³, and improving the extraction of intracellular compounds⁴. One of the main PEF targets in cells is the plasma membrane, which can be substantially and controllably permeabilized (electroporated)⁵ for desired applications. We have shown previously that PEF can induce cell death via metacaspase activation⁶ and permeabilize both cell membranes and yeast cell walls⁷. The experimental data indicated that cellular responses are dependent on electric field strength, pulse duration, and pulse number⁸.

The cellular state after PEF is usually determined by measuring various parameters, including permeability⁹, oxidative state¹⁰, lipid peroxidation¹¹, and other markers related to aging¹² or death¹³. The measurement of increased molecular transport across the membrane is the most common way to confirm electroporation¹⁴. The extent of permeabilization can be evaluated by measuring the leakage of intracellular compounds¹⁵ as well as signals generated by exogenous compounds after entering the cell¹⁶. To successfully detect permeabilization, exogenous compounds should not enter intact cells and should be easily detectable. On the other hand, some physical methods like measurement of conductivity¹⁷, impedance¹⁸, or cell swelling¹⁹ can assist investigation and detect electroporation without exogenous probes. There is a high number of substances and methods, yet each comes with a set of disadvantages and often indicates only single very specific characteristic or parameter of a system reliably. Furthermore, although PEF is widely applied, electroporation effects on the output signals of various detection methods are poorly understood as most methods are primarily used for analyzing intact cells. Moreover, development of new methods for electroporation detection is very important for understanding the mechanism of electroporation and for investigating the cellular state after exposure to PEF.

Electrochemical methods provide the ability to monitor redox processes inside the intact cells, thus reflecting the intracellular state^{20,21}. Such experiments are often conducted by transferring whole cells^{22,23}, or their parts²⁴ onto surface of an electrode. To achieve the electron transfer between the electrode and redox centers of the enzymes in the cell, an electroactive mediator is used. The mediator shuttles the electrons between the electrode and the redox centers of the enzymes, thus providing information about redox activity of cells. Yet

State Research Institute, Center for Physical Sciences and Technology, Saulėtekio al. 3, Vilnius, Lithuania. ✉email: simonis.povilas@gmail.com

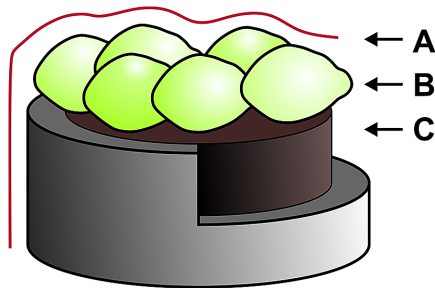


Figure 1. Yeast-modified carbon paste electrode. A membrane; B yeast cells; C carbon paste.

currently electrochemical methods such as potentiometry or amperometry are not widely used for investigating PEF effects on cells.

In this study, we set out to employ amperometry at yeast-modified electrodes to elucidate pulsed electric field effects on (1) plasma membrane/cell wall permeability, (2) metabolic activity, and (3) to investigate the prospects for controlled sensitivity/applicability improvement of whole-cell sensors.

Materials and methods

Cultivation and preparation of yeast cells. *S. cerevisiae* BY4742 (*MAT α* ; *his3 Δ 1*; *leu2 Δ 0*; *lys2 Δ 0*; *ura3 Δ 0*) yeast cells (Euroscarf, Germany) were grown on solid media YPD (1% yeast extract (Biocorp, Poland), 2% peptone ex casein (Carl Roth GmbH, Germany), 2% glucose (Merck KGaA, Germany), 1.3% agar (Alfa Aesar, Germany) at 30 °C in the incubator for 48 h. Cells were then collected. 40 mg of cells were washed twice with electroporation buffer (EPB) (20 mmol/L Tris (Applichem, Germany), HCl (Merck KGaA, Germany), pH 7.4), and resuspended in 0.5 ml of it. Conductivity of final suspension was ≈ 1.5 mS/cm (Seven2Go conductivity meter with Inlab 738-ISM sensor, Mettler Toledo, USA). Where noted, such cell suspension was lyophilized and kept at 4 °C before use in experiments.

Electrode preparation. Plain carbon paste was prepared by mixing 100 mg of graphite powder (Fluka, Germany) with 50 μ l of paraffin oil (Fluka, Germany)²⁵. The paste was packed into an electrode body consisting of a plastic tube (diameter 2.9 mm) and a copper wire serving as a contact for an electrode. The layers of the yeast cells on the surfaces of plain carbon paste electrodes were formed by covering the conducting area with 10 μ l of cell suspension in EPB. The electrodes were allowed to dry at room temperature for 15–20 min and were then covered with a dialysis membrane (Sigma-Aldrich, USA) (Fig. 1). Due to relatively long electrode preparation procedure (when compared to membrane resealing time), investigation of permeability is limited to irreversible electroporation.

Electrochemical measurements. Electrochemical experiments were carried out according to previously described procedure²⁵ on a BAS-Epsilon Bioanalytical system (USA) and a three-electrode cell arranged with a magnetic stirrer. The platinum wire and Ag/AgCl in 3 M NaCl served as counter and reference electrodes, respectively. Amperometry was carried out in a stirred solution at an operating potential 0.3 V (vs. Ag/AgCl, 3 M NaCl). The yeast-modified carbon paste electrode served as a working electrode. All electrochemical measurements were performed at room temperature.

Hydrophilic mediator. To analyze hydrophilic mediators, yeast cells were employed as biosensors for lactic acid detection²⁵. Amperometry for lactic acid-sensing was performed in phosphate buffer: 0.1 M potassium phosphate (Riedel-de Haën, Germany); 0.1 M potassium chloride (Fluka, Germany); potassium hydroxide (Sigma Aldrich, USA) at pH 7.3 and containing 0.5 mM of mediator: *N*-Methylphenazonium methyl sulfate (PMS) (Fluka, Germany), 2,6-Dichlorindophenol sodium salt hydrate (DCPIP) (Fluka, Germany), Potassium ferricyanide (PFC) (Fluka, Germany), 1,2-Naphthoquinone-4-sulfonic acid sodium salt (NQSA) (Fluka, Germany). After reaching steady state of the background current at the operating potential (0.3 V), L-lactic acid (Riedel-de Haën, Germany) was added into the solution (final concentration 0.2 mM). Data was collected and represented as a change in current strength after the steady-state current was achieved.

Lipophilic mediator. Amperometry for menadione-mediated (Sigma-Aldrich, USA) current detection was performed in phosphate buffer at pH 6.5. The electrode was poised at an operating potential (0.3 V) until the steady-state of the background current was obtained. After that, menadione [dissolved in absolute ethanol (VWR, France)] was added up to final concentration of 67 μ M. Change in current was evaluated after the steady-state current was reached. Redox activity monitoring was performed by adding NADH disodium salt (VWR, USA) or NADPH tetrasodium salt (MP Biomedicals, France) to a final concentration of 1 mM.

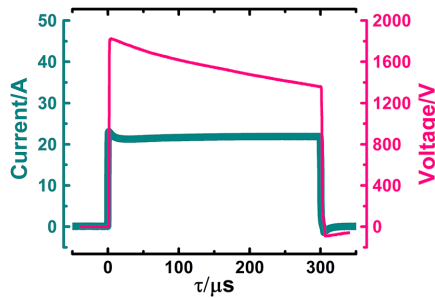


Figure 2. Voltage and current across the cuvette during the generation electric field pulse.

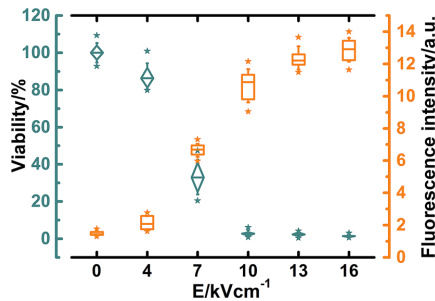


Figure 3. PEF effects on the viability (blue diamonds) and permeability (orange rectangular) of yeast cells. Whiskers of box plots indicate values of standard deviation while stars beside respective boxes indicate highest and lowest values within the distribution of 10 experiments.

PEF generation system. A pulse generator assembled in the Center for Physical Sciences and Technology was used in the experiments²⁶. 100 μ l of yeast cell suspension was placed into a cuvette with 1 mm gap between electrodes (Fisher Scientific, US) and exposed to a single square-shaped pulse with pulse length of 300 μ s and an electric field strength (E) of up to 16 kV/cm ($I = 22 \pm 0.5$ A). Pulses of voltage and current are shown in Fig. 2. Temperature of suspension before and after exposure was evaluated by thermal camera (FLIR One Pro LT, FLIR Systems, US). Electric field pulse raised the temperature of suspension by up to 7 °C.

Evaluation of the viability and permeability. The viability was evaluated by plating treated cell suspension onto a solid YPD medium and then incubating in the INCU-Line (VWR, USA) incubator at 30 °C for 48–72 h. After incubation, the number of colony-forming units (CFU) was evaluated. As a control, PEF untreated suspension was used.

Permeability of the plasma membrane was measured by employing Sytox Green (Thermo Fisher Scientific, USA). Dye was diluted in anhydrous dimethyl sulfoxide (Thermo Fisher Scientific, USA) to a final concentration of 0.25 mM. During the whole procedure, cells were kept on ice. The solution was transferred to the cell suspension (final concentration—125 nM) one hour after exposure to PEF. After incubation for 60 s, fluorescence intensity was measured using luminescence spectrometer Perkin Elmer LS—50b (PerkinElmer, USA). The excitation wavelength was 480 nm. Emission was measured within range of 500–600 nm with scanning speed of 100 nm/min.

Leakage of intracellular cofactors was measured by exciting supernatant with 340 nm and measuring fluorescence at 430 nm²⁷.

Results and discussion

PEF effects on yeast viability and membrane permeability. We started the investigation by evaluating viability and permeability of yeast cells with standard methods. Viability was assessed by counting colony-forming units (Fig. 3). After exposure to PEF the viability started to decrease considerably when electric field strengths (E) were higher than 4 kV/cm. After exposing yeast cells to a pulse with E stronger than 10 kV/cm, viability decreased to ~2%. Therefore, we concluded that viability decreased due to cellular damage. Only viable cells can replicate and form detectable colonies; thus, we eliminate misinterpretation of cells' death state²⁸.

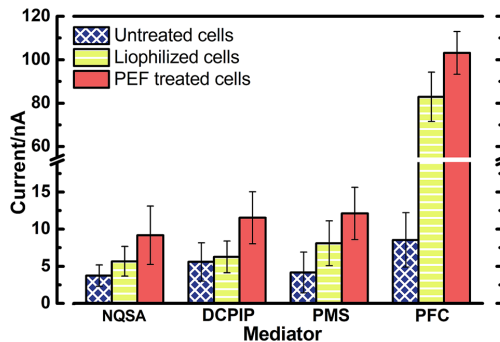


Figure 4. Current dependence on yeast pretreatment and mediator ($C = 0.5$ mM) used for lactic acid sensing. NQSA—1,2-Naphthoquinone-4-sulfonic acid sodium salt, DCPIP—2,6-Dichloroindophenol sodium salt hydrate, PMS—*N*-Methylphenazonium methyl sulfate, PFC—Potassium ferricyanide. Each mean was obtained from at least 10 experimental data points.

Adjustments in composition of media can also indicate respiration deficiency²⁹ and sublethal injuries³⁰, but in this study we focused on evaluating the irreversible damage.

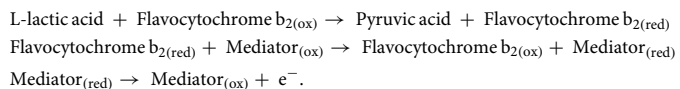
Permeability was evaluated with membrane-impermeable Sytox green dye intercalating into nucleic acids. Some cells were permeable to the Sytox green fluorescent dye even before exposure to PEF, possibly due to the non-uniform age of cells³¹ or nonspecific damage during preparation of cell suspension. The rise in membranes' permeability after the exposure to PEF showed an inverse pattern to the change in the viability. Weak electric field pulses ($E < 4$ kV/cm) did not change either of the measured parameters. Even if membrane was permeabilized, it effectively resealed without further damage to cells. Most considerable changes were observed when cells were exposed to a pulse with electric field strength between 4 and 10 kV/cm. Stronger electric fields permeabilized yeast cells irreversibly, causing a decrease in the viability, potentially due to the leakage of intracellular compounds. Eukaryotic cells can repair their membrane damage and continue to grow at later times³². To avoid misinterpretation of such cases, permeability was measured 1 h after exposure to PEF.

The possibility of using PEF for inactivation of microorganisms is already widely explored and exploited both for research and commercial applications³³. Full inactivation of the yeast cells was not detected, probably due to differences in cell size, shape³⁴ and some volume of suspension being above the electrodes in untreated areas, and non-homogeneous electric field distribution³⁵.

Hence, we showed that exposure to a single electric pulse with a duration of 300 μ s induces irreversible electroporation and causes a decrease in the viability of yeast cells.

Yeast pretreatment enhances the signal of current mediated via hydrophilic mediators. One of the factors limiting the usage of hydrophilic mediators in combination with intact cells is permeability of membranes. To test cell pretreatment procedures we chose irreversible electroporation and lyophilization which is typical for the preparation of biosensors³⁶. After pretreatment, yeast cells were immobilized on carbon paste electrodes, immersed into the solution with the single hydrophilic mediator, and analyzed.

The system we employed was previously suggested for amperometric biosensing of lactic acid²⁵. The scheme for mediated electrocatalytic oxidation of lactic acid can be represented as follows:



The results showed marked differences in the responses of electrodes covered with untreated, lyophilized, and electroporated yeast cells (Fig. 4). Current generated by PEF treated cells in a solution with ferricyanide was strongest ($I = 103 \pm 10$ nA) followed by lyophilized ($I = 83 \pm 11$ nA) and untreated yeasts ($I = 9 \pm 4$ nA). Exposure to PEF increased permeability to all mediators resulting in stronger currents.

In a similar study, the rise in ferricyanide current strength after chemical pretreatment was most notable as well³⁷. It remains to be elucidated whether current strengths generated by NQSA, DCPIP, and PMS during lactic acid-sensing are limited by permeability of the membrane and cell wall or by charge transfer³⁸. Since pretreatment by lyophilization and exposure to PEF resulted in generation of stronger currents we suggest that limiting factor is charge transfer and not permeability. Even though lyophilization provides convenient solution for long term storage of yeast cells, the permeability of cell populations is non-homogeneous³⁹. PEF treatment was superior to lyophilization, while ferricyanide was shown to be the most efficient mediator and was used for further investigation of the electroporation effects.

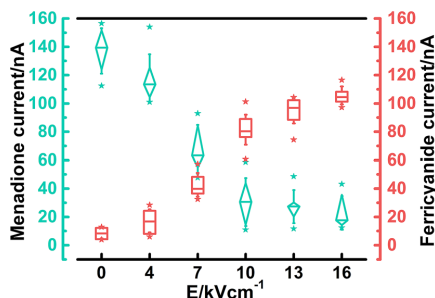
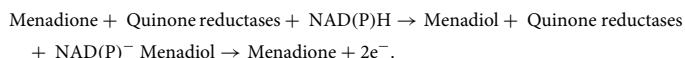


Figure 5. Effect of electric field strength on the current responses to 0.2 mM lactic acid at yeast-modified electrodes at the operating potential 0.3 V in phosphate buffer at pH 7.3 containing 0.5 mM mediator $K_3[Fe(CN)_6]$ (pink rectangles), and to 67 μ M menadione at an operating potential 0.3 V in phosphate buffer at pH 6.5 (teal diamonds). Whiskers of box plots indicate values of standard deviation while stars beside respective boxes indicate highest and lowest values of distribution.

PEF modulates signals of yeast-modified electrodes. Usually, redox processes occurring in intact cells are studied using double mediator systems containing both lipophilic and hydrophilic mediators^{40,41}. The lipophilic mediator can penetrate membrane and interact with intracellular redox centers while hydrophilic mediator facilitates transferring charge from cell to electrode surface. To note the changes in measured current at yeast modified electrodes we pretreated cells with different electric field strength and tested them with common mediators from double mediator system separately (Fig. 5).

After exposure to weak electric fields ($E \leq 4$ kV/cm) measured current mediated with PFC slightly increased from 9 ± 4 up to 17 ± 8 nA. The further rise in electric field resulted in ever-increasing currents. Yet after exposure to pulses stronger than 10 kV/cm, increments of rise in current strength decreased. Such a profile could imply that with the increase in E, more yeast cells are permeabilized irreversibly, and the ever-smaller fraction of cells remain untreated/unpermeabilized. These results indicate that PEF treatment can be used to circumvent the usage of double mediator systems and increase signal mediated by hydrophilic mediators in a controlled manner. After the pretreatment, hydrophilic mediators can efficiently enter cells and participate in electron transfer from intracellular enzymes, which remain intact after PEF treatment. The membrane is a barrier to various hydrophilic mediators⁴², so permeabilized cells can be used in combination with much wider range of mediators providing new insights into cellular machinery. It remains to be elucidated whether hydrophilic mediators could be employed in conjunction with reversible electroporation.

To test how permeabilization affects signal mediated by the lipophilic mediator, we employed menadione. The suggested scheme of charge transfer is the following⁴²:



When electrodes were covered with untreated cells ($E = 0$ kV/cm), current of 138 ± 15 nA was detected. After exposure to weak electric fields ($E = 4$ kV/cm), current slightly decreased down to 117 ± 14 nA. The further rise in electric field strength ($E = 10$ kV/cm) resulted in even weaker current of 32 ± 15 nA. Exposure to the strongest electric field (16 kV/cm) resulted in further decrease in current down to 23 ± 12 nA.

Menadione can freely cross the cell membrane and enter the cytoplasm where it is then reduced to menadiol by the cytosolic and mitochondrial enzymes catalyzing the electron transfer from NAD(P)H to quinone substrates. It was previously proposed that menadione-mediated current depend on intracellular NAD(P)H content and decrease with its depletion⁴³. Intracellular concentrations of NAD(P)H could decrease due to intracellular perturbations like oxidative stress and leakage of these small cofactors. We decided to investigate the latter by measuring fluorescence²⁷ of the supernatant from treated ($E = 16$ kV/cm) and untreated cell suspensions. Specimens were excited with 340 nm light. Fluorescence intensity at 430 nm after pretreatment was eightfold higher. Such results indicate excessive leakage of intracellular compounds. During preparation of electrodes treated cells are transferred onto electrode surface and subsequently into electrochemical cell with higher solution volume, cofactors become highly diluted.

We performed the further investigation by adding NAD(P)H into the electrolyte during current measurement (Fig. 6). We showed that the decrease in menadione current of PEF treated cells could be complemented entirely by adjusting extracellular concentration of NADH to 1 mM. The addition of NADPH resulted in stronger current as well, but not as high as after addition of NADH. Supplementing untreated cells with NAD(P)H raised current strength by up to 10%. Such findings suggest that the decrease of menadione current is indeed observed due to the leakage of intracellular reducing species through permeable membranes. We, therefore, conclude that formation of hydrophilic pores should not significantly affect the entry of a lipophilic mediator and cause decrease in current strength by itself.

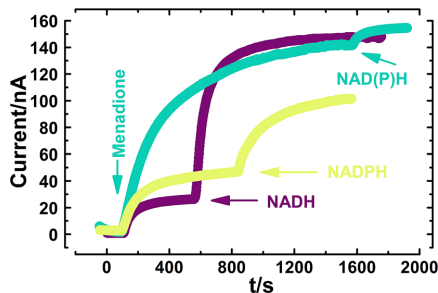
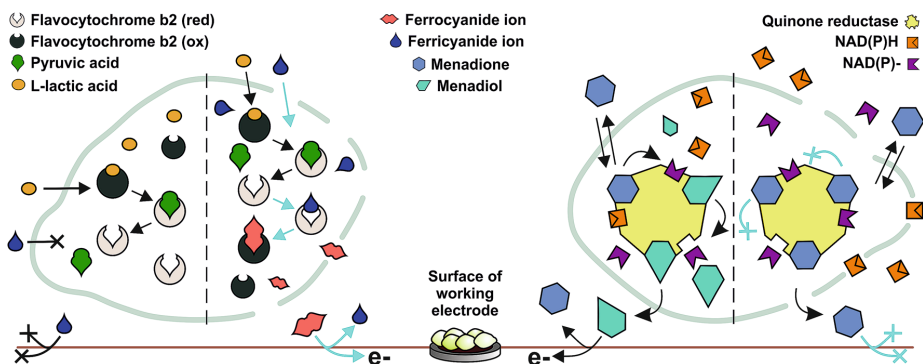


Figure 6. Typical real-time current responses of yeast cells immobilized on carbon paste electrode. Teal curve—untreated cells. Yellow and violet—PEF treated cells ($E = 16 \text{ kV/cm}$). Electrolyte composition was $67 \mu\text{M}$ menadione at an operating potential 0.3 V in phosphate buffer at pH 6. Final concentration of NAD(P)H in the electrolyte was 1 mM .



Scheme 1. Schematic overview of permeabilization effects on amperometric signal of yeast-modified electrodes.

The entire process of exposing cells to redox mediators can be considered as redox stress, which must be counterbalanced by NAD(P)H and the cellular dehydrogenases. Eukaryotic cells use NAD(P)H for multiple purposes, and decrease in its concentration can result in impaired metabolism, calcium homeostasis, gene expression as well as reduction in antioxidative capacity⁴⁴. NADPH is a primary cofactor utilized by cells when reducing artificial mediators⁴³. Khlupova et al. showed that membranes of permeabilized and lyophilized cells lose integrity and become NAD(P)H permeable. Such loss of reducing species can be a major cause of why weaker currents are generated³⁹. We confirmed that PEF could change permeability leading to the loss of NAD(P)H. Furthermore, we showed that permeabilization could be performed in a controlled way leading to an adjustable signal of the whole-cell sensors.

Conclusions

We showed that after exposure to PEF, the permeability of the cell wall/membrane increased and remained so for at least an hour. Yeast-modified electrode responses to lactic acid were dependent on exposure to PEF and increased with the rise in electric field strength (Scheme 1). Traditional methods for the preparation of yeast cells like lyophilization or chemical treatment (salts, alcohols, acids, detergents) are relatively unspecific and will affect intracellular structures as well as machinery while PEF treatment primarily focuses on the plasma membrane.

PEF treated yeast cells also showed lower redox activity and viability, which decreased with rise in electric field strength. The decrease in menadione current of PEF treated cells could be compensated entirely by adjusting extracellular concentration of NADH to 1 mM . Such results raise attention to the viability kits employing quinone-like mediators. If such mediators are applied to analyze abiotic treatments affecting membrane permeability, they can give ambiguous results. In our study menadione current in PEF treated cells decreased from 100 to $\sim 17\%$ while the viability decreased down to $\sim 2\%$, thus highlighting possible inconsistency between methodologies. The complete picture of cellular death, membrane permeability and redox kinetics upon PEF exposure remain to be elucidated.

Our investigation shows that PEF technology can be effectively used to modulate the amperometric signal of yeast-modified electrodes and that they can be used for real-time study of cellular responses to PEF treatment.

Such pretreatment can also open the gateways to intracellular enzymes without extraction and allow investigation of both permeability as well as cellular death mechanisms. We conclude that permeabilization in combination with different combinations of growth conditions, inhibitors, mediators, substrates, cofactors will pave the way for the investigation of biochemical pathways through multistep processes.

Received: 21 November 2019; Accepted: 22 October 2020

Published online: 05 November 2020

References

- Esmaili, N. & Friebe, M. Electrochemotherapy: a review of current status, alternative IGP approaches, and future perspectives. *J. Healthc. Eng.* **2019**, 2784516 (2019).
- Schmitt, M. A., Friedrich, O. & Gilbert, D. F. Portoprotorator: a portable low-cost electroporation device for gene transfer to cultured cells in biotechnology, biomedical research and education. *Biosens. Bioelectron.* **131**, 95–103 (2019).
- Timmermans, R. A. H., Nederhoff, A. L., Nierop Groot, M. N., van Boekel, M. A. J. S. & Mastwijk, H. C. Effect of electrical field strength applied by PEF processing and storage temperature on the outgrowth of yeasts and moulds naturally present in a fresh fruit smoothie. *Int. J. Food Microbiol.* **230**, 21–30 (2016).
- Kotnik, T. *et al.* Electroporation-based applications in biotechnology. *Trends Biotechnol.* **33**, 480–488 (2015).
- Weaver, J. C. & Chizmadzhev, Y. A. Theory of electroporation: a review. *Bioelectrochem. Bioenergy* **41**, 135–160 (1996).
- Simonis, P. *et al.* Caspase dependent apoptosis induced in yeast cells by nanosecond pulsed electric fields. *Bioelectrochemistry* **115**, 19–25 (2017).
- Stirke, A. *et al.* The link between yeast cell wall porosity and plasma membrane permeability after PEF treatment. *Sci. Rep.* **9**, 14731 (2019).
- Simonis, P. *et al.* Pulsed electric field effects on inactivation of microorganisms in acid whey. *Int. J. Food Microbiol.* **291**, 128–134 (2019).
- Zhang, Y., Chen, X., Gueydan, C. & Han, J. Plasma membrane changes during programmed cell deaths. *Cell Res.* **28**, 9–21 (2018).
- Farrugia, G. & Balzan, R. Oxidative stress and programmed cell death in yeast. *Front. Oncol.* <https://doi.org/10.3389/fonc.2012.00064> (2012).
- Eisenberg, T. & Büttner, S. Lipids and cell death in yeast. *FEMS Yeast Res.* **14**, 179–197 (2014).
- Carmona-Gutierrez, D. & Büttner, S. The many ways to age for a single yeast cell. *Yeast* **31**, 289–298 (2014).
- Carmona-Gutierrez, D. *et al.* Guidelines and recommendations on yeast cell death nomenclature. *Microbial Cell* **5**, 4–31 (2018).
- Batista Napotnik, T. & Miklavčič, D. In vitro electroporation detection methods—an overview. *Bioelectrochemistry* **120**, 166–182 (2018).
- Ganeva, V. & Galutzov, B. Electropulsation as an alternative method for protein extraction from yeast. *FEMS Microbiol. Lett.* **174**, 279–284 (1999).
- Peterson, A. D., Jaroszeski, M. J. & Gupta, V. K. Fluorometric assay to compensate for non-viable cells during electroporation. *J. Fluoresc.* **25**, 159–165 (2015).
- Pavlin, M. *et al.* Effect of cell electroporation on the conductivity of a cell suspension. *Biophys. J.* **88**, 4378–4390 (2005).
- Granot, Y., Ivorra, A., Maor, E. & Rubinsky, B. In vivo imaging of irreversible electroporation by means of electrical impedance tomography. *Phys. Med. Biol.* **54**, 4927–4943 (2009).
- Romeo, S., Wu, Y. H., Levine, Z. A., Gundersen, M. A. & Vernier, P. T. Water influx and cell swelling after nanosecond electroporation. *Biochim. Biophys. Acta Biomembr.* **1828**, 1715–1722 (2013).
- Heiskanen, A. *et al.* Mediator-assisted simultaneous probing of cytosolic and mitochondrial redox activity in living cells. *Anal. Biochem.* **384**, 11–19 (2009).
- Garjonyte, R., Melyvydas, V. & Malinauskas, A. Mediated amperometry reveals different modes of yeast responses to sugars. *Bioelectrochemistry* **107**, 45–49 (2016).
- Wu, S. *et al.* Extracellular electron transfer mediated by flavins in Gram-positive *Bacillus* sp. WS-XY1 and yeast *Pichia stipitis*. *Electrochim. Acta* **146**, 564–567 (2014).
- Chelikani, V. *et al.* Investigating yeast cell responses to oestrogen by electrochemical detection. *Electrochim. Acta* **73**, 136–140 (2012).
- Giroud, F., Nicolo, T. A., Koepke, S. J. & Minter, S. D. Understanding the mechanism of direct electrochemistry of mitochondria-modified electrodes from yeast, potato and bovine sources at carbon paper electrodes. *Electrochim. Acta* **110**, 112–119 (2013).
- Garjonyte, R., Melyvydas, V. & Malinauskas, A. Mediated amperometric biosensors for lactic acid based on carbon paste electrodes modified with baker's yeast *Saccharomyces cerevisiae*. *Bioelectrochemistry* **68**, 191–196 (2006).
- Stankevicius, V. *et al.* Compact square-wave pulse electroporator with controlled electroporation efficiency and cell viability. *Symmetry* **12**, 412 (2020).
- Blacker, T. S. *et al.* Separating NADH and NADPH fluorescence in live cells and tissues using FLIM. *Nat. Commun.* **5**, 1–9 (2014).
- Madeo, F. *et al.* Caspase-dependent and caspase-independent cell death pathways in yeast. *Biochem. Biophys. Res. Commun.* **382**, 227–231 (2009).
- Sugiyama, K. I., Kawamura, A., Izawa, S. & Inoue, Y. Role of glutathione in heat-shock-induced cell death of *Saccharomyces cerevisiae*. *Biochem. J.* **352**, 71–78 (2000).
- Kethireddy, V., Oey, L., Jowett, T. & Bremer, P. Critical analysis of the maximum non inhibitory concentration (MNIC) method in quantifying sub-lethal injury in *Saccharomyces cerevisiae* cells exposed to either thermal or pulsed electric field treatments. *Int. J. Food Microbiol.* **233**, 73–80 (2016).
- Eisenberg, T. *et al.* Induction of autophagy by spermidine promotes longevity. *Nat. Cell Biol.* **11**, 1305–1314 (2009).
- Blazek, A. D., Paleo, B. J. & Weisleder, N. Plasma membrane repair: a central process for maintaining cellular homeostasis. *Physiol. Oxyg.* **6**, 438–448 (2015).
- Buckow, R., Ng, S. & Toepfl, S. Pulsed electric field processing of orange juice: a review on microbial, enzymatic, nutritional, and sensory quality and stability. *Compr. Rev. Food Sci. Food Saf.* **12**, 455–467 (2013).
- Kotnik, T., Pucihar, G. & Miklavčič, D. Induced transmembrane voltage and its correlation with electroporation—mediated molecular transport. *J. Membr. Biol.* **236**, 3–13 (2010).
- Knoerzer, K., Baumann, P. & Buckow, R. An iterative modelling approach for improving the performance of a pulsed electric field (PEF) treatment chamber. *Comput. Chem. Eng.* **37**, 48–63 (2012).
- Jarque, S., Bittner, M. & Hilscherová, K. Freeze-drying as suitable method to achieve ready-to-use yeast biosensors for androgenic and estrogenic compounds. *Chemosphere* **148**, 204–210 (2016).
- Garjonyte, R., Melyvydas, V. & Malinauskas, A. Effect of yeast pretreatment on the characteristics of yeast-modified electrodes as mediated amperometric biosensors for lactic acid. *Bioelectrochemistry* **74**, 188–194 (2008).
- Smutok, O., Gayda, G., Gonchar, M. & Schuhmann, W. A novel L-lactate-selective biosensor based on flavocytochrome b2 from methylotrophic yeast *Hansenula polymorpha*. *Biosens. Bioelectron.* **20**, 1285–1290 (2005).

39. Khlupova, M., Kuznetsov, B., Gonchar, M., Ruzgas, T. & Shleev, S. Amperometric monitoring of redox activity in intact, permeabilised and lyophilised cells of the yeast *Hansenula polymorpha*. *Electrochem. Commun.* **9**, 1480–1485 (2007).
40. Ino, K., Onodera, T., Fukuda, M. T., Nashimoto, Y. & Shiku, H. Combination of double-mediator system with large-scale integration-based amperometric devices for detecting NAD(P)H:quinone Oxidoreductase 1 activity of cancer cell aggregates. *ACS Sens.* **4**, 1619–1625 (2019).
41. Baronian, K., Downard, A., Lowen, R. & Pasco, N. Detection of two distinct substrate-dependent catabolic responses in yeast cells using a mediated electrochemical method. *Appl. Microbiol. Biotechnol.* **60**, 108–113 (2002).
42. Heiskanen, A. *et al.* Amperometric monitoring of redox activity in living yeast cells: comparison of menadione and menadione sodium bisulfite as electron transfer mediators. *Electrochem. Commun.* **6**, 219–224 (2004).
43. Spégel, C. F. *et al.* Amperometric response from the glycolytic versus the pentose phosphate pathway in *Saccharomyces cerevisiae* cells. *Anal. Chem.* **79**, 8919–8926 (2007).
44. Ying, W. NAD⁺/NADH and NADP⁺/NADPH in cellular functions and cell death: regulation and biological consequences. *Antioxid. Redox Signal.* **10**, 179–206 (2008).

Acknowledgements

We want to thank Edvardas Golovinas and Gediminas Drabavičius for helpful comments and proofreading.

Author contributions

P.S.: conceptualization, investigation, data curation, writing—original draft preparation, visualization; R.G.: methodology, validation, resources; A.S.: writing—review & editing, supervision, project administration.

Competing interests

The authors declare no competing interests.

Additional information

Correspondence and requests for materials should be addressed to P.S.

Reprints and permissions information is available at www.nature.com/reprints.

Publisher's note Springer Nature remains neutral with regard to jurisdictional claims in published maps and institutional affiliations.



Open Access This article is licensed under a Creative Commons Attribution 4.0 International License, which permits use, sharing, adaptation, distribution and reproduction in any medium or format, as long as you give appropriate credit to the original author(s) and the source, provide a link to the Creative Commons licence, and indicate if changes were made. The images or other third party material in this article are included in the article's Creative Commons licence, unless indicated otherwise in a credit line to the material. If material is not included in the article's Creative Commons licence and your intended use is not permitted by statutory regulation or exceeds the permitted use, you will need to obtain permission directly from the copyright holder. To view a copy of this licence, visit <http://creativecommons.org/licenses/by/4.0/>.

© The Author(s) 2020

Paper 4

Caspase dependent apoptosis induced in yeast cells by
nanosecond pulsed electric fields

Simonis, P., Kersulis, S., Stankevich, V., Kasetas, V., Lastauskiene, E.,
Stirke, A.

Bioelectrochemistry **115**, 19-25 (2017).
<https://doi.org/10.1016/j.bioelechem.2017.01.005>



Caspase dependent apoptosis induced in yeast cells by nanosecond pulsed electric fields

Povilas Simonis^a, Skirmantas Kersulis^b, Voitech Stankevich^b, Vytautas Kaseta^{a,c}, Egle Lastauskiene^{a,d}, Arunas Stirke^{a,d,*}

^a Laboratory of Bio-Nanotechnology, State Research Institute, Center for Physical Sciences and Technology, Sauletekio ave. 3, LT-10257 Vilnius, Lithuania

^b High Power Pulse Laboratory, State Research Institute, Center for Physical Sciences and Technology, Sauletekio ave. 3, LT-10257 Vilnius, Lithuania

^c State Research Institute Center for Innovative Medicine, Santariškių 5, LT-08406 Vilnius, Lithuania

^d Department of Microbiology and Biotechnology, Faculty of Natural Sciences, Vilnius University, Sauletekio ave. 7, LT-10257 Vilnius, Lithuania



ARTICLE INFO

Article history:

Received 25 November 2016

Received in revised form 18 January 2017

Accepted 31 January 2017

Available online 6 February 2017

Keywords:

Yeast

Apoptosis

Metacaspase

Electroporation

Nanosecond

ABSTRACT

Saccharomyces cerevisiae yeast cells were used as a model organism to investigate the effects of various pulsed electric fields on the programmed death of such cells. These were exposed to electric field pulses with field strengths (E) of up to 220 kV/cm. The effects of square shaped pulses having different durations ($\tau = 10$ –90 ns) and different pulse numbers ($pn = 1$ –5) were then analysed. The obtained results show that nanosecond pulses can induce the death of such cells, which in turn is dependent on the electric field pulse parameters and increase with the rise in E , τ and pn . The decrease of the cells' viability was accompanied by an increase in the active form of intracellular yeast metacaspases. It was thus shown that nanosecond electric field pulses induced the caspase-dependent yeast cell death.

© 2017 Elsevier B.V. All rights reserved.

1. Introduction

The effects that are induced by exposing biological tissues and cell suspensions to electric fields are intensively investigated. It had been previously established that repetitive electric field pulses, namely that pulsed electric fields (PEFs) are an effective method for improving conventional procedures such used in chemotherapy [1], gene transfer [2], microbiological inactivation in food preservation [3] [4] and the extraction of intracellular compounds [5] [6]. The responses of such cells when exposed to electric fields are mostly dependent on the electric field strength (E), the pulse length (τ), shape, polarization and the number of pulses used [6] [7]. When a cell is exposed to an electric field, the electric potential difference across its insulating membrane changes (induced transmembrane voltage) and this superimposes a physiological resting transmembrane voltage. Such increased transmembrane voltage can result in the electroporation of the cell membrane [8] and even the inhibition of its voltage-gated channels [9] [10]. It has been previously shown that in mammalian cells, a nanosecond pulsed electric field (nsPEF) can improve the permeability of the plasma membrane [11], alter gene expression [12], cause phosphatidylserine translocation

[13], affect the distribution of intracellular ions [14] and even lead to the death of the cell [15] [16]. The effects of nanosecond pulses on such membranes were theoretically investigated using molecular dynamics simulation. The formation of hydrophobic pores, translocation of phosphatidylserine, the flow of water and various dyes after exposure to high voltage nsPEF treatment were modelled and were in agreement with the obtained experimental data [11] [17]. Even though there is a large body of knowledge concerning the effects of nsPEF on higher eukaryotic cells (a recent systematic review analysed the effects of high voltage nanosecond electric pulses on eukaryotic cells (*in vitro*) and covered data from 203 articles [18]), there is still a lack of sufficient data related to the effects of nsPEF on yeast cells. One of the conclusions summarized in this systematic review was that nsPEF pulses with moderate duration ($\tau = 11$ –100 ns) were the most likely to cause intracellular effects. We thus conducted our experiments within similar parameters ($\tau = 10$ –90 ns).

Budding yeast (*Saccharomyces cerevisiae*) is one of the most well-studied and understood eukaryotic organisms. It is an irreplaceable component in the food industry, where it is used in the preparation of fermented foods and beverages and in the pharmaceutical and biotechnology sectors, where it is used for the production of recombinant proteins. In addition, it is also a highly useful organism for theoretical and practical modelling. Yeasts have been used for studying genetic networks and have contributed to a better understanding of the programmed deaths of cells. In 1997, apoptotic markers were described in yeast for

* Corresponding author at: Laboratory of Bio-Nanotechnology, State Research Institute, Center for Physical Sciences and Technology, Sauletekio ave. 3, LT-10257 Vilnius, Lithuania.

E-mail address: arunas.stirke@ftmc.lt (A. Stirke).

the first time [19]. This was followed by the characterization of several orthologues of metazoan apoptotic regulators (yeast metacaspase, protein Yca1p/Mca1p [20], the apoptosis-inducing factor Aif1p [21], the Htr2A/Omi serine protease Nma11p [22], the inhibitor of apoptosis protein (IAP) Bir1p [23], the mitochondrial endonuclease G Nuclp [24]) and the analysis of distinct death pathways [25]. Such programmed cell death (PCD) can be induced using various lethal insults, which lead to caspase-dependent or caspase-independent death pathways. Unlike mammalian caspases, which are crucial for the initiation and regulation of apoptosis, yeast metacaspases, depending on the source of the lethal stimulus, participate in approximately 40% of PCD cases [25].

Research on apoptosis in yeasts provides an advantage as the use of yeasts avoids one of the technical problems that effect research on the death of mammalian cells, such as when the detection of cell death relies on apoptotic markers, which can yield false positive and negative results [26]. Moreover, the genetic tractability of yeast is unique and allows the simultaneous overexpression of one gene and the knockout of another gene, helping to establish hierarchies among the cell death executors. This makes yeast a useful model organism when attempting to identify the effects of nsPEF on PCD.

The aim of this study was to elucidate the effects of nsPEFs on yeast cells. We show that i) high voltage square shaped electric field pulses of nanoseconds order duration can induce the programmed, caspase-dependent death of yeast cells, and ii) that such cell death is in turn dependent on the parameters of such electric field pulses (E , τ and pulse number).

2. Materials and methods

2.1. Yeast strain and cultivation

Saccharomyces BY4741 (*MATA*; *his3Δ1*; *leu2Δ0*; *met15Δ0*; *ura3Δ0*) yeast cells (Euroscarf, Germany) were grown in a 6 mL of YPD (1% yeast extract, 2% peptone, 2% glucose, Merck KGaA, Germany) at 30 °C in a reciprocal shaker operating at 200 rpm.

The cell concentration was measured by optical density (OD) using an absorption spectrophotometer (Halo RB-10; Dynamica Scientific Ltd., GB) operating at a 600 nm wavelength. In order to collect cells more sensitive to these physical treatments, the yeast cells were harvested after reaching 0.9–1.1 OD (early exponential phase). These cells were then collected, washed twice with phosphate buffered saline, pH 7.4 (Sigma-Aldrich, USA) and then suspended in 2–3 mL of electroporation buffer (EPB) (1 mol/L sorbitol, Applichem GmbH, Germany; 20 mmol/L Tris, Applichem, Germany; HCl Merck KGaA, Germany;

pH = 7.4), while keeping the final concentration of the yeasts at $(6-9) \times 10^7$ colony forming units (CFU)/mL.

2.2. PEF generation system

A nanosecond generator based on coaxial line discharge by an optically triggered spark-gap switch was used for the generation of the electrical pulses. A schematic diagram of the experimental setup was described previously [27] and is shown with some modifications in Fig. 1. Changing the discrete length (L) of the coaxial pulse-forming line and charging it from the DC high voltage power supply up to 30 kV (Technix, France) makes it possible to generate rectangular shaped electrical pulses with durations of 10, 20, 40, 60 and 90 ns and with rise time ≈ 0.5 ns. A 400 ps laser pulse was used for the triggering of the spark gap switch. A cuvette having cylindrical-shaped electrodes (diameter $D = 6$ mm) made from stainless steel and spaced at a $d = 1$ mm distance was used for electroporation of the biological cells dispersed in EPB. The cuvette was connected to the end of transmission line. Depending on the resistivity of the investigated suspension, electric fields with strengths of up to 220 kV/cm were achieved.

The system operates as follows: when the cuvette is filled with a suspension, the system is triggered by a laser pulse. The waveforms and amplitudes of the incident and the reflected pulses are then recorded using a real-time oscilloscope. The voltage (V) applied between the electrodes of the cuvette was calculated according to the formula: $V = V_{in} + V_{ref}$, where V_{in} and V_{ref} are the amplitudes of the incident and reflected pulses respectively. The resistance (R) of the sample inside the cuvette was calculated using the following equation: $R = Z \times (V_{in} + V_{ref}) / (V_{in} - V_{ref})$, where $Z = 75 \Omega$ is the impedance of the transmission line [27]. During our experiments, the resistance of the suspension was $\approx 300 \Omega$. The calculation of the temperature change in the suspension inside the cuvette after each pulse was performed by assuming that the heating was adiabatic and homogeneous. It was calculated that even at the strongest electrical field and when using the longest pulses, the temperature change was less than 1 degree per pulse. This means that even after 5 pulses, the rise in temperature was too small to affect the viability of the yeast cells significantly [28].

2.3. Evaluation of cell viability

After exposure to the electric field, the yeast cells were kept in EPB for at least an hour, and were then diluted in 1 M sorbitol, plated onto a solid YPD medium with 1.3 g/mL agar (Merck KGaA, Germany) and then incubated in the INCU-Line (VWR, USA) incubator at 30 °C for 48–72 h. After incubation, the number of colony forming units (CFU) was evaluated. As a control, cells which were untreated by nsPEF were

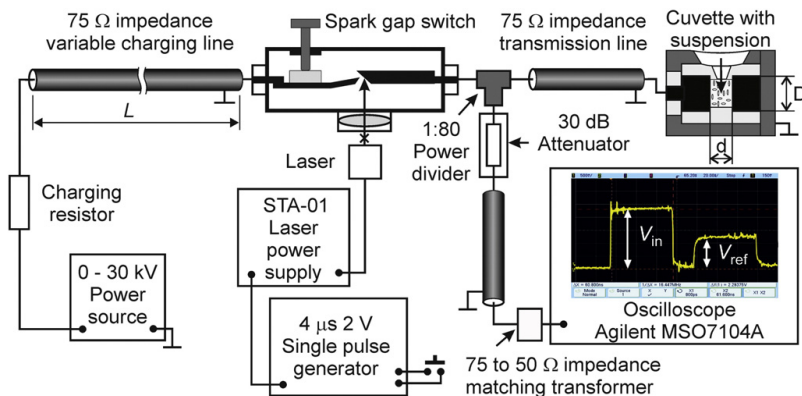


Fig. 1. Principal Scheme of the nanosecond pulse generation system.

used. To determine the possible changes in the buffer composition during PEF treatment that affected the viability of the yeasts, the yeasts were kept in the nsPEFs treated EPB.

2.4. Detection of apoptotic markers

The effect of nsPEFs on PCD was evaluated using the CaspACE™ FITC-VAD-FMK *in situ* marker (Promega, USA), propidium iodide (Carl Roth GmbH + Co.-KG, Germany), Annexin V-FITC (Biovision, USA) and a FragEL™ DNA Fragmentation Detection Kit (Merck KGaA, Germany). Caspase detection and DNR fragmentation assays were performed according to the producer protocols. Propidium iodide was added to the yeast cell suspensions immediately or 1.5–2 h after exposure to nsPEFs at a final concentration of 2.5 µg/mL. For the phosphatidylserine externalisation analysis before Annexin V-FITC staining, the cells were washed twice with a sorbitol buffer (1.2 M sorbitol, 0.5 mM MgCl₂ (Merck KGaA, Germany), 35 mM KPO₄ (Merck KGaA, Germany), pH = 6.8) and the cells walls were digested with 30 U/mL lyticase (Sigma-Aldrich, USA) in a sorbitol buffer. After a 2 h incubation at 30 °C, the cells were then collected and washed with a binding buffer (10 mM HEPES, Sigma-Aldrich, USA; NaOH, Sigma-Aldrich, USA; 140 mM NaCl, Sigma-Aldrich, USA; 2.5 mM CaCl₂, Applchem GmbH, Germany; pH = 7.4) with 1.2 M sorbitol and suspended in it. 1 µL Annexin V-FITC was then added to 40 µL of cell suspension and incubated for 20 min. The cells were then washed 3 times and suspended in a binding buffer.

For the preparation of the microscopy slides, 0.1% (w/v) poli-L-lizine (Sigma-Aldrich, USA) was used. The fluorescence of at least 200 fixed cells was evaluated on each slide.

In the flow cytometry experiments, at least 20,000 cell events were acquired for each sample with an Amnis FlowSight Imaging Flow Cytometer (Merck Millipore, Germany) and IDEAS v6.1 software was used for data analysis. The acquired images included a brightfield image, a forward scatter (FSC) (Channel1 457/45 nm), a side scatter (SSC) (Channel6 772/35 nm), FITC (Channel2 532/55 nm) and PI (Channel4 610/30 nm). The FITC, PI and SSC were then excited by 488 nm, 561 nm and a 785 nm lasers, respectively. The gating strategy, as detailed in the results and discussion section, was used to assess the event count and the signal intensity of the cells of interest. Non-stained and appropriate single and double stained controls for compensation and gate setting were used. The yeast cells in the EPB supplemented with acetic acid, pH = 2.5 (Merck KGaA, Germany) were used as a positive control for the detection and evaluation of the apoptotic markers [20].

3. Results and discussion

3.1. Electric field effects on yeast viability

The number of CFUs was evaluated by the plate counting method, thus avoiding misinterpreting fluorescent markers and evaluating the effects of abiotic impact [25]. After exposure to a single electric field pulse ($\tau = 10\text{--}90$ ns, $E = 25\text{--}220$ kV/cm), the decrease in viability was detected and is shown in Fig. 2. Pulses with durations of 10 ns even with strong electric fields ($E = 185$ kV/cm) showed a weak effect (CFU = $94 \pm 6\%$). The smallest number of CFUs ($40 \pm 3\%$) was observed after exposure of the yeast suspensions to a single 60 ns pulse when $E = 190$ kV/cm. Despite the large standard deviation in our results, the tendency for the cells' viability to decrease was dependent on the pulse length and strength.

To evaluate the effect of repetitive exposure to the electric field, five consecutive pulses were used. The lethal dose of the electric field that was necessary to inactivate 50% of the cells (LD50E) was dependent on the pulse lengths: $\tau = 20$ ns (LD50E ≈ 167 kV/cm), $\tau = 40$ ns (LD50E ≈ 115 kV/cm); $\tau = 60$ ns (LD50E ≈ 125 kV/cm); $\tau = 90$ ns (LD50E ≈ 40 kV/cm). After five 50 kV/cm electric field pulses with durations of 90 ns, the viability of the yeast cells decreased by 68%. Stronger electric fields affected their viability only slightly, reaching its lowest value (CFU = 19%), when $E = 218$ kV/cm. The cumulative effect of such nsPEFs was detected when $\tau = 90$ ns and the multiplication factor was 1.9–2.5 times compared to that of the single pulse treatment.

It had been previously discovered that depending of pulse parameters, an electric field with the nanosecond duration could cause both cumulating [7] and neutralizing [14] effects. It is difficult to evaluate the contribution of each consecutive pulse, since the whole system changes such as the position, permeability and the structure of the membranes as well as the permeability of the cell walls [28] [29]. CFU values exceeding 100% could be explained by aggregation phenomena. If exposure to the electric field cause change of cell surface charge, this could lead to dispersion of aggregates due to repulsion between their cells thus giving greater number of viable CFU [29] [30]. Therefore, the effect of five pulses on the viability of the yeast was greater compared to that of a single pulse treatment. Full inactivation of the yeast cells was not detected, probably due to the electrically insulating features of the yeast aggregates [31] [32] and cell size [16]. So we showed that square shaped pulses of nanosecond duration can be a quite effective method for the reduction of the viability of yeast cells. This in turn is dependent on the parameters of the electric field pulses and their decrease with the rise in E , τ and the number of pulses.

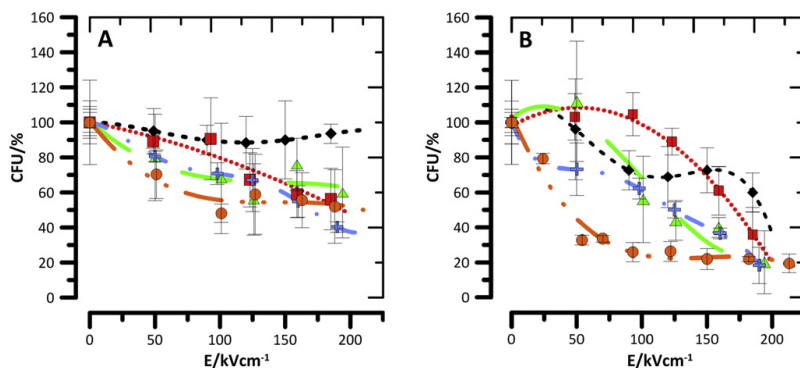


Fig. 2. Colony forming units after exposure to electric field pulses: A, cell suspension was exposed to single pulse; B, cell suspension was exposed to five consecutive pulses. Symbols represent pulse length: ♦ (diamond) – 10 ns; ■ (square) – 20 ns; ▲ (triangle) – 40 ns; + (plus) – 60 ns; ● (circle) – 90 ns; dotted lines of respective colour in this and following graphs represent fit to an eye.

3.2. Analysis of PCD markers

3.2.1. nsPEFs induce externalisation of phosphatidylserine but not DNR fragmentation

The externalisation of phosphatidylserine is one of the PCD markers. After exposure to an electric field, the cell walls were removed and the protoplasts were incubated with Annexin-V-FITC. Externalisation of phosphatidylserine was detected by fluorescent microscopy and this is shown in Fig. 3. It is known that phosphatidylserine can be externalised due to the nsPEFs effect, but since we treated regular cells with cell walls, we could not evaluate whether it was externalised as part of the programmed cell death or during exposure to nsPEFs. Due to the low stability of protoplasts obtained from nsPEFs treated cells ($\tau = 90$ ns, $E = 100$ kV/cm), quantitative analysis was not performed.

To analyse DNA fragmentation, a TUNEL assay was carried out 1.5–3 h after treatment with nsPEFs ($\tau = 10$ –90 ns, $E =$ up to 190 kV/cm). DNA fragmentation, which has previously been defined as an apoptotic marker in yeast [19], was not observed in our experiments (DNA fragmentation was detected in less than 2% of the cells and this was independent of nsPEF treatment parameters). Such results could mean that in nsPEF treated cells, metacaspase activation is the primary event and that DNR fragmentation occurs only later during the process of apoptosis. In our analysis, when nsPEF treated cells were tested for DNA fragmentation, they were still in the early stages of programmed cell death and DNA fragmentation was therefore not detected [33].

3.2.2. nsPEFs induced activation of metacaspase

For the detection of cells with active metacaspases (YCA1 +), the caspase inhibitor FITC-VAD-FMK was used. Cells with active caspase showed bright green fluorescence and were detected by using fluorescence microscopy (Fig. 3). The specimens were treated with 5 consecutive nsPEF pulses. The number of yeast cells with activated metacaspases was greatest (YCA1 + = 61 ± 4%) after treatment with strong (164 kV/cm) and long pulses (90 ns) (Fig. 4). A similar portion of YCA1 + cells (YCA1 + = 58 ± 9%) was detected with pulse durations of 60 ns when $E = 209$ kV/cm, which showed that with shorter pulses, a stronger electric field is required to achieve same result. When we used strong electric field pulses ($E = 196$ kV/cm), the lowest number of cells with active metacaspases (YCA1 + = 17 ± 2%) was detected when the shortest pulses were used ($\tau = 10$ ns). Meanwhile, in untreated suspensions (possibly due to aging [20]), metacaspases were activated in ≈ 3% of yeast cells.

To obtain more quantitative results and to establish a possible link between metacaspase activation and the effects of the electric fields on membrane permeability, the yeast cells were treated with propidium iodide, a caspase inhibitor and analysed using a flow cytometer (Fig. 5).

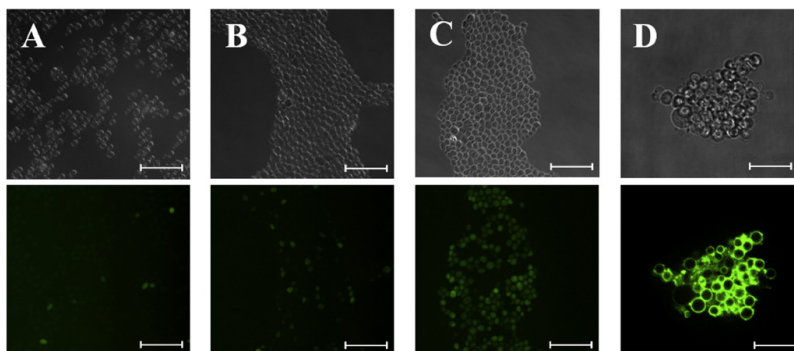


Fig. 3. Bright-field (up) and fluorescence (down) microscopy images of yeast cells after exposure to five consecutive nanosecond pulses. Yeast cells with activated metacaspases: A, when $\tau = 10$ ns, $E = 52$ kV/cm; B, when $\tau = 10$ ns, $E = 196$ kV/cm; C, when $\tau = 90$ ns, $E = 164$ kV/cm; D is phosphatidylserine externalisation in yeast protoplasts obtained from PEF treated yeast cells. The scale bar represents 22 μ m.

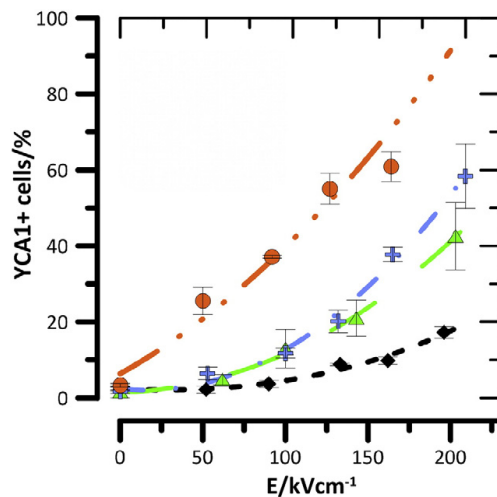


Fig. 4. Number of yeast cells with activated metacaspases (YCA1 +) by counting fluorescent cells and its dependence on electric field strength after exposure to 5 consecutive pulses. Symbols represent pulse length: \blacklozenge (diamond) – 10 ns; \blacktriangle (triangle) – 40 ns; \blackplus (plus) – 60 ns; \bullet (circle) – 90 ns.

As was previously shown in Fig. 4, the strongest effect of nsPEFs on metacaspase activation (YCA1 + = 61 ± 4%) was obtained after the cells were treated with 164 kV/cm electric field strength and 90 ns duration pulses. Thus, for further analysis, 90 ns duration electrical pulses were used.

After exposure to nsPEFs and staining, the cells were grouped into four subpopulations based on the following gating scheme: viable cells (YCA1 −, PI −), cells with active metacaspases, but impermeabilised membranes (YCA1 +, PI −), cells with permeabilised membranes, but inactive metacaspases (YCA1 −, PI +) and those with active metacaspases and permeabilised membranes (YCA1 +, PI +). The size of these populations and their dependence on electric field strength are shown in Fig. 6.

After exposure to a single nsPEF pulse, the sizes of the cell populations with one detectable PCD marker (YCA1 +, PI − and YCA1 −, PI +) were similar to each other. When the electric field was not applied (YCA1 +, PI −), the population size was 0.9 ± 0.6%, while along a whole range of E values, the average was 8.2 ± 1.9%. The size of the (YCA1 −, PI +) population was 2.2 ± 1.1% when $E = 0$ kV/cm, and this was

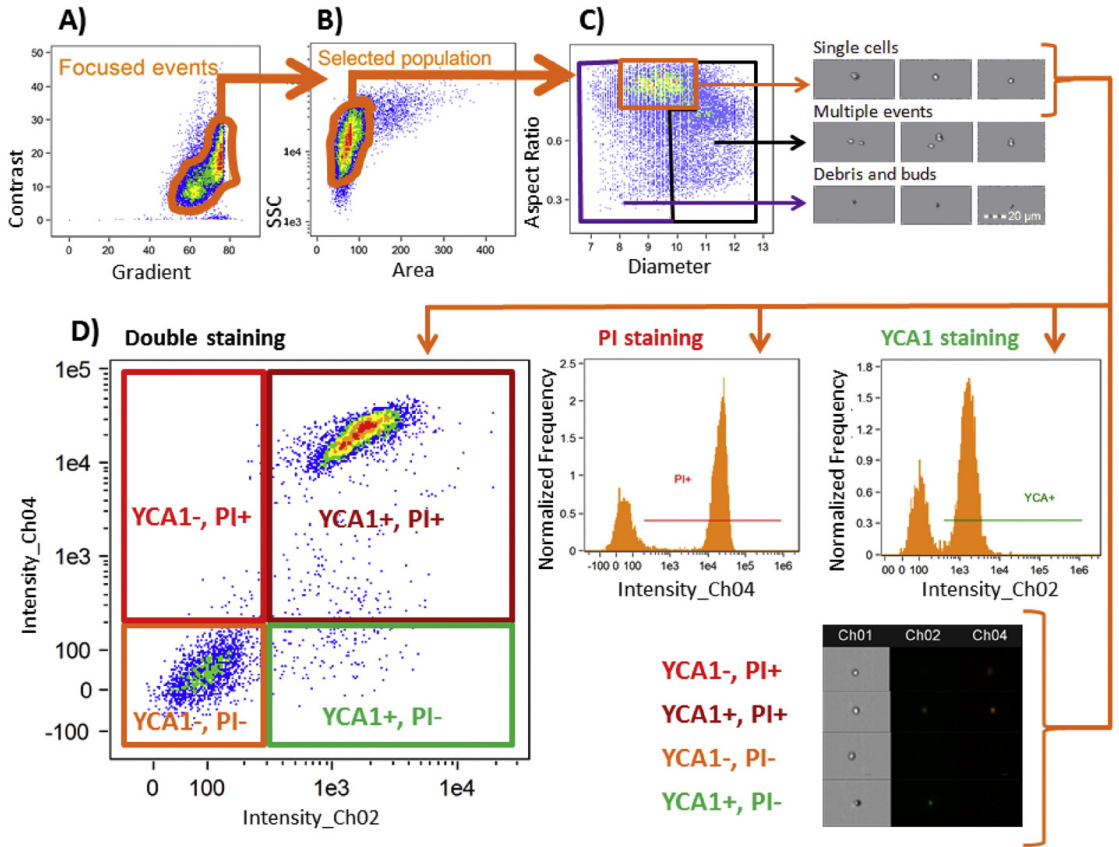


Fig. 5. The scheme used for imaging flow cytometry analysis was the gating strategy for the identification and quantification of metacaspases activity and membrane permeability of yeast cells. The focused events were gated using a gradient and the contrast features of bright field scans (A). The in-focus events were gated on a forward scatter/side scatter (area/ssc) dot plot (B) and refined to remove events with more than one cell by using the size and aspect ratios of the minor and major axes features of the bright field scans (C). The identification of properly-focused, focused single cell events was followed by YCA1 and PI staining analysis in channel 02 (Ch02) and channel 04 (Ch04), respectively (D).

consistent in the whole range of E values ($2.6 \pm 1.3\%$). The sizes of populations (YCA1 +, PI+) and (YCA1 -, PI-), which were considered as apoptotic and viable were respectively inversely proportional. The

apoptotic population before exposure was $3 \pm 1.2\%$, when $E = 54 \text{ kV/cm}$ - $4.3 \pm 2.3\%$ and this had been consistently increasing up to $58.7 \pm 6\%$ when $E = 219 \text{ kV/cm}$. When the yeast cells were exposed

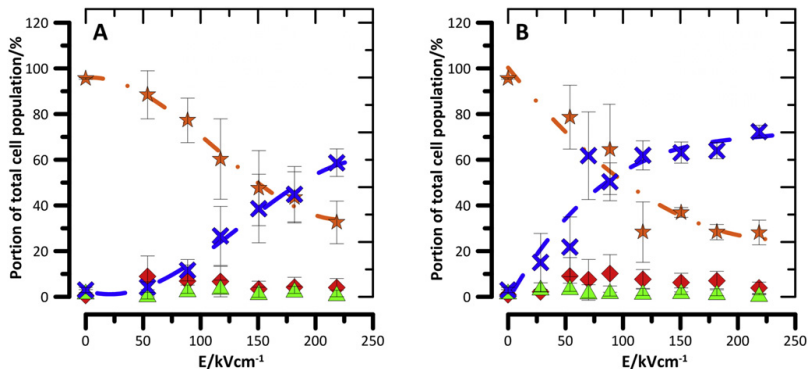


Fig. 6. Yeast cell populations with activate (YCA1+) or inactive (YCA1-) metacaspases and permeable (PI+) or impermeable (PI-) to propidium iodide after exposure to electric field when $\tau = 90 \text{ ns}$: A. populations after exposure to one pulse; B. populations after exposure to 5 consecutive pulses. Symbols represent different cell populations: \star (star) - YCA1 -, PI -; \times ("x") - YCA1 +, PI +; \blacktriangle (triangle) - YCA1 +, PI -; \blacklozenge (diamond) - YCA1 -, PI +.

to 5 consecutive pulses, the size of the (YCA1⁻, PI⁺) population was $6.7 \pm 2.6\%$, while the (YCA1⁺, PI⁻) population contained $2.6 \pm 1\%$ of the total cells. Both populations were consistent along the whole range of E values. Apoptotic and viable populations were inversely proportional as in the single pulse experiment. The apoptotic population after exposure to 5 nsPEF pulses with $E = 28$ kV/cm was $15 \pm 12.7\%$. A rise in E up to 117 kV/cm produced a fast increase of this apoptotic population up to $61.9 \pm 6.4\%$. A further increase ($E = 219$ kV/cm) only slightly affected the population after reaching a maximum size of $72.7 \pm 2.7\%$. After exposure to a single nsPEF, LD50E was ≈ 190 kV/cm, while exposure to 5 consecutive pulses with $E = 70$ – 90 kV/cm were strong enough to achieve same decrease in the cells' viability.

The change in the viability is dependent on the pulse parameters and shows a similar pattern as in the activity of metacaspases in cells treated with pulses with increasing electric field strength (Fig. 7). Over the whole range of E (except ≈ 50 kV/cm), the average number of dead cells is greater up to 10% and the spread of the results overlaps with the YCA1⁺ values. These results show that yeast cell death is dependent on the electric field pulse parameters which cause membrane permeability and subsequent metacaspase activity leading to a decrease in the CFU number.

This decrease in the cells' viability followed a similar pattern to the increase of the active form of the intracellular yeast metacaspases, thus suggesting oxidative stress [20]. It is known that increased intracellular reactive oxygen and the concentration of oxidised protein lead to the activation of metacaspases. Another possible cause leading to the activation of yeast metacaspases could be a disturbance of Ca^{2+} homeostasis. It is known that pulses with nanosecond duration can modulate intracellular Ca^{2+} concentration [34] which is needed for the activation of yeast metacaspases [35]. It was proposed that the initial pulses could cause the release of calcium from the endoplasmic reticulum, leading to calcium redistribution within the cytoplasm. Pulse exposure would facilitate the penetration of calcium ions into mitochondrial membranes leading (at least in metazoan cells) to changes that trigger a release of cytochrome c and other death molecules [36]. Loss of membrane integrity and permeability to propidium iodide is considered as a marker of necrosis or late apoptosis [37]. In our research, permeability appeared instantly after treatment (data not shown) and can be considered as an upstream factor for PCD induction. The dynamics of membrane permeability were not evaluated. If membrane integrity or the cell wall integrity pathways could be activated due to nsPEF treatment, this can lead to the initiation of the cell death pathway [38]. In addition, it is known, that an electric current can generate hydrogen peroxide [39], which in turn can activate the cell wall integrity pathways, change the

membrane permeability and cause oxidative stress [40]. For the evaluation of the electric field effects on the electroporation buffer, the yeast cells were suspended in EPB treated with 5 to 20 pulses ($\tau = 90$ ns) with electric field strengths of up to 200 kV/cm. No changes in their viability were detected, therefore it was concluded that the programmed cell death is induced due to the direct nsPEFs impact on yeast cells.

4. Conclusions

We analysed the effects of square shaped electrical pulses of different duration ($\tau = 10$ – 90 ns) and pulse number ($pn = 1$ – 5) with electric field strength E up to 220 kV/cm and showed that nanosecond pulses can induce the cell death, which in turn is dependent on the electric field pulse parameters and increase with the rise in E, τ and pulse number. Since nsPEFs which treated the electroporation buffer did not cause any reduction in the viability, we concluded that nsPEFs affects yeast cells directly. Exposure of yeast cells to nsPEFs was accompanied by metacaspase activation, membrane permeability to propidium iodide and the externalisation of phosphatidylserine. We conclude that square shaped electric field pulses with nanosecond durations induce caspase-dependent apoptosis in yeast cells, which in turn can be used as a model for more detailed analysis of the programmed cell death analysis induced by nsPEFs.

References

- [1] D. Miklavčič, B. Mali, B. Kos, R. Heller, G. Serša, Electrochemotherapy: from the drawing board into medical practice, *Biomed. Eng. Online* 13 (1) (2014) 29.
- [2] M. Suga, T. Hatakeyama, High-efficiency electroporation by freezing intact yeast cells with addition of calcium, *Curr. Genet.* 43 (3) (2003) 206–211.
- [3] E. Ortega-Rivas, I. Salmerón-Ochoa, Non-thermal food processing alternatives and their effects on taste and flavor compounds of beverages, *Crit. Rev. Food Sci. Nutr.* 52 (2) (2014) 190–207.
- [4] G. Saldaña, I. Álvarez, S. Condón, J. Raso, Microbiological aspects related to the feasibility of PEF technology for food pasteurization, *Crit. Rev. Food Sci. Nutr.* 54 (11) (2014) 1415–1426.
- [5] A. Golberg, M. Sack, J. Teissie, G. Pataro, U. Pliquett, G. Saulis, T. Stefan, D. Miklavčič, E. Vorobiey, W. Frey, Energy-efficient biomass processing with pulsed electric fields for bioeconomy and sustainable development, *Biotechnol. Biofuels* 9 (1) (Dec. 2016) 1–22.
- [6] D. Liu, N.I. Lebovka, E. Vorobiey, Impact of electric pulse treatment on selective extraction of intracellular compounds from *Saccharomyces cerevisiae* yeasts, *Food Bioprocess Technol.* 6 (2) (2013) 576–584.
- [7] A.G. Pakhomov, E. Gianulis, P.T. Vernier, I. Semenov, S. Xiao, O.N. Pakhomova, Multiple nanosecond electric pulses increase the number but not the size of long-lived nanopenes in the cell membrane, *Biochim. Biophys. Acta Biomembr.* 1848 (4) (2015) 958–966.
- [8] T. Kotnik, G. Purihar, D. Miklavčič, Induced transmembrane voltage and its correlation with electroporation-mediated molecular transport, *J. Membr. Biol.* 236 (1) (2010) 3–13.
- [9] V. Nesin, A.G. Pakhomov, Inhibition of voltage-gated Na⁺ current by nanosecond pulsed electric field (nsPEF) is not mediated by Na⁺ influx or Ca²⁺ signaling, *Bioelectromagnetics* 33 (6) (2012) 443–451.
- [10] V. Nesin, A.M. Bowman, S. Xiao, A.G. Pakhomov, Cell permeabilization and inhibition of voltage-gated Ca²⁺ and Na⁺ channel currents by nanosecond pulsed electric field, *Bioelectromagnetics* 33 (5) (2012) 394–404.
- [11] P.T. Vernier, Y. Sun, M.A. Gundersen, Nanosecond-pulse-driven membrane perturbation and small molecule permeabilization, *BMC Cell Biol.* 7 (37) (2006).
- [12] S.J. Beebe, J. White, P.F. Blackmore, Y. Deng, K. Somers, K.H. Schoenbach, Diverse effects of nanosecond pulsed electric fields on cells and tissues, *DNA Cell Biol.* 22 (12) (2003) 785–796.
- [13] P.T. Vernier, Y. Sun, L. Marcu, C.M. Craft, M.A. Gundersen, Nanosecond-pulse-induced phosphatidylserine translocation, *Biophys. J.* 86 (6) (2004) 4040–4048.
- [14] K.H. Schoenbach, A.G. Pakhomov, I. Semenov, S. Xiao, O.N. Pakhomova, B.L. Ibe, Ion transport into cells exposed to monopolar and bipolar nanosecond pulses, *Bioelectrochemistry* 103 (2015) 44–51.
- [15] S.J. Beebe, P.M. Fox, L.J. Rec, E.L.K. Willis, K.H. Schoenbach, Nanosecond, high-intensity pulsed electric fields induce apoptosis in human cells, *FASEB J.* 17 (14) (2003) 1493–1495.
- [16] K.H. Schoenbach, R.P. Joshi, J.F. Kolb, N. Chen, M. Stacey, P.F. Blackmore, E.S. Buescher, S.J. Beebe, Ultrashort electrical pulses open a new gateway into biological cells, *Proc. IEEE* 92 (7) (2004) 1122–1136.
- [17] M. Ho, M. Casciola, Z.A. Levine, P.T. Vernier, Molecular dynamics simulations of ion conduction in field-stabilized nanoscale lipid electropores, *J. Phys. Chem.* 117 (13) (2013) 11633–11640.
- [18] T.B. Napotnik, M. Reberšek, P.T. Vernier, B. Mali, D. Miklavčič, Effects of high voltage nanosecond electric pulses on eucaryotic cells (in vitro): a systematic review, *Bioelectrochemistry* 110 (2016) 1–12.

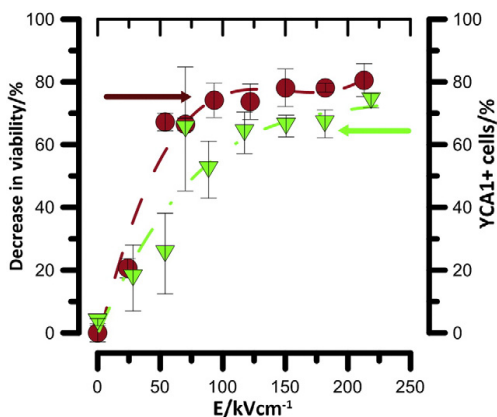


Fig. 7. Decrease in viability and YCA1⁺ activation dependence on the electric field strength after exposure to 5 pulses with durations of 90 ns.

- [19] F. Madeo, E. Fröhlich, K.U. Fröhlich, A yeast mutant showing diagnostic markers of early and late apoptosis, *J. Cell Biol.* 139 (3) (1997) 729–734.
- [20] F. Madeo, E. Herker, C. Maldener, S. Wissing, S. Lachelt, M. Herlan, M. Fehr, K. Lauber, S.J. Sigrist, S. Wesselborg, K.U. Fröhlich, A caspase-related protease regulates apoptosis in yeast, *Mol. Cell* 9 (4) (2002) 911–917.
- [21] S. Wissing, P. Ludovico, E. Herker, S. Buttner, S.M. Engelhardt, T. Decker, A. Link, A. Proksch, F. Rodrigues, M. Corte-Real, K.U. Fröhlich, J. Manns, C. Cande, S.J. Sigrist, G. Kroemer, F. Madeo, An AIF orthologue regulates apoptosis in yeast, *J. Cell Biol.* 166 (7) (2004) 969–974.
- [22] B. Fahrenkrog, U. Sauder, U. Aebi, The *S. cerevisiae* HtrA-like protein Nma111p is a nuclear serine protease that mediates yeast apoptosis, *J. Cell Sci.* 117 (Pt 1) (2004) 115–126.
- [23] D. Walter, S. Wissing, F. Madeo, B. Fahrenkrog, The inhibitor-of-apoptosis protein Bir1p protects against apoptosis in *S. cerevisiae* and is a substrate for the yeast homologue of Omi/HtrA2, *J. Cell Sci.* 119 (9) (2006) 1843–1851.
- [24] S. Buttner, T. Eisenberg, D. Carmona-Gutierrez, D. Ruli, H. Knauer, C. Ruckenstein, C. Sigrist, S. Wissing, M. Kollroser, K.U. Fröhlich, S. Sigrist, F. Madeo, Endonuclease G regulates budding yeast life and death, *Mol. Cell* 25 (2) (2007) 233–246.
- [25] F. Madeo, D. Carmona-Gutierrez, J. Ring, S. Buttner, T. Eisenberg, G. Kroemer, Caspase-dependent and caspase-independent cell death pathways in yeast, *Biochem. Biophys. Res. Commun.* 382 (2) (2009) 227–231.
- [26] D. Wlodkovic, W. Telford, J. Skommer, Z. Darzynkiewicz, Apoptosis and Beyond: Cytometry in Studies of Programmed Cell Death, vol. 103, 2011.
- [27] S. Balevicius, V. Stankevicius, N. Zurauskienė, E. Shatkovskis, A. Stirke, A. Bitinaite, R. Saule, R. Maciuleviciene, G. Saulis, System for the nanoporation of biological cells based on an optically-triggered high-voltage spark-gap switch, *IEEE Trans. Plasma Sci.* 41 (10) (2013) 2706–2711.
- [28] A. Stirke, A. Zimkus, S. Balevicius, V. Stankevicius, A. Ramanaviciene, A. Ramanavicius, N. Zurauskienė, Permeabilisation of yeast *Saccharomyces cerevisiae* cells using nanosecond high power electrical pulses, *Appl. Phys. Lett.* 105 (253701) (2014) 1–4.
- [29] A. Stirke, A. Zimkus, A. Ramanaviciene, S. Balevicius, N. Zurauskienė, G. Saulis, L. Chaustova, V. Stankevicius, A. Ramanavicius, Electric field-induced effects on yeast cell wall permeabilization, *Bioelectromagnetics* 35 (2) (Feb. 2014) 136–144.
- [30] T.C. Tomov, L.C. Tsoneva, Changes in the surface charge of cells induced by electrical pulses, *Bioelectrochem. Bioenerg.* 22 (1989) 127–133 (no. October 1988).
- [31] Q. Zhang, A. Monsalve-Gonzalez, B.L. Qin, G.V. Barbosa-Canovas, B.G. Swanson, Inactivation of *Saccharomyces cerevisiae* in apple juice by square-wave and exponential-decay pulse electric fields, *J. Food Process Eng.* 17 (4) (1994) 469–478.
- [32] H. El Zakhem, J.-L. Lanoisellé, N.I. Lebovka, M. Nonus, E. Vorobiev, The early stages of *Saccharomyces cerevisiae* yeast suspensions damage in moderate pulsed electric fields, *Colloids Surf. B: Biointerfaces* 47 (2) (Feb. 2006) 189–197.
- [33] S. Elmore, Apoptosis: a review of programmed cell death, *Toxicol. Pathol.* 35 (4) (2007) 495–516.
- [34] P.T. Vernier, Y. Sun, L. Marcu, S. Salemi, C.M. Craft, M.A. Gundersen, Calcium bursts induced by nanosecond electric pulses, *Biochem. Biophys. Res. Commun.* 310 (2) (2003) 286–295.
- [35] A.H.H. Wong, C. Yan, Y. Shi, Crystal structure of the yeast metacaspase Yca1, *J. Biol. Chem.* 287 (35) (2012) 29251–29259.
- [36] J.C. Weaver, K.C. Smith, A.T. Esser, R.S. Son, T.R. Gowrishankar, A brief overview of electroporation pulse strength-duration space: a region where additional intracellular effects are expected, *Bioelectrochemistry* 87 (2012) 236–243.
- [37] D. Carmona-Gutierrez, T. Eisenberg, S. Büttner, C. Meisinger, G. Kroemer, F. Madeo, Apoptosis in yeast: triggers, pathways, subroutines, *Cell Death Differ.* 17 (2010) 763–773.
- [38] C. Jin, A.V. Parshin, I. Daly, R. Strich, K.F. Cooper, The cell wall sensors Mtl1, Wsc1, and Mid2 are required for stress-induced nuclear to cytoplasmic translocation of cyclin C and programmed cell death in yeast, *Oxidative Med. Cell. Longev.* 2013 (2013) 1–15.
- [39] P. Drogui, S. Elmaleh, M. Rumeau, C. Bernard, A. Rambaud, Hydrogen peroxide production by water electrolysis: application to disinfection, *J. Appl. Electrochem.* 31 (2001) 877–882.
- [40] G. Farrugia, R. Balzan, Oxidative Stress and Programmed Cell Death in Yeast, *Front. Oncol.* 2 (2012) 1–21 (June).

Paper 5

Pulsed electric field effects on inactivation of microorganisms in acid whey

Simonis, P., Kersulis, S., Stankevich, V., Sinkevic, K., Striguniene, K.,
Ragoza, G., Stirke, A.

International journal of food microbiology **291**, 128-134 (2019).
<https://doi.org/10.1016/j.ijfoodmicro.2018.11.024>



Contents lists available at ScienceDirect

International Journal of Food Microbiology

journal homepage: www.elsevier.com/locate/ijfoodmicro

Pulsed electric field effects on inactivation of microorganisms in acid whey

Povilas Simonis^a, Skirmantas Kersulis^b, Voitech Stankevich^b, Kamilija Sinkevici^a,
Kristina Striguniene^c, Gregoz Ragoza^c, Arunas Stirke^{a,*}

^a Laboratory of Bioelectrochemistry, State Research Institute, Center for Physical Sciences and Technology, Sauletekio ave. 3, LT-10257 Vilnius, Lithuania

^b High Power Pulse Laboratory, State Research Institute, Center for Physical Sciences and Technology, Sauletekio ave. 3, LT-10257, Vilnius, Lithuania

^c Pieno Zvaigzdes Kaunas Department, Taikos ave. 90, LT-51181 Kaunas, Lithuania



ARTICLE INFO

Keywords:

Acid-whey

PEF

Non-thermal

Yeast

Selectivity

ABSTRACT

Prospects of pulsed electric field technology application on acid whey concentrate pretreatment were analyzed. Stationary and flow pre-treatment systems were combined with different treatment parameters: electric field strength ($E = 39$ kV/cm, 95 kV/cm, 92 kV/cm), pulse duration ($\tau = 60$ ns, 90 ns, 1000 ns) and pulse number ($pn =$ up to 100 pulses). Isolates of *Saccharomyces* sp. and *Lactobacillus* sp. were predominant in concentrate. Significant non-thermal inactivation effect was achieved after PEF treatment. Exposure to short pulses selectively inactivated yeast cells, as a result PEF technology can be applied for low-energy acid whey processing.

1. Introduction

Acid whey, also known as sour whey is a byproduct of manufacturing process of acidic dairy products such as cottage cheese or strained yoghurt. Nowadays consumers pay a major attention to food quality as well as health benefits therefore healthier options, e.g., cultured buttermilk and yoghurt are often selected for healthy diet. As a result, food manufacturers are interested in possibilities to reprocess production byproducts such as sweet and acid whey (Chen et al., 2016; Helen Shiphrah et al., 2013; Panesar et al., 2010; Pescuma et al., 2008). Acid whey contains significant amounts of lactose, galactose, calcium phosphate and lactic acid. These components can be further reused in manufacturing of functional foods as well as in improving their color, texture or flavor (Alsaed et al., 2013; Lievore et al., 2015; Pescuma et al., 2010; Yang and Silva, 1995). Moreover, whey contains unique bioactive compounds, e.g., α -lactalbumin, β -lactoglobulin, glycomacropeptide, lactoferrin, lactoperoxidase, lysozyme, growth factors, cytokines, serum albumin, immunoglobulins which can be used as supplements in their active form (Park and Haenlein, 2013). It was previously shown that low-fat dairy products can be beneficial in certain human disease management, e.g., hypertension, type 2 diabetes, cardiovascular diseases, reduce oxidative and inflammatory stresses, facilitate obesity control (Aihara et al., 2005; Baer et al., 2011; McGregor and Poppitt, 2013; Mills et al., 2011). Some proteins are suggested to be active components regulating intestinal enzymes and hormones that play a role in satiety (Luhovyy et al., 2007) and digestion, other proteins are possible mediators for prevention of certain

cancer types, e.g., colon cancer (Parodi, 2007).

In addition to nutritious compounds, whey also contains the microorganisms. Some of them are beneficial for the human gut microbiota, yet others can be harmful and cause food poisoning. Microorganisms may also decrease product shelf life. Seeking an effective assimilation of whey beneficial properties, it is important to apply specific concentration and pasteurization methods. Whey concentrates are usually contaminated, therefore they should be pasteurized and processed immediately. During pasteurization food products are treated with heat to eliminate pathogens and extend shelf life. On the downside, pasteurization affects physicochemical properties of food including changes in appearance, flavor and quality of proteins (Qi et al., 2015; Rynne et al., 2004), fats, minerals, vitamins. One of mentioned chemical changes is formation of advanced glycation products (Uribarri et al., 2010) which are related to diabetes and several chronic diseases (Clarke et al., 2016). Since thermal pasteurization of acid whey leads to secondary straining, i.e., formation of insoluble protein aggregates, non-thermal pasteurization methods are on demand.

Some methods such as centrifugation and microfiltration, high-pressure treatment, ultra-sonication, ultraviolet light, ionizing radiation were suggested and, in some specific cases, are even applied in production of dairy foods. Yet whey is often considered as a byproduct and no specific treatment is applied. Pulsed electric field (PEF) is an emerging technology in dairy product industry (McAuley et al., 2016). PEF technology has been previously applied for pasteurization of various liquid food products (Buckow et al., 2013; Milani et al., 2015; Min

* Corresponding author.

E-mail address: arunas.stirke@ftmc.lt (A. Stirke).

<https://doi.org/10.1016/j.ijfoodmicro.2018.11.024>

Received 5 July 2018; Received in revised form 8 November 2018; Accepted 20 November 2018

Available online 22 November 2018

0168-1605/ © 2018 Published by Elsevier B.V.

et al., 2003). It has also been applied in combination with other pasteurization methods and/or substances for improved efficiency (Caminiti et al., 2011; Pataro et al., 2014a; Saldaña et al., 2014). When a cell in a suspension or a tissue is exposed to electric field, electric potential difference across insulating membrane changes and it may lead to membrane integrity loss. Efficacy of PEF treatment usually depends on the following parameters: electric field strength (E), pulse length (τ), pulse number (pn) and pulse shape (Schoenbach et al., 2015; Pakhomov et al., 2015; Weaver and Chizmadzhev, 1996). PEF based pasteurization technologies inactivate the microorganisms by irreversibly permeabilizing the membranes.

In this study, we aim to elucidate PEF effects on i) acid whey solution, ii) inactivation efficiency, iii) effects on different microorganisms in acid whey concentrate and iv) energy-related aspects of the treatment.

2. Materials and methods

2.1. Whey composition

Acid whey was collected and concentrated at a dairy company (Pieno žvaigždės, Lithuania) during cottage cheese production process. Milk was incubated with a mixture of mesophilic cultures Ceska-star G-700 (CSK, Netherlands) until whey separated from cottage cheese. Whey composition measurements were performed by the manufacturer according to international standards: ISO 9622:2013 (IDF 141:2013). The composition (except the content of viable microorganisms) remained constant prior and after the PEF treatment (Table 1.) and this is in accordance with data from previous milk pasteurization research (Al-Hilphy, 2012). Freshly prepared whey concentrate contained bacterial ($> 10^6$ cells per mL) and yeast ($< 10^4$ cells per mL) cells. During storage at 4 °C, yeast cell count reached approximately 10^5 cells per mL. The PEF treatment was performed at room temperature.

Conductivity was measured with a conductivity meter AD3000 AC/TDS (ADWA, Hungary). Log reduction was evaluated by a plate counting method on a solid MRS media (10 g/L peptone from casein (Merck KGaA, Germany), 10 g/L meat extract (Merck KGaA, Germany), 4 g/L yeast extract (Merck KGaA, Germany), 20 g/L glucose (Merck KGaA, Germany), 2 g/L disodium hydrophosphate (SIGMA-ALDRICH, USA), 1 g/L Tween 80 (Merck KGaA, Germany), 2 g/L diammonium hydroxide (SIGMA-ALDRICH, USA), 5 g/L sodium acetate (SIGMA-ALDRICH, USA), 0.2 g/L magnesium sulphate (SIGMA-ALDRICH, USA), 0.04 g/L manganese sulphate (Merck KGaA, Germany), 12 g/L agar (Merck KGaA, Germany).

2.2. Evaluation of viability

Efficacy of microbial inactivation was evaluated by log reduction (LR), defined by equation:

$$LR = -\log\left(\frac{N}{N_0}\right) \quad (1)$$

N and N_0 are numbers of colony forming units in treated and untreated suspensions respectively. Experimental data of log reduction was analyzed by mathematical model (Mafart et al., 2002):

$$LR = \left(\frac{pn}{pn_{red1}}\right)^{\rho} \quad (2)$$

Table 1
Chemical composition of acid whey.

Fat, %	Protein, %	Dry solids, %	Conductivity, mS/cm	pH
0.026 ± 0.005	2.26 ± 0.02	17.78 ± 0.05	~8.33	4.54 ± 0.01

Table 2

List of primers.

Primer	Primer sequence (Sanchez and Sanz, 2011; White et al., 1990)
27F	5'-GAGAGTTTGATCTGGCTCAG-3'
1495R	5'-CTACGGCTACCTGTTACGA-3'
ITS1	5'-TCCGTAGTGAACCTGGCG-3'
ITS4	5'-TCCTCCGCTTATTGATATGC-3'

Eq. (2) includes data from our experiments (LR, pn) and computed generated parameters (pn_{red1} , ρ). pn_{red1} describes pulse number required viable cell count reduction by one log and ρ is the parameter of curve shape. Convex curves are described by $\rho > 1$, concave curves are described by $\rho < 1$, $\rho = 1$ represents linear change. Data lines approximated with this model are survival curves.

2.3. Microorganism identification

To identify species of isolated microorganisms, 16S rRNA gene sequence from bacterial isolate (Sanchez and Sanz, 2011) and highly variable Internal Transcribed Spacer (ITS) regions of fungal ribosomal DNA from yeast isolate (White et al., 1990) were amplified and analyzed. The amplification reactions were performed by a colony PCR method. Two pairs of primers were selected (Table 2): 27F and 1495R for 16S rRNA gene amplification, ITS1 and ITS4 for amplification of ITS region sequences. All primers were synthesized by Metabion (Germany).

Microorganism isolation was performed on chloramphenicol glucose agar (Sharlau Chemie S.A., Spain) and plate count skim milk agar (Merck KGaA, Germany) growth media. Single dominant bacterial and yeast isolates were then separated and cultured overnight at 30 °C on MRS agar and YPD agar plates (20 g/L peptone from casein (Merck KGaA, Germany), 10 g/L yeast extract (Merck KGaA, Germany), 20 g/L glucose (Merck KGaA, Germany), 12 g/L agar (Merck KGaA, Germany) respectively in INCULine (VWR, USA) incubator. Single colonies from overnight cultures of each isolate were re-suspended in 50 μ L of ultrapure water and mixed. Cells were lysed at 95 °C for 10 min. 2 μ L of each lysate was added to prepared PCR reaction mixtures. 50 μ L PCR reaction mixture contained 2 μ L of template DNA, 1.25 U of DreamTaq DNA Polymerase (Thermo Scientific, Lithuania), 5 μ L of 10 \times Dream Taq buffer, 1 μ M of forward and 1 μ M of reverse primer, 4 mM of MgCl₂, 0.4 mM of each of four dNTPs. Amplification was performed under the following conditions: 2 min of initial denaturation at 98 °C; 35 cycles of denaturation (30 s at 96 °C), annealing (30 s at 51 °C for samples with 27F and 1495R primers, 54 °C for samples with ITS1 and ITS4 primers), extension (1 min at 72 °C) and final extension at 72 °C for 10 min. Amplification products were analyzed on 0.9% (wt/vol) agarose gel, purified using a GeneJET Gel Extraction and a DNA Cleanup Micro Kit (Thermo Scientific, Lithuania). Purified fragments were sequenced by BaseClear B.V. (The Netherlands).

The consensus sequences were obtained using BioEdit software package version 7.0.5 (North Carolina State University, Raleigh, USA) and compared to those in the NCBI database (<http://www.ncbi.nlm.nih.gov/BLAST/>). Yeast isolate was ascribed to the species showing the highest matched sequence identity. In case of bacterial isolate, sequences showing highest identity were chosen to generate phylogenetic tree and determine evolutionary relationships. Sequences were aligned using ClustalW method. The phylogenetic tree was generated using neighbor-joining method from phylogenetic distances calculated by the Jukes-Cantor method with MEGA v. 7 software (Pennsylvania State University, USA). Bootstrap values were obtained after 1000 replicates.

2.4. PEF generation systems

Two different PEF generation systems were used for acid whey

treatment. Square-wave monopolar pulses (duration of 60 and 90 ns) were formed by a generator based on an optically triggered spark-gap switch. In these experiments, the coaxial line (75 Ω) was charged up to 23 kV resulting in generation of electric field $E = 95$ kV/cm across a cuvette with resistance of approximately 50 Ω . 60 and 90 ns pulses generated 0.11 J and 0.16 J of energy respectively. A schematic diagram of the experimental setup and working parameters were previously described by Balevicius et al., 2013. A cuvette with cylinder shaped stainless-steel electrodes (diameter $D = 5.3$ mm), spaced at a distance of $d = 0.75$ mm, was used in stationary system (SS). Another experimental set-up involved a seven-stage Marx generator operating in free-running mode up to 10 Hz. In these experiments, the Marx generator was charged to 1.8 kV (threshold voltage for used spark-gaps) and discharged into the cuvette with liquid samples. A unipolar exponential damped pulse of about 1 μ s duration (full width at half maximum) was achieved. For flow system (FS), a polytetrafluoroethylene (PTFE) cell with stainless steel electrodes was used. Acid whey was delivered to the treatment chamber by MasterFlex L/S (Cole-Parmer, USA) peristaltic pump at a flow rate of 2 mL/min. The active area of the electrodes was 130 mm². The distance between the plates of the electrodes was 2 mm. 0.26 mL of cell suspension was placed in a cuvette. Number of pulses per volume was adjusted by changing pulse frequency and flow speed. Pulse frequency was adjusted by adjusting a power supply voltage. In a stationary cuvette experiments, the electrical energy of about 1.8 J was produced with each pulse. Electric field of about 92 kV/cm was generated across a cuvette. In flow system experiments, the energy was about 2.6 J per pulse when electric field was approximately $E = 39$ kV/cm. To determine PEF effects on whey only, microorganisms were separated by centrifugation for 20 min at 20,000g (Jouan KR25i, Thermo Fisher Scientific, USA). Fig. 1 shows a rough experimental scheme and a summary of treatment parameters.

3. Results and discussion

3.1. Indirect effects on the viability of microorganisms

Research was started by analyzing indirect PEF effects on the viability of microorganisms, i.e., generation of toxic reactive oxygen species (Drogui et al., 2001) as well as electrolysis and electrode corrosion products (Pataro et al., 2014a, b; Saulis et al., 2015). To test PEF induced chemical effects, whey was centrifuged, and the supernatant was exposed to PEF ($\tau = 1$ μ s; $E = 39$ kV/cm; $pn = 32$). The pellet was resuspended immediately after PEF treatment and subsequently plated on solid media. It was shown that LR increase up to 0.287 ± 0.094 can be attributed to indirect effects. Some of LR was achieved by centrifugation ($LR = 0.159 \pm 0.076$) that could have caused formation of aggregates as well as cell death due to shear forces and, therefore, lead to decrease in the number of colony-forming units. It was concluded that LR of approximately 0.128 was caused by PEF generated chemical toxicity.

It is known that thermal treatment may lead to permanent inactivation of microorganisms. To test thermal impact on LR values, acid whey was incubated in water bath for 2 min and plated on solid medium immediately afterwards. It was observed that the temperature of 40 °C can act as a signal for proliferation or induce aggregate dispersion, therefore, lowering LR values (-0.046 ± 0.044). The viability of microorganisms in a sample that was incubated at 50 °C was similar to the control sample. The highest increase in LR (0.196 ± 0.066) was observed after incubating the sample at 60 °C. The conclusion was drawn that the temperature does affect the viability of microorganisms, therefore, to distinguish PEF effects from those caused by thermal pasteurization, it is important to monitor the sample temperature.

3.2. Electroporation in flow chamber

For further whey processing, a continuous flow system was used ($E = 39$ kV/cm, $\tau = 1$ μ s). The viability of microorganisms was shown to be affected by the velocity of a fluid flow (data not presented): microorganisms were less viable at higher velocity rates. Hence, the flow speed was set to a constant 2 mL/min value that did not influence the viability of microorganisms. Pulse number was adjusted by changing frequency of pulses (up to 32 pulses per volume). Higher LR values were observed with raise in pulse number and the results are shown in Fig. 2. The highest value of microbial LR was achieved after 32 pulses ($LR = 1.14 \pm 0.08$). Whey exposure to electric field also caused the rise of its temperature and it was dependent on pulse number applied. The highest temperature ($T = 50.10 \pm 4.05$ °C) was measured after 32 pulses, however, it is too low for thermal pasteurization. Therefore, it can be presumed that LR in our experiments was achieved by direct as well as indirect effects of PEF treatment but not by thermal effect only. It was concluded that PEF can be effectively applied for non-thermal acid whey concentrate pasteurization in the flow system. Since LR values changed when the number of pulses was increased, it suggests that the results could also be improved by changing E and/or τ .

3.3. Microorganism isolation

To evaluate PEF effects on specific microorganisms, isolation was performed. Two dominant microorganisms were chosen for identification by 16S rRNA gene and ITS region sequencing. The analysis of yeast ITS region sequences resulted in 99% match with the sequences of *Saccharomyces cerevisiae* strains published in NCBI database. The BLAST analysis showed significant bacterial isolate identity ($> 98\%$) to *Lactobacillus* genus bacteria. Phylogenetic analysis indicated that a species most closely related to bacterial isolate is *L. rhamnosus* (Fig. 3). In general, bacteria from *Lactobacillus* genus are recognised as safe and are designated the GRAS status (Salminen et al., 1998). *L. rhamnosus* has significant positive impact on the intestinal microbiota and epithelial barrier functions (Johnson-Henry et al., 2008), it also relieves diarrhoea (Guandalini et al., 2000), displaces the pathogenic bacteria (Vesterlund et al., 2006), stimulates hosts' immune system (Saxelin et al., 2005) and plays a role in maintaining homeostasis of intestinal epithelial cells (Yan and Polk, 2002). Furthermore, *L. rhamnosus* strains act as probiotics for prevention of oral cavity disorders (Ahola et al., 2002) and respiratory infections (Hojsak et al., 2010).

PEF effects on each microorganism were analyzed separately. For simplicity purposes, PEF parameters are shown as $LR_{\text{microorganism_pulselength(ns)_fieldstrength_pulsenummer}}$.

3.4. Selective pasteurization

PEF effects on acid whey microorganisms were further analyzed in a static treatment chamber. The suspension was poured into a cuvette and exposed to various numbers of electric field pulses ($pn = 1, 5, 10, 30, 50, 70, 100$) of different pulse length ($\tau = 60$ ns, 90 ns, 1000 ns) and field strength ($E = 95$ kV/cm, 92 kV/cm). When shorter pulses < 1000 ns were applied, minimal increase of bacterial LR values was observed ($LR_{B,60,95,100} = 0.08 \pm 0.01$ and $LR_{B,90,95,100} = 0.08 \pm 0.01$; Fig. 4). However, higher sensitivity of yeast cells was observed ($LR_{Y,60,95,100} = 0.99 \pm 0.08$, $LR_{Y,90,95,100} = 1.34 \pm 0.36$) and it suggests that PEF can be used for selective pasteurization. At pulse lengths of 60 ns and 90 ns yeast cells were at least ten times more sensitive to PEF treatment than bacterial cells. After whey exposure to longer pulses LR values were higher, but the difference of PEF effects on yeast and bacterial cells was less significant ($LR_{Y,1000,92,50} = 1.79 \pm 0.12$; $LR_{B,1000,92,50} = 1.47 \pm 0.05$).

Shorter pulses may cause selective effects by targeting mitochondria in yeast, yet the difference in size of the cells can be an alternative explanation of our results (Schoenbach et al., 2004). It was previously shown

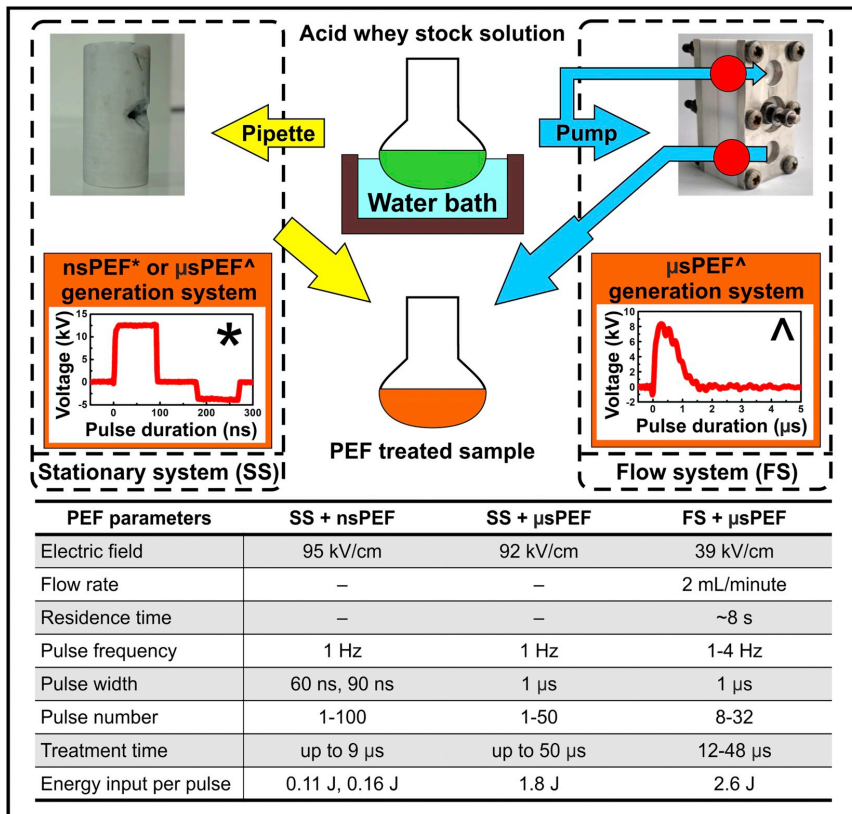


Fig. 1. Scheme of PEF treatment setup and parameters. Residence time – is the time which specimen spends in PEF treatment area in flow system; treatment time – is the duration of an actual exposure to PEF of the specimen; ★ – pulse shape formed by nsPEF generation system; ▲ – pulse shape formed by μsPEF generation system; ● – thermocouples.

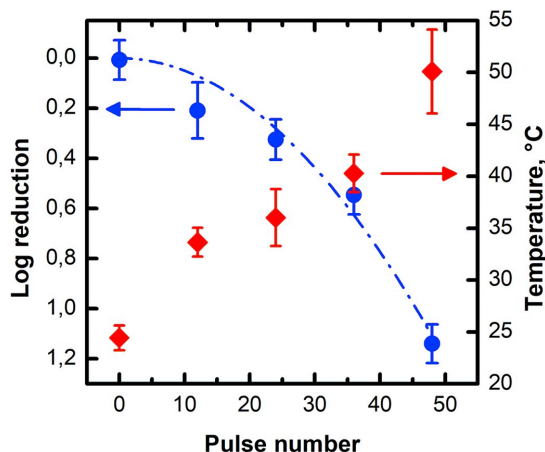


Fig. 2. Log reduction of total colony forming unit number (blue circles) and temperature (red diamonds) change dependence on pulse number in flow system (FS). Dash-dotted line represents survival curve by data fitting using Eq. (2) (Adj, R-square = 0,96,576). (For interpretation of the references to color in this figure legend, the reader is referred to the web version of this article.)

that pulse duration of 90 ns can induce apoptosis in yeast cells – number of colony forming units (CFU) of *S. cerevisiae* cells decreased ($CFU_{Y_{90,96,1}} = 62 \pm 6\%$, $CFU_{Y_{90,96,5}} = 59 \pm 5\%$) (Simonis et al., 2017). If we present whey LR_Y results as CFU, where 100% represents number of yeast colony forming units in untreated samples, we get similar decrease values ($CFU_{Y_{90,95,1}} = 63 \pm 29\%$, $CFU_{Y_{90,95,5}} = 66 \pm 16\%$). However, cell treatment medium was different in both studies in terms of acidity and osmolarity. It suggests that acidity and osmolarity were secondary factors affecting yeast cell viability during/after PEF treatment (Saldaña et al., 2009). PEF effects on yeast and bacteria in same media were studied previously (Puértolas et al., 2009). Puértolas et al. demonstrate similar results: *Lactobacillus* strains were more resistant to PEF treatment than *S. bayanus*, but no significant selectivity was detected. Puértolas' team applied electric field strengths ranging from 16 to 31 kV/cm, number of pulses ranged from 0 to 100, specific energies per pulse ranged from 1.02 to 3.77 kJ/kg, pulse frequency was 1 Hz. Treatment of microorganisms in wine media was more energy efficient probably due to lower conductivity (~4 times lower than whey). In both of our studies (flow and stationary) increase in LR (for all whey microorganisms) was dependent on pn, τ and E, resulting in greater values with higher pn, longer τ and stronger E.

3.5. Efficiency analysis

Efficiency of PEF treatment was evaluated by calculating energy

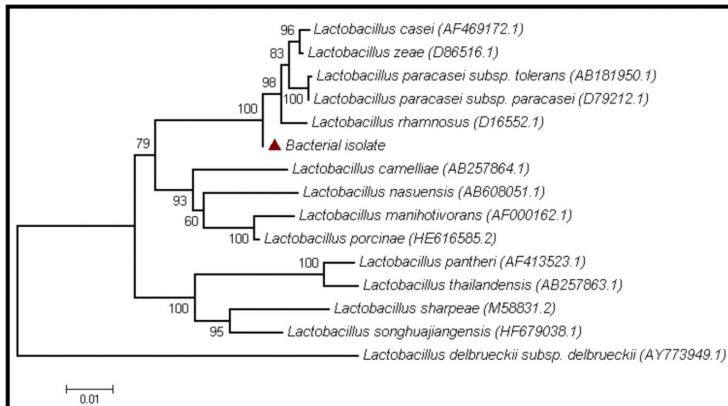


Fig. 3. Phylogenetic tree highlighting the position of bacterial isolate relative to other *Lactobacillus* species. The tree was constructed based on 16S rRNA gene sequences. GenBank accession numbers are presented in parentheses. The scale bar indicates an estimated 0.01 nucleotide change per nucleotide position. Horizontal distances correspond to genetic distances; vertical distances are arbitrary. Numbers at the nodes indicate the bootstrap values on neighbor-joining analysis.

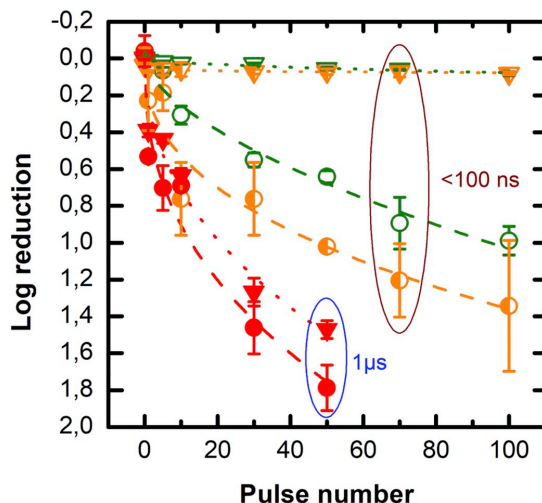


Fig. 4. Selective inactivation of acid whey concentrates in stationary system. Circles – yeast cells; triangles – bacteria; hollow symbols, green color – $E = 95\text{ kV/cm}$, $\tau = 60\text{ ns}$; half-filled symbols, orange color – $E = 95\text{ kV/cm}$, $\tau = 90\text{ ns}$; filled symbols, red color – $E = 92\text{ kV/cm}$, $\tau = 1\mu\text{s}$; dashed and dotted curves were obtained by fitting with Eq. (2) for yeast and bacteria cells respectively. (For interpretation of the references to color in this figure legend, the reader is referred to the web version of this article.)

Table 3

Log reduction analysis through model assessed data. SS – stationary system, FS – flow system, Y – yeast cells, B – bacteria, T – yeast and bacteria.

PEF system	SS	SS	SS	SS	SS	FS
Microorganisms	Y	Y	Y	B	T	T
E, kV/cm	95	95	92	92	92	39
Pulse width	60 ns	90 ns	1 μs	1 μs	1 μs	1 μs
Pnred1	94.37	47.34	12.75	20.77	19.69	30.36
ρ	0.61	0.41	0.41	0.46	0.45	1.98
Energy per 1 LR, kJ/L	189.52	137.63	417.27	679.75	644.4	303.6

required for log reduction (Table 3). Pnred1 and ρ values were calculated from eq. (2). In order to increase LR_Y by one, when $\tau = 90\text{ ns}$ and $E = 95\text{ kV/cm}$, 137.63 kJ/L of energy was consumed. Same LR_Y was achieved after exposure of whey to multiple pulses when $\tau = 1\mu\text{s}$ and

$E = 92\text{ kV/cm}$. Such treatment required 417.27 kJ/L of energy. It was shown that selective PEF treatment is an energy efficient process. In addition, overall microbial inactivation in flow system demonstrated significantly higher energy efficiency compared to stationary system (303.6 kJ/L in flow system and 644.4 kJ/L in stationary system when 1 μs pulses with 92 kV/cm electric field strength were used). In order to avoid electrical discharges, extra liquid was added into stationary treatment chamber. Untreated volume could have caused lower efficiency.

Another parameter obtained from the model was ρ which describes the shape of the curve (Cebrián et al., 2016; Mafart et al., 2002). The only convex curve ($\rho = 1.98$) was observed in log reduction pattern of flow system. This could mean that not all cells were affected equally (due to shear forces, turbulence inside treatment chamber, uneven flow) in the system and specific number of pulses should be applied to compensate this phenomenon. In stationary system all curves were concave with $\rho < 1$ suggesting that most of the cells were affected during the treatment. Some cells remained untreated possibly due to uneven electric field distribution, cell size difference or involvement in aggregates. In theory, if we multiply applied pulses by factor ten, LR in stationary system will increase up to ~ 4 times. LR would reach plateau due to our particular setup where some of the cells remain outside the treatment chamber. On the other hand, in FS, tenfold raise in pulse number, theoretically would result in ~ 95 -fold higher LR suggesting that in our setup some cells remained untreated, but they would be if exposed to higher number of pulses. It was concluded that electric field pulses of nanosecond duration can be used for selective and energy efficient pasteurization of the product, yet it is very important to optimize treatment parameters as well as treatment chamber.

4. Conclusions

We analyzed prospects of PEF application on acid whey concentrate in flow and stationary treatment chambers. We demonstrate that a significant microbial reduction can be achieved ($LR_{T,1000,92,50} = 1.47 \pm 0.05$). As the current flows through the chamber during PEF application, the temperature of the sample increases and toxic compounds are potentially produced. In flow system, $LR_{T,1000,39,60} = 1.14 \pm 0.08$ was achieved with $\Delta T = 27.41 \pm 3.26\text{ }^\circ\text{C}$. Temperature raise was not high enough to significantly affect LR. This suggests that PEF could be applied as a non-thermal pasteurization technology and it could be used for treatment of heat sensitive products. To lower the temperature of the system and to achieve log reduction of higher values, multiple treatment chambers with different PEF parameters could be used in combination with cooling lines.

Efficiency of electroporation is not significantly affected by pulse shape and primarily depends on time during which the amplitude

of pulse exceeds a certain critical value (Kotnik et al., 2003). In our study, we showed that PEF pulses of different duration can result in selective LR of different cell types (in our case yeast and bacterial cells) making it applicable for food processing technologies where beneficial bacteria are required to be preserved. On the other hand, yeast cells usually play an undesirable role as spoilage microorganisms and preferably should be inactivated (Fleet and Mian, 1987). Yeast can survive in acidic and/or cool environments and are resistant to physicochemical stresses, therefore, they can grow in manufacturing lines of certain dairy products (e.g., yoghurt) (Jakobsen and Narvhus, 1996). PEF technology enables pre-treatment and non-thermal pasteurization of various food products including cottage cheese, yoghurt and acid whey preserving the beneficial strains of bacteria for further fermentation.

Acknowledgements

The authors want to thank Rytis Baltutis and Sandra Gandzelyte for their contribution in experiments. We thank Justina Kavaliauskaitė for helpful comments on the manuscript.

References

- Ahola, A.J., Yli-Knuutila, H., Suomalainen, T., Poussa, T., Ahlström, A., Meurman, J.H., Korpela, R., 2002. Short-term consumption of probiotic-containing cheese and its effect on dental caries risk factors. *Arch. Oral Biol.* 47 (11), 799–804.
- Aihara, K., Kajimoto, O., Hirata, H., Takahashi, R., Nakamura, Y., 2005. Effect of powdered fermented milk with *Lactobacillus helveticus* on subjects with high-normal blood pressure or mild hypertension. *J. Am. Coll. Nutr.* 24 (4), 257–265.
- Al-hilphy, A.R.S., 2012. Electrical field (AC) for non-thermal milk pasteurization. *J. Nutr. Food Sci.* 2 (10). <https://doi.org/10.4172/2155-9600.1000177>.
- Alsaed, A.K., Ahmad, R., Aldoomy, H., El-Qader, S.A., Saleh, D., Sakejha, H., Mustafa, L., 2013. Characterization, concentration and utilization of sweet and acid whey. *Pak. J. Nutr.* 12 (2), 172–177. <https://doi.org/10.3923/pjn.2013.172.177>.
- Baer, D.J., Stote, K.S., Paul, D.R., Harris, G.K., Rumpler, W.V., Clevidence, B.A., 2011. Whey protein but not soy protein supplementation alters body weight and composition in free-living overweight and obese adults. *J. Nutr.* 141 (8), 1489–1494. <https://doi.org/10.3945/jn.111.139840>.
- Balevicius, S., Stankevicius, V., Zurauskienė, N., Shatkovskis, E., Stirke, Arunas, Bitinaite, A., Saule, R., Maciuleviciene, R., Saulis, G., 2013. System for the nonoperation of biological cells based on an optically-triggered high-voltage spark-gap switch. *IEEE T. Plasma Sci.* 41 (10), 2706–2711. <https://doi.org/10.1109/TPS.2013.2280376>.
- Buckow, R., Ng, S., Toepfl, S., 2013. Pulsed electric field processing of orange juice: a review on microbial, enzymatic, nutritional, and sensory quality and stability. *Compr. Rev. Food Sci. Food Saf.* 12 (5), 455–467. <https://doi.org/10.1111/1541-4337.12026>.
- Caminiti, L.M., Palgan, I., Noci, F., Muñoz, A., Whyte, P., Cronin, D.A., Morgan, D.J., Lyng, J.G., 2011. The effect of Pulsed Electric Fields (PEF) in combination with High Intensity Light Pulsed (HILP) on *Escherichia Coli* inactivation and quality attributes in apple juice. *Innov. Food Sci. Emerg. Technol.* 12 (2), 118–123. <https://doi.org/10.1016/j.ifset.2011.01.003>.
- Cebrián, G., Condón, S., Mañas, P., 2016. Influence of growth and treatment temperature on *Staphylococcus aureus* resistance to pulsed electric fields: relationship with membrane fluidity. *Innov. Food Sci. Emerg. Technol.* 37, 161–169. <https://doi.org/10.1016/j.ifset.2016.08.011>.
- Chen, G.Q., Eschbach, F.I.L., Weeks, M., Gras, S.L., Kentish, S.E., 2016. Removal of lactic acid from acid whey using electrodialysis. *Sep. Purif. Technol.* 158, 230–237. <https://doi.org/10.1016/j.seppur.2015.12.016>.
- Clarke, R.E., Dordevic, A.L., Tan, S.M., Ryan, L., Coughlan, M.T., 2016. Dietary advanced glycation end products and risk factors for chronic disease: a systematic review of randomised controlled trials. *Nutrients* 8 (3), 125. <https://doi.org/10.3390/nu8030125>.
- Drogui, P., Elmaleh, S., Rumeau, M., Bernard, C., Rambaud, A., 2001. Hydrogen peroxide production by water electrolysis: application to disinfection. *J. Appl. Electrochem.* 31 (8), 877–882.
- Fleet, G.H., Mian, M.A., 1987. The occurrence and growth of yeasts in dairy products. *Int. J. Food Microbiol.* 4 (2), 145–155. [https://doi.org/10.1016/0168-1605\(87\)90021-3](https://doi.org/10.1016/0168-1605(87)90021-3).
- Guandalini, S., Pensabene, L., Zikri, M.A., Dias, J.A., Casali, L.G., Hoekstra, H., Kolacek, S., Massar, K., Micetic-Turk, D., Papadopoulos, A., de Sousa, J.S., Sandhu, B., Szajewska, H., Weizman, Z., 2000. *Lactobacillus GG* administered in oral rehydration solution to children with acute diarrhea: a multicenter European trial. *J. Pediatr. Gastroenterol. Nutr.* 30 (1), 54–60.
- Hojšak, I., Snovak, N., Abdović, Slaven, Szajewska, Hania, Mišak, Zrinjka, Sanja, Kolaček, 2010. *Lactobacillus GG* in the prevention of gastrointestinal and respiratory tract infections in children who attend day care centers: a randomized, double-blind, placebo-controlled trial. *Clin. Nutr.* 29 (3), 312–316. <https://doi.org/10.1016/j.clnu.2009.09.008>.
- Jakobsen, M., Narvhus, J., 1996. Yeasts and their possible beneficial and negative effects on the quality of dairy products. *Int. Dairy J.* 6 (8–9), 755–768. [https://doi.org/10.1016/0958-6946\(95\)00071-2](https://doi.org/10.1016/0958-6946(95)00071-2).
- Johnson-Henry, K.C., Donato, K.A., Shen-Tu, G., Gordanpour, M., Sherman, P.M., 2008. *Lactobacillus rhamnosus* strain GG prevents Enterohemorrhagic *Escherichia coli* O157:H7-induced changes in epithelial barrier function. *Infect. Immun.* 76 (4), 1340–1348. <https://doi.org/10.1128/IAI.00778-07>.
- Kotnik, T., Pucihar, G., Reberser, M., Miklavcic, D., Mir, L.M., 2003. Role of pulse shape in cell membrane electroporation. *Biochim. Biophys. Acta* 1614 (2), 193–200. [https://doi.org/10.1016/S0005-2736\(03\)00173-1](https://doi.org/10.1016/S0005-2736(03)00173-1).
- Lievore, P., Simões, D.R., Silva, K.M., Drunkler, N.L., Barana, A.C., Nogueira, A., Demiate, I.V., 2015. Chemical characterisation and application of acid whey in fermented milk. *J. Food Sci. Technol.* 52 (4), 2083–2092. <https://doi.org/10.1007/s13197-013-1244-z>.
- Luhovyy, B.L., Akhavan, T., Anderson, G.H., 2007. Whey proteins in the regulation of food intake and satiety. *J. Am. Coll. Nutr.* 26 (6), 704S–712S.
- Mafart, P., Couvert, O., Gaillard, S., Leguerinel, I., 2002. On calculating sterility in thermal preservation methods: application of the Weibull frequency distribution model. *Int. J. Food Microbiol.* 72 (1–2), 107–113.
- McAuley, C.M., Singh, T.K., Haro-Maza, J.F., Williams, R., Buckow, R., 2016. Microbiological and physicochemical stability of raw, pasteurised or pulsed electric field-treated milk. *Innov. Food Sci. Emerg. Technol.* 38, 365–373. <https://doi.org/10.1016/j.ifset.2016.09.030>.
- McGregor, R.A., Poppitt, S.D., 2013. Milk protein for improved metabolic health: a review of the evidence. *Nutr. Metab. (Lond.)* 10 (1), 46. <https://doi.org/10.1186/1743-7075-10-46>.
- Milani, E.A., Alkhalafji, S., Silva, F.V.M., 2015. Pulsed electric field continuous pasteurization of different types of beers. *Food Control* 50, 223–229. <https://doi.org/10.1016/j.foodcont.2014.08.033>.
- Mills, S., Ross, R.P., Hill, C., Fitzgerald, G.F., Stanton, C., 2011. Milk intelligence: mining Milk for bioactive substances associated with human health. *Int. Dairy J.* 21 (6), 377–401. <https://doi.org/10.1016/j.idairyj.2010.12.011>.
- Min, S., Jin, Z.T., Zhang, Q.H., 2003. Commercial scale pulsed electric field processing of tomato juice. *J. Agric. Food Chem.* 51 (11), 3338–3344. <https://doi.org/10.1021/jf0260444>.
- Pakhomov, A.G., Gianulis, E., Vernier, P.T., Semenov, I., Xiao, S., Pakhomova, O.N., 2015. Multiple nanosecond electric pulses increase the number but not the size of long-lived nanopores in the cell membrane. *Biochim. Biophys. Acta* 1848 (4), 958–966. <https://doi.org/10.1016/j.bbame.2014.12.026>.
- Panesar, P.S., Kennedy, J.F., Knill, C.J., Kosseva, M., 2010. Production of L(+) lactic acid using *Lactobacillus casei* from whey. *Braz. Arch. Biol. Technol.* 53 (1), 219–226. <https://doi.org/10.1590/S1516-89132010000100027>.
- Park, Y.W., Haenlein, G.F.W., 2013. Milk and Dairy Products in Human Nutrition Production, Composition and Health. John Wiley & Sons Ltd.
- Parodi, P.W., 2007. A role for milk proteins in cancer prevention. *Curr. Pharm. Des.* 13 (8), 813–828.
- Pataro, G., De Lisi, M., Donsi, G., Ferrari, G., 2014a. Microbial inactivation of *E. coli* cells by a combined PEF–HPCD treatment in a continuous flow system. *Innov. Food Sci. Emerg. Technol.* 22, 102–109. <https://doi.org/10.1016/j.ifset.2013.12.009>.
- Pataro, G., Falcone, M., Donsi, G., Ferrari, G., 2014b. Metal release from stainless steel electrodes of a PEF treatment chamber: effects of electrical parameters and food composition. *Innov. Food Sci. Emerg. Technol.* 21, 58–65. <https://doi.org/10.1016/j.ifset.2013.10.005>.
- Pescuma, M., Hebert, E.M., Mozzi, F., de Valdez, G.F., 2008. Whey fermentation by thermophilic lactic acid bacteria: evolution of carbohydrates and protein content. *Food Microbiol.* 25 (3), 442–451. <https://doi.org/10.1016/j.fm.2008.01.007>.
- Pescuma, M., Hebert, E.M., Mozzi, F., de Valdez, G.F., 2010. Functional fermented whey-based beverage using lactic acid bacteria. *Int. J. Food Microbiol.* 141 (1–2), 73–81. <https://doi.org/10.1016/j.jfoodmicro.2010.04.011>.
- Puértolas, E., López, N., Condón, S., Raso, J., Álvarez, I., 2009. Pulsed electric fields inactivation of wine spoilage yeast and bacteria. *Int. J. Food Microbiol.* 130 (1), 49–55. <https://doi.org/10.1016/j.jfoodmicro.2008.12.035>.
- Qi, P.X., Ren, D., Xiao, Y., Tomasula, P.M., 2015. Effect of homogenization and pasteurization on the structure and stability of whey protein in milk. *J. Dairy Sci.* 98 (5), 2884–2897. <https://doi.org/10.3168/jds.2014.8920>.
- Rynne, N.M., Beresford, T.P., Kelly, A.L., Guinee, T.P., 2004. Effect of milk pasteurization temperature and in situ whey protein denaturation on the composition, texture and heat-induced functionality of half-fat cheddar cheese. *Int. Dairy J.* 14 (11), 989–1001. <https://doi.org/10.1016/j.idairyj.2004.03.010>.
- Saldaña, G., Puértolas, E., López, N., García, D., Álvarez, I., Raso, J., 2009. Comparing the PEF resistance and occurrence of sublethal injury on different strains of *Escherichia coli*, *Salmonella typhimurium*, *Listeria monocytogenes* and *Staphylococcus aureus* in media of PH 4 and 7. *Innov. Food Sci. Emerg. Technol.* 10 (2), 160–165. <https://doi.org/10.1016/j.ifset.2008.11.003>.
- Saldaña, G., Álvarez, I., Condón, S., Raso, J., 2014. Microbiological aspects related to the feasibility of PEF Technology for Food Pasteurization. *Crit. Rev. Food Sci. Nutr.* 54 (11), 1415–1426. <https://doi.org/10.1080/10408398.2011.638995>.
- Salminen, S., von Wright, A., Morelli, L., Marteau, P., Brassart, D., de Vos, W.M., Fondén, R., Saxelin, M., Collins, K., Mogensen, G., Birkeland, S.E., Mattila-Sandholm, T., 1998. Demonstration of safety of probiotics - a review. *Int. J. Food Microbiol.* 44 (1–2), 93–106.
- Sanchez, E., Sanz, Y., 2011. *Lactobacillus*. In: Liu, D. (Ed.), *Molecular Detection of Human Bacterial Pathogens*. Taylor & Francis/CRC Press, pp. 257–267.
- Saulis, G., Rodaitė-Riševičienė, R., Damauskaitė, V.S., Saulė, R., 2015. Electrochemical processes during high-voltage electric pulses and their importance in food processing technology. In: Rai, R.V. (Ed.), *Advances in Food Biotechnology*. Wiley, Chichester, pp. 575–592. <https://doi.org/10.1002/9781118864463>.
- Saxelin, M., Tynkkynen, S., Mattila-Sandholm, T., de Vos, W.M., 2005. Probiotic and other functional microbes: from markets to mechanisms. *Curr. Opin. Biotechnol.* 16

- (2), 204–211. <https://doi.org/10.1016/j.copbio.2005.02.003>.
- Schoenbach, K.H., Joshi, R.P., Kolb, J.F., Chen, N., Stacey, M., Blackmore, P.F., Buescher, E.S., Beebe, S.J., 2004. Ultrashort electrical pulses open a new gateway into biological cells. *Proc. IEEE* 92 (7), 1122–1136. <https://doi.org/10.1109/JPROC.2004.829009>.
- Schoenbach, K.H., Pakhomov, A.G., Semenov, I., Xiao, S., Pakhomova, O.N., Ibey, B.L., 2015. Ion transport into cells exposed to monopolar and bipolar nanosecond pulses. In: *Bioelectrochemistry*. 103. Elsevier B.V., pp. 44–51. <https://doi.org/10.1016/j.bioelechem.2014.08.015>.
- Shiphrah, V.H., Sahu, S., Thakur, A.R., Chaudhuri, S.R., 2013. Screening of bacteria for lactic acid production from whey water. *Am. J. Biochem. Biotechnol.* 9 (2), 118–123. <https://doi.org/10.3844/ajbbsp.2013.118.123>.
- Simonis, P., Kersulis, S., Stankevich, V., Kaseta, V., Lastauskiene, E., Stirke, A., 2017. Caspase dependent apoptosis induced in yeast cells by nanosecond pulsed electric fields. *Bioelectrochemistry* 115, 19–25. <https://doi.org/10.1016/j.bioelechem.2017.01.005>.
- Uribarri, J., Woodruff, S., Goodman, S., Cai, W., Chen, X., Pyzik, R., Yong, A., Striker, G.E., Vlassara, H., 2010. Advanced glycation end products in foods and a practical guide to their reduction in the diet. *J. Am. Diet. Assoc.* 110 (6), 911–916. <https://doi.org/10.1016/j.jada.2010.03.018>. Advanced.
- Vesterlund, S., Karp, M., Salminen, S., Ouwehand, A.C., 2006. *Staphylococcus aureus* adheres to human intestinal mucus but can be displaced by certain lactic acid bacteria. *Microbiology* 152 (6), 1819–1826. <https://doi.org/10.1099/mic.0.28522-0>.
- Weaver, J.C., Chizmadzhev, Y.A., 1996. Theory of electroporation: a review. *Bioelectrochem. Bioenerg.* 41 (2), 135–160. [https://doi.org/10.1016/S0302-4598\(96\)05062-3](https://doi.org/10.1016/S0302-4598(96)05062-3).
- White, T.J., Bruns, T., Lee, S., Taylor, J., 1990. Amplification and direct sequencing of fungal ribosomal RNA genes for phylogenetics. In: Innis, M., Gelfand, D., Shinsky, J., White, T. (Eds.), *PCR Protocols: a Guide to Methods and Applications*. Academic Press, San Diego, pp. 315–322. <https://doi.org/10.1016/B978-0-12-372180-8.50042-1>.
- Yan, F., Polk, D.B., 2002. Probiotic bacterium prevents cytokine-induced apoptosis in intestinal epithelial cells. *J. Biol. Chem.* 277 (52), 50959–50965. <https://doi.org/10.1074/jbc.M207050200>.
- Yang, S.T., Silva, E.M., 1995. Novel products and new Technologies for use of a familiar carbohydrate, Milk lactose. *J. Dairy Sci.* 78 (11), 2541–2562. [https://doi.org/10.3168/jds.S0022-0302\(95\)76884-9](https://doi.org/10.3168/jds.S0022-0302(95)76884-9).

Vilnius University Press
9 Saulėtekio Ave., Building III, LT-10222 Vilnius
Email: info@leidykla.vu.lt, www.leidykla.vu.lt
Print run copies 25